UPLIFT IN GRAVITY DAMS

and Associated Problems

by JAMES PARK, B.Sc.

Dissertation submitted for the degree of Master of Science at the University of Edinburgh, October 1956

ACKNOWLEDGEMENTS

The author wishes to express his thanks for the assistance of Professor R. N. Arnold, Regius Professor of Engineering at the University of Edinburgh, Dr. O. C. Zienkiewicz whose constant encouragement and advice made the work possible, Mr. J. Griffiths for his invaluable help in the reproduction of the final manuscript, and the various friends who have taken a kind interest in the work.

Notation for Chapters 6 and 7

a, b	internal and external radii of a cylinder
c	intermediate radius of a cylinder, $a < c < b$
α	apex angle of triangular dam
β	drainage angle of triangular dam
γ	ω_s/ω
δ	Dirac's delta function
∇^2	Laplacian operator $\left(\frac{\partial^2}{\partial x^2} + \frac{\partial^2}{\partial y^2}\right)$ or $\left(\frac{\partial^2}{\partial r^2} + \frac{1}{r}\frac{\partial}{\partial r} + \frac{1}{r^2}\frac{\partial^2}{\partial \theta^2}\right)$
∇^4	$\nabla^2 . \nabla^2$
e^{-mt}	Laplace transformation factor
f or $f(\theta)$	a function of θ
F	a stress function
ϕ	Airy's stress function
H	unit step function
∞	infinity
k	$\frac{1-2\nu}{1-\nu}$
k'	$\frac{\nu}{1-\nu}$
ν	Poisson's ratio
n	area factor
p	pore pressure
p_a, p_b	pressures applied at radii a and b of a cylinder
ψ or $\psi(\theta)$	function of θ governing pressure distribution
Q	$n(p_a - p_b)/(1-\nu)\log a/b$
Q'	$na\,p_a/(1-\nu)\log c/a$
r, θ	Polar co-ordinates in a two-dimensional system
$\sigma_x, \sigma_y, \tau_{xy}$	plane strain components of stress (Cartesian)
$\sigma_r, \sigma_\theta, \tau_{r\theta}$	plane strain components of stress (Polar)
t	$\log_e r/a$
u, v	radial and tangential displacements
V	potential function representing all body forces
ω	unit weight of water
ω_s	unit weight of saturated porous material
x, y	Cartesian co-ordinates in a two-dimensional system.

CONTENTS

Chapter 1

INTRODUCTION

The complex nature of a gravity dam including its galleries, drain-holes, roads and ancillary buildings, the variable nature of concrete, the heterogeneous foundation, the indeterminacy of the forces acting on the dam including the restraint of the foundation and abutments, all lead to a three-dimensional problem as complex and insolvable in exact terms as could possibly be met in engineering design. The design of gravity dams is then, of necessity, based upon a number of simplifying assumptions, perhaps the most important of which is to consider the problem in two dimensions and limit calculations to finding the stress distribution on a cross-section at right angles to the longitudinal axis of the dam. If the dam and foundation are considered to be made of one homogeneous, elastic material, an exact solution is then theoretically possible if the applied forces are known. It is not generally possible to determine exactly the magnitude of the applied forces which consist mainly of the weight of the material, the internal and external action of the impounded water, and in some locations ice pressure, silt pressure and earthquake shocks. In addition the uneven cooling and shrinkage of concrete set up forces which are inherent in massive structures. The dependence of most of these forces on the elements of nature makes them subject to uncertain variation, but in most cases a good degree of approximation can be reached. This is the result of many years of exhaustive research which has reduced enormously the approximation and guesswork in early dam designs.

It is paradoxical that the action of water pressure, which the dam, primarily, is meant to withstand, should have been misunderstood through centuries of dam building and even to-day eludes complete understanding. The early dams were built like walls, with broad rectangular profiles intended to resist the horizontal thrust of water in their impounded reservoirs. These structures, "designed" by purely empirical methods, generally possessed factors of safety far in excess of those permitted by present day economy or demanded by present day practice. With the advent of competitive industry and the development of mechanical sciences, dam design became more scientific.

Because the horizontal thrust of water on a structure increases linearly with depth, it was soon realised that the ideal profile for a dam was a triangle with a vertical upstream face. Dam profiles, therefore, became gradually more slender, tending towards the ideal shape, and in the latter part of the 19th century this reduction reached a significant stage.

Around the turn of the century a number of large dams in Europe and in the United States of America failed because of the movement downstream of one of their sections and the subsequent collapse of the remaining structure under the onrushing water. The resulting loss of life and property was catastrophic and serious investigations had to be made into the causes.

It was gradually realised, as postulated by a few advanced thinkers of that time, notably Levy[25] in France and Intze[23] in Germany, that water under pressure could not only push horizontally on the structure but could also penetrate into the concrete or masonry of the dam and its foundation probably, it was thought, through cracks and fissures, and so cause an upward as well as a forward overturning force. This upward or "uplift" force reduced the effective weight of the dam and diminished the shear

25. Numbers refer to bibliography.

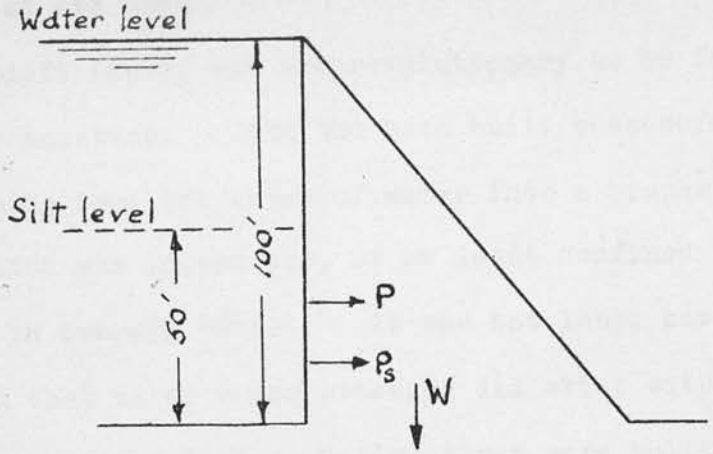

Fig. 1

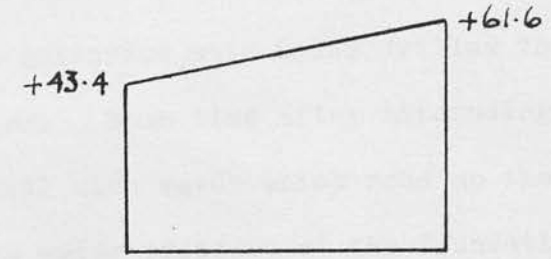

W + P

Fig. 1a

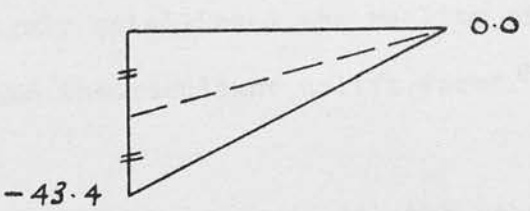

Uplift

Fig. 1b

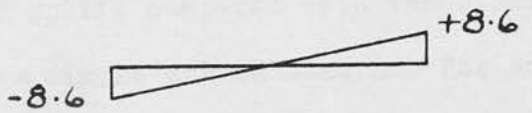

Silt

Fig. 1c

Ice

Fig. 1d

Stress diagrams

Scale: 1 inch to 50 lb./sq. in. Compression plotted above axis

resistance at its base.

The uplift theory was too revolutionary to be immediately and universally accepted. Dams had been built successfully for hundreds of years assuming that the entry of water into a properly constructed dam or its foundation was impossible, or at least confined to local fissures and negligible in overall effect. It was not long, however, before evidence established that water under pressure did exist within "solid" dams, at least near the foundation. Hollow pipes were built into new structures, connecting inspection galleries with holes drilled through the joint between dam and foundation. Some time after impounding the reservoir these holes were found to fill with water which rose up the pipesto heights which indicated considerable water pressure at the foundation. The evidence of these measurements firmly established the reality of water under pressure beneath a structure and the resultant uplift force.*

Importance of Uplift.

The importance of uplift compared with the other applied forces can be clearly seen from a few simple stress diagrams for an idealised triangular dam profile with a vertical water face. The diagrams in Figure 1 show the vertical stresses on the base section caused by (i) the weight of the material and the horizontal thrust of the water, (ii) uplift pressure, (iii) silt pressure, (iv) ice pressure.

Stress Calculations.

It will be assumed here that the stress distribution is linear over all sections, an assumption which is sufficiently accurate for the purpose of comparison. It is discussed in relation to exact elastic analysis in

*See for example reference 16 bibliography.

the introduction to **Chapter** 6.

a) Weight of masonry w_s and horizontal thrust P.

Data: Apex angle = 40°; total height, h = 100 feet; base width, b = 83.9; specific gravity of masonry = 2.42; weight of water = 6.25 lb./cu.ft. Stress due to weight of masonry at upstream end

$$= \frac{100 \times 2.42 \times 62.5}{144} = +105.0 \text{ lb./sq.in.}$$

This stress decreases linearly to zero at the downstream end of the section. Horizontal thrust, $P = \frac{w h^2}{2} = 312{,}500$ lb. Bending moment, M = 312,500 x 100/3 ft. lb. Section modulus, $Z = \frac{1}{6}b^2$ (1 foot wide strip) = 1,174 ft. units. Maximum stress = M/Z = $\pm$61.6 lb./sq.in. Nett stress due to weight of masonry and horizontal thrust is then +43.4 lb./sq.in. at upstream end and +61.6 lb./sq.in. at downstream end. (See Figure 1a).

b) Uplift. "Full uplift" is assumed, i.e., a linear variation from full reservoir pressure at the upstream end to zero at the downstream end acting over 100% of the area of the section. For design purposes this is generally considered the most severe case likely to develop. In this case the resulting stress is identical in magnitude and distribution to the uplift pressure (see Figure 1b). Maximum stress = wh = -43.4 lb./sq.in.

c) Silt pressure. The dam is considered to be silted up to half its height, a severe condition which would not normally be anticipated. Submerged density of silt, w_{sub} = 70 lb./cu.ft. Angle of internal friction of silt, $\phi = 0^\circ$. The horizontal thrust P_s, caused by the silt is given by the Rankine formula

$P_s = \frac{w_{sub} h^2}{2} \cdot \frac{(1 - \sin \phi)}{(1 + \sin \phi)} = 87{,}500$ lb. (h in this case being the depth of the silt). Bending moment, M = 87,500 x 50/3 ft.lb. Maximum stress = M/Z = $\pm$8.6 lb./sq.in. (See Figure 1c).

d) Ice pressure. A pressure of 5,000 lb./ft. run is assumed to act at the top of the dam. This is the upper limit of Professor E. Brown's recommendation of 3,000 to 5,000 lb./ft. run, used in general practice.[7] Bending moment, M = 5,000 x 100 ft. lb. Maximum stress = M/Z = $\pm$3.0 lb./sq.in. (See Figure 1d).

Uplift is a constant threat to the stability of a dam, not merely a locational or occasional one such as silt and ice pressure. Figure 1 clearly demonstrates that its magnitude makes uplift one of the fundamental factors in dam design and as such it demands the fullest attention and investigation.

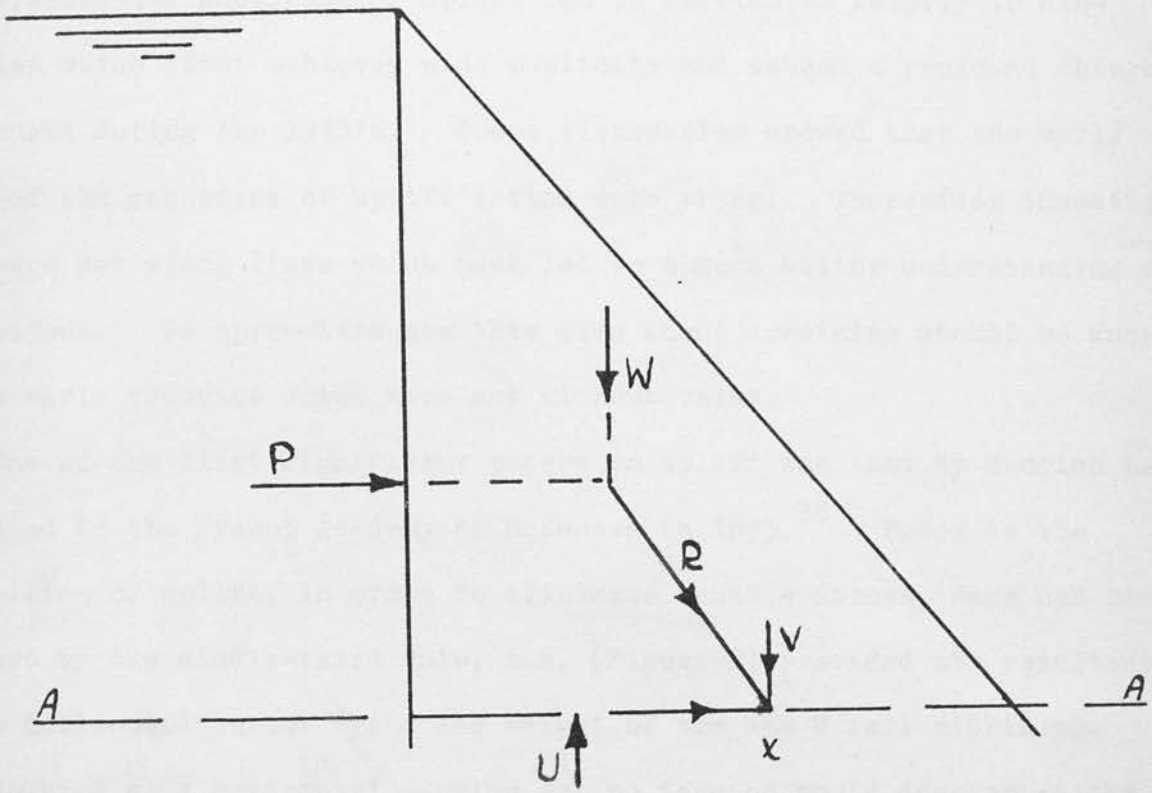

Figure 2

Chapter 2

EARLY AND MODERN CONCEPTIONS OF UPLIFT

Present-day knowledge of uplift can be attributed largely to discoveries which first achieved wide publicity and caused a profound change of thought during the 1930's. These discoveries showed that the early ideas of the mechanics of uplift action were wrong. Thereafter investigations were set along lines which have led to a much better understanding of the subject. To appreciate how this came about something should be known of the early theories which were not without value.

One of the first significant papers on uplift was that by Maurice Levy presented to the French Academy of Sciences in 1895.[24] Prior to the recognition of uplift, in order to eliminate tensile stress, dams had been designed by the middle-third rule, i.e. (Figure 2) provided the resultant R of the horizontal thrust P and the weight of the dam W fell within the middle-third of a horizontal section AA, no tension would develop at the upstream end of the section. This is a form of the well-known middle-third rule for an eccentrically loaded column. The line of action of R meets the section at a point X; provided X lies within the middle-third, the total vertical component V, (numerically equal to W) also lies within the middle-third and no tensile stress will develop at the upstream face.

This rule is quite legitimate for an impervious structure, but Levy pointed out that it was inadequate when uplift forces were acting. Any appreciable uplift force U would reduce the effective vertical component V, and the resultant R of all forces acting on AA would almost certainly be

pushed outside the middle-third. Levy visualized water entering a crack in the face of the dam, (caused for example by temperature expansion and contraction), and penetrating into the structure under full hydrostatic head. The result of this wedging action would be an uplift force, a vertical tensile stress at the upstream face and the danger of progressive failure as the water penetrated further into the crack. To prevent this occurrence Levy recommended that the dam should be so designed to create a vertical compressive stress at all elevations of the upstream face equal at least to the hydrostatic pressure in the reservoir. In this way all fissures in the material would be so tightly closed that water would be unable to enter.

Levy's rule was applied for many years, especially in France, until practice showed that it was excessive and led to costly sections, particularly when uplift relieving devices were employed. The reason for this was an erroneous conception of the mechanics of uplift action which only became generally recognised thirty to forty years later.

Water Pressure as an Internal Force.

P. Fillunger in 1913[9] was the first to advance the theory that water could penetrate into a masonry dam independently of cracks in the structure, simply because masonry, and particularly the cement matrix, is porous. In this way uplift could be caused by the presence of water under pressure in the pores, and some at least of the horizontal thrust on the dam would arise from friction between the penetrating water and the internal surfaces of the masonry.

Fillunger's theory did not receive general recognition until many years later as the literature of that time shows. This may have been partly because it was published in an Austrian engineering journal and not

widely read, and partly because engineers were unwilling to immediately accept the idea that the whole structure of a masonry dam was porous. As late as 1934 D. C. Henny[16] published a paper on the stability of gravity dams in which his views on uplift action differ very little from those of Levy in 1895. This paper was hailed by prominent members of the profession as a great advance in clarifying the various problems in dam design, among them uplift. Henny acknowledges that water might penetrate a dam because of the porosity of the material and quotes experiments which prove that it is porous, but he maintains that uplift pressures develop primarily from the entry of water into cracks and fissure.

A feature of the uplift phenomenon which troubled Henny and his predecessors and is still in dispute today is the area factor, i.e. THE PROPORTION OF THE AREA OF A PLANE SECTION ON WHICH UPLIFT SHOULD BE ASSUMED TO ACT FOR THE PURPOSE OF STRESS CALCULATIONS. If uplift were mainly due to the pressure of water in fissures, then the area factor is indeterminable. (Henny attempted to estimate a maximum value for the area factor by considering the stresses acting in a number of existing dams which were considered to be stable. He arrived at a value of 40%). If some uplift develops in the pores of the concrete then in this region the area factor, according to Henny, is the proportion of voids cut by a plane section. This proportion is statistically the same as the volumetric porosity of the material which, in ordinary concrete, is about 12%. It was assumed that the equivalent area factor applying to uplift caused by fissures, although it was indeterminate, would be considerably greater than 12% and so uplift in the pores of the material was of little consequence. The area factor will be discussed in much greater detail in Chapter 4, but Henny's views are discussed here because his paper was the last one of

importance belonging, so far as uplift is concerned, to the "old" school of thought which had not changed basically since Levy's time.

Fillunger's theory, which he reiterated at the Second World Power Conference in 1930,[10] began to receive some attention at this time. Fillunger believed that the area factor was equal to the difference in porosity between the cement matrix and the masonry of the dam as a whole. This idea is now known to be wrong, but his theory that water pressure acts as an internal force within the natural voids of a dam was gradually accepted as being essentially correct. Fillunger's idea of internal pore pressure was not identical with the present day conception. He believed that high uplift pressure were likely to develop in regions of high permeability, but that such regions need not necessarily exist in a well constructed dam.

Credit for firmly establishing the theory of internal pore pressure must go largely to K. Terzaghi. In a paper published in 1936[38] Terzaghi took the bold step of plainly stating that because masonry or concrete are porous materials, a continuous but imperceptible flow of water passes through a dam from the upstream to the downstream face. Evaporation occurs at the downstream face as soon as the water arrives there, so that it never appeares wet. Uplift is due primarily to the presence of water in the pores of the material, and the area factor, as shown by his laboratory experiments, has a very high value and is in no way associated with the porosity of the material. Measurements made subsequently at existing structures confirm that water penetrates deeply into the dam and that high water pressures develop in the voids.

The discoveries of Fillunger and Terzaghi made Levy's hypothetical cracks unnecessary to the conception of uplift. It became evident that

uplift would exist in any part of the structure where water could penetrate, irrespective of the state of stress, and was caused by pore pressure rather than the wedging action associated with Levy's theory. The value of the latter's theory is that of pioneering work, for it was the first successful attempt to approach the problem in a rational manner and provide a basis for safe design.

Horizontal Thrust.

It had always been assumed by designers of dams that the horizontal thrust of the water in the reservoir was exerted entirely on the upstream face. In view of the new knowledge of pore pressure this assumption was seen to be wrong. The idea of pore water pressure had led Fillunger to the important conclusion that the horizontal thrust was at least partly due to friction between the seeping water and the internal surfaces of the masonry. To state the function of water pressure more explicitly, water can penetrate into a structure and in so doing its pressure is subjected to a gradual reduction from its original value, viz. that of the hydrostatic pressure in the reservoir, to zero, when it is intercepted by a drain or arrives at the downstream face. This reduction is caused by friction between the percolating water and the internal surfaces of the minute pores and channels within the concrete, in a way similar to the head lost by water in percolating through a granular mass. Thus, the water experiences a decreasing pressure gradient and the material of the dam is subjected to a body force due to friction in the direction of the falling pressure gradient. Put more generally, the horizontal thrust experienced by a dam is not applied at the upstream face, but gradually along the lines of flow of the percolating water.

Distribution of Pressure within a Dam.

It is apparent, since horizontal thrust and uplift are both in some way due to pore pressure, that they are two results of a single phenomenon. The connection can be demonstrated with the aid of a flow net for the triangular dam profile. The profile can be regarded either as the top section of a dam of infinite height or as a dam on an impervious foundation. The flow conditions for the two cases are identical.

It is assumed in drawing the flow net that the dam is perfectly homogeneous with respect to permeability. It is also assumed that flow obeys Darcy's law of seepage which can be expressed in the form

$$v = ki$$

where v = apparent velocity of flow,
i = hydraulic gradient,
k = a constant depending on the permeability.

'Apparent velocity of flow' denotes discharge from a plane section divided by the total area of the section, and not the true velocity of the water particles passing through the voids in the concrete.

'Hydraulic gradient' is defined as the limit of the difference in hydraulic head between two points divided by the shortest distance between them.

There are limits to the strict applicability of Darcy's law depending on the Reynold's Number of the flow, and it is by no means certain that the law is strictly applicable to the flow of water through concrete. However, since existing evidence provides no better alternative, it will be assumed that the law is applicable. The factors affecting its applicability are briefly discussed on page 22.

The flow of water from the upstream face to the downstream face of the dam follows the shortest possible route under maximum hydraulic gradient.

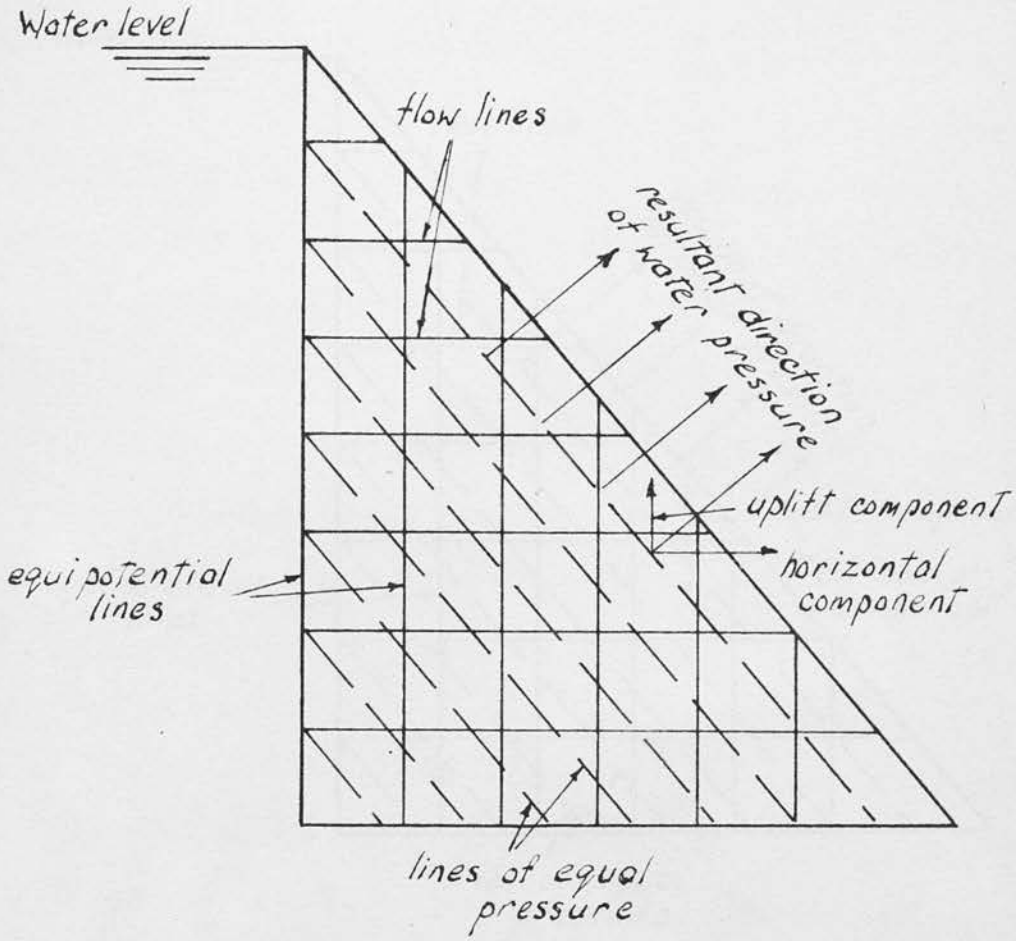

Figure 3

Flow net for triangular dam

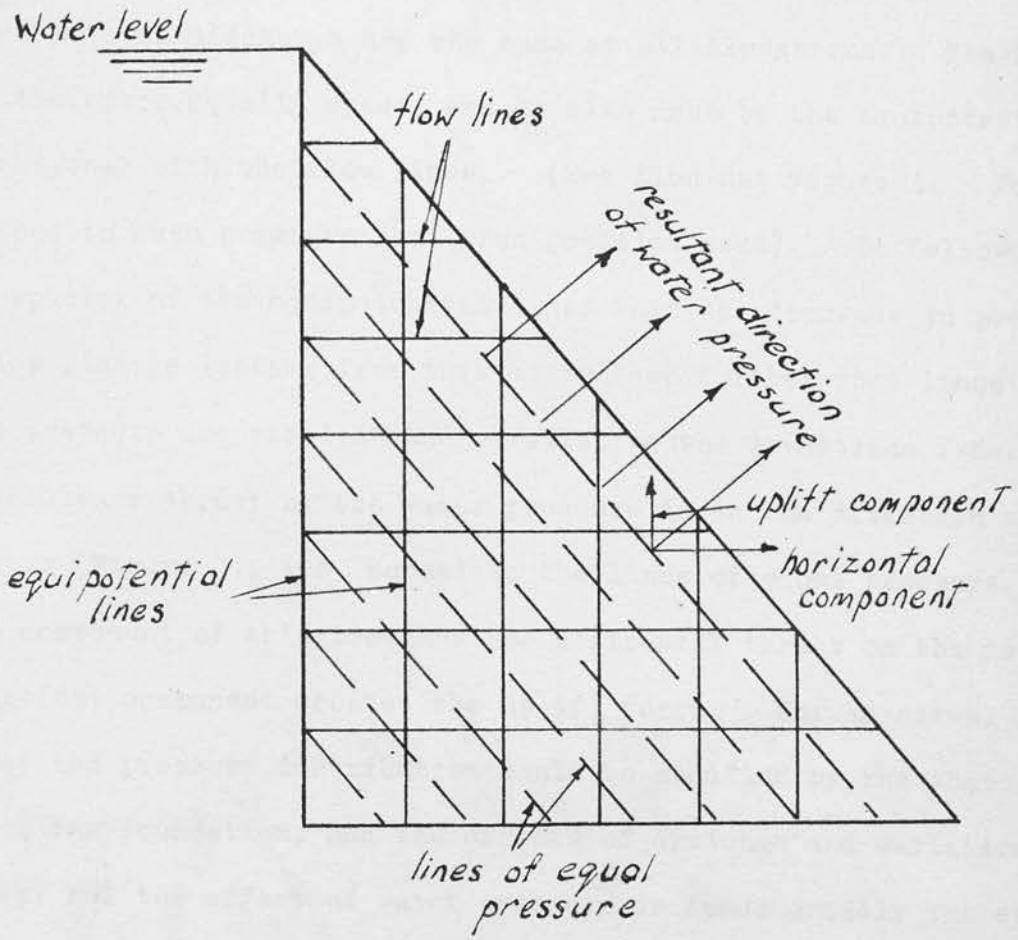

Figure 3

Flow net for triangular dam

Flow lines are therefore horizontal and there is no free surface to distort the flow pattern. The hydraulic gradient at all sections has the same value because of the shape of the dam, and so by Darcy's law the velocity of flow and rate of discharge are the same at all elevations. The flow lines are therefore equally spaced and so also must be the equipotential lines, orthogonal with the flow lines. (See flow net Figure 3. Potential is understood to mean pressure head plus position head). It follows from the equal spacing of the equipotential lines that the decrease in pressure along a flow line is linear; from this it follows further that lines of equal pore pressure are straight and parallel to the downstream face.

The resultant thrust by the water pressure is in the direction shown by the arrows (Figure 3), i.e. normal to the lines of equal pressure. The horizontal component of this provides the horizontal thrust on the material and the vertical component creates the uplift force. For an actual dam, the flow net and pressure distribution would be modified by the shape of the profile, the foundation, and the effects of drainage and variations in permeability; but the effect of water pressure is fundamentally the same, i.e. at acts at all times at right angles to the lines of equal pressure.

For the purpose of dam design it is more convenient to consider separately the two pore pressure components, thrust and uplift; but in order to understand the effect of water pressure on the structure, the foregoing theory is essential and has done much to clarify uplift problems.

Chapter 3

FACTORS AFFECTING THE DEVELOPMENT OF PORE PRESSURE IN CONCRETE

The process by which a dam reaches its ultimate state of saturation, and the flow of pore water reaches a steady state, is an extremely complex one which may progress throughout the life of the dam. Numerous variables are involved, none of which is fully determinable, and because of the intricate and unexplained internal structure of concrete, it has not in the past been possible, by deductive reasoning, to draw many conclusions regarding the physical interaction between pore water and porous material. The most valuable information about the movement of water through concrete has therefore come from direct permeability tests which show how permeability, measured in arbitrary units, is affected by various known parameters. A series of such tests, carried out by W. H. Glanville,[12] is discussed below, and some conclusions are drawn connecting the results with the development of water pressure within a dam. Following this, later sections will deal with the other factors thought to affect uplift development, including recently discovered evidence about the structure of hydrated cement paste.

Permeability.

Permeability can be defined as the property by which a material allows water under pressure to pass through it. It is distinct from capillarity by which a material can absorb water, a phenomenon which is caused by surface tension forces between the water and the walls of connecting pores. The flow of water through a porous body is at first influenced by the combined actions of water pressure and capillary forces, but once seepage has

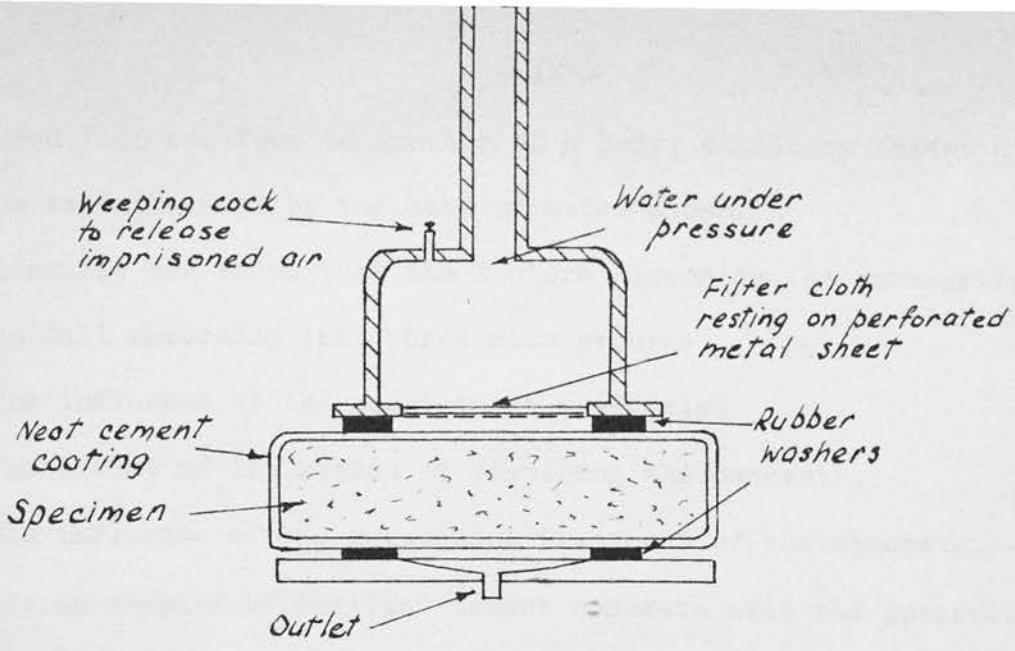

Figure 4

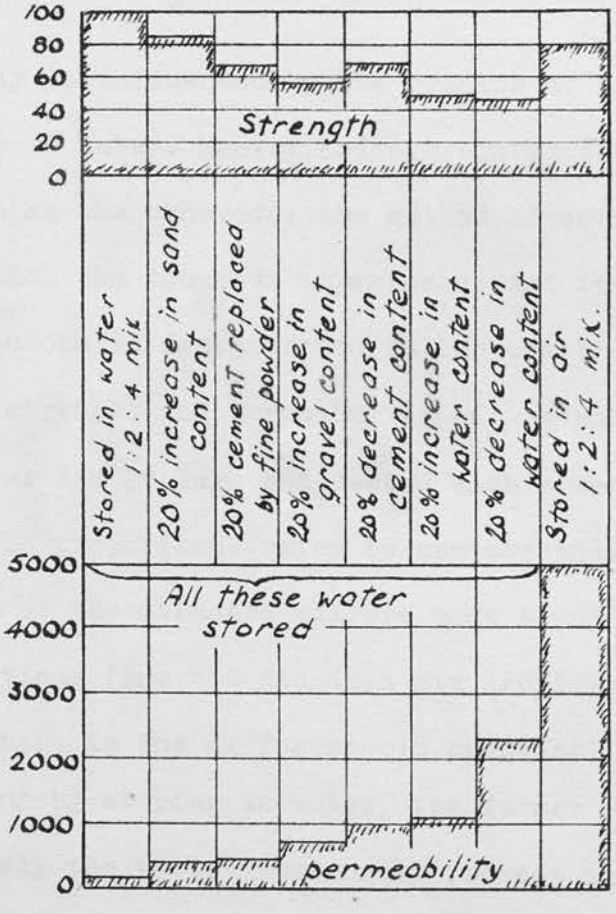

Figure 5

penetrated from one face to another of a body, capillary forces disappear and flow is influenced by the head of water alone.

Glanville has shown that the factors governing the permeability of concrete fall naturally into three main groups:

a) The influence of the constituent materials,

b) The effect of the method of preparing the concrete,

c) The influence of the subsequent treatment of the concrete.

His tests on samples of Portland cement concrete with the apparatus shown in Figure 4 yielded a number of positive results. These are too numerous to present in detail because of the large number of variables investigated, but those which interest the present discussion can be briefly summarized as follows:

(i) Permeability is influenced by the grading of aggregates and the relative proportions of water, cement and aggregate; the care taken in mixing, casting and ramming the concrete; the method of curing; the subsequent conditions to which the concrete is exposed; and its age. The effect of some of these factors is demonstrated in the chart of Figure 5. The chart is based on the strength and permeability of a standard 1:2:4 (by weight) mix cured in water for 28 days and tested with a water pressure of 100 lb.per sq.in. (the proportions refer to cement:sand:gravel). The strength and permeability of the standard mix are each taken as 100 units and some results of deviations from the standard mix are illustrated. The dominant feature of the chart is the difference in permeability of samples cured by storing in air and by storing in water, the former being 50 times the latter. Obviously the wetter the curing process in practice, the more impermeable will be the concrete.

(ii) Air cured and water cured concrete reach an almost permanent state of

permeability after 14 and 28 days respectively assuming that they are subject thereafter to similar conditions. However, a concrete which has not been well cured at an early stage, i.e. through insufficient wetting, can be made considerably less permeable if submitted to water under pressure for a long period.

(iii) Rich mixes, i.e. those containing a high proportion of cement, are generally less permeable than lean mixes, though this depends to a large extent on the curing conditions.

(iv) Initial permeability may decrease with time if the concrete acts as a filter to fine particles carried by the water.

From the above summary of results the following conclusions can be drawn:

1. Care in the choice of materials and the mixing, placing and curing of the concrete, can all contribute towards decreasing its permeability.

2. Careful curing is essential to low permeability at an early stage, but in time the permeability may be reduced by the continual effect of water under pressure.

3. The practice of using a richer concrete at the upstream face of a dam will reduce its permeability.

4. The deposition by water of fine particles may in time reduce the permeability in some regions. Such particles may be silt carried from the reservoir, or loose particles carried from the upstream regions of the dam to positions further downstream.

It should be noted that the foregoing paragraphs have dealt only with the permeability of concrete. At this stage it is necessary to consider the relation, if any, between permeability and pore pressure for they are by no means inseparable. High pore pressure may exist with little or no

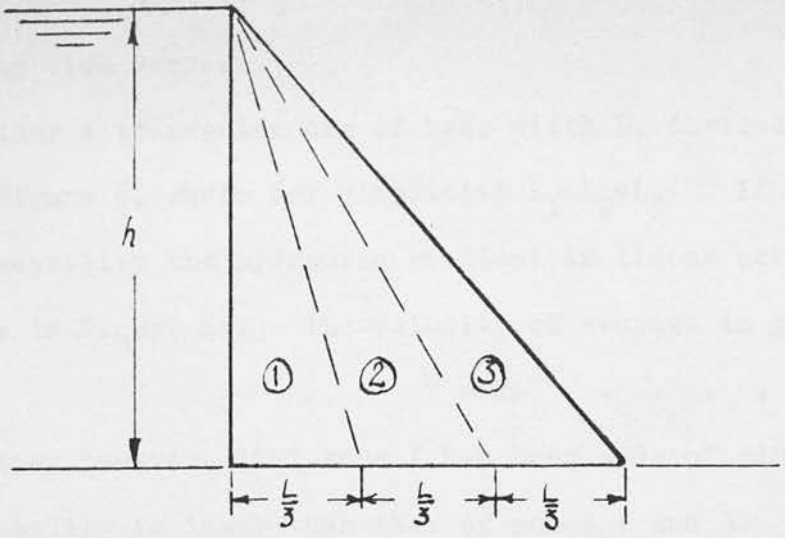

Fig. 6

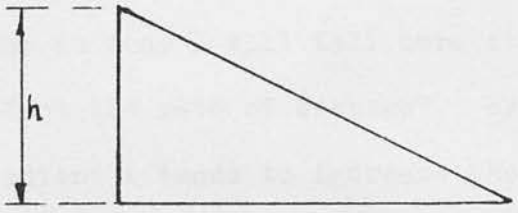

Fig. 6a

$k_1 = k_2 = k_3$

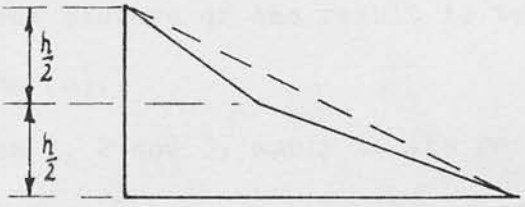

Fig. 6b

$k_1 = 1/2\ k_{2,3}$

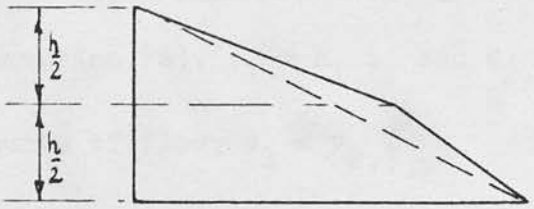

Fig. 6c

$k_{1,2} = 1/2\ k_3$

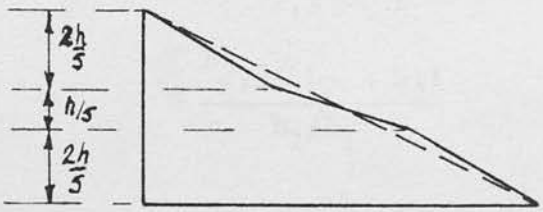

Fig. 6d

$k_1 \cdot 2k_2 = k_3$

Pressure diagroms

seepage and vice versa.

Consider a triangular dam of base width L, divided into three zones as shown in Figure 6, where for simplicity $L_1=L_2=L_3$. If all zones are of equal permeability the hydraulic gradient is linear across a horizontal section as in Figure 6a. The velocity of seepage is given by Darcy's law

$$v = ki \quad . \ . \ . \ . \ . \ . \ . \ . \ . \ . \ (a)$$

Suppose, however, that zone 1 has been made of richer concrete so that its permeability is lower than that of zones 2 and 3. Obviously the hydraulic gradient in zone 1 will fall more steeply as in Figure 6b, but how will this affect the rate of seepage? By Darcy's law an increase in the hydraulic gradient i tends to increase the rate of seepage but at the same time the decrease in permeability k tends to decrease it. The only way to get a clear picture of the result is to work out a simple example based on equation (a).

The suffixes 1, 2 and 3, apply to the respective zones.

Assume that zone 1 has one half the permeability of zones 2 and 3, i.e. $k_1 = \frac{1}{2}k_{2,3}$. Total head available = h.

Applying equation (a), $v_1 = k_1 i_1$ and $v_{2,3} = k_{2,3} i_{2,3}$

For continuity of flow, $v_1 = v_{2,3}$

so that

$$\frac{k_1}{k_{2,3}} = \frac{i_{2,3}}{i_1}$$

$$= \frac{h_{2,3}/(L_2 + L_3)}{h_1/L_1}$$

$$= \frac{1}{2} \cdot \frac{h_{2,3}}{h_1}$$

and since $\frac{k_1}{k_{2,3}} = \frac{1}{2}$, then $h_{2,3} = h_1 = \frac{1}{2} h$.

Therefore, $v_1 = k_1 i_1 = \frac{1}{2} k_{2,3} \cdot \frac{h_1}{L_1}$ . . . . . .(b)

$$= \frac{1}{2} k_{2,3} \cdot \frac{\frac{1}{2}h}{L}$$

$$= \frac{3}{4} k_{2,3} \frac{h}{L}$$

$$= \frac{3}{4} v, \quad \text{if } k_{2,3} = k \text{ in equation (a)}$$

i.e. if the permeability of zone 1 is reduced to one half its original value, half the available head is dissipated in zone 1 and the rate of flow is reduced to $\frac{3}{4}$ its original value. (See Figure 6b).

Consider now the case where the permeability of zone 3 is reduced to half the value of that in zones 1 and 2. Equation (b) now becomes

$$\frac{k_{1,2}}{k_3} = \frac{i_3}{i_{1,2}}$$

$$= \frac{h_3/L_3}{h_{1,2}/(L_1 + L_2)}$$

$$= 2 \frac{h_3}{h_{1,2}}$$

and since $k_{1,2} = 2k_3$ then $h_3 = h_{1,2} = \frac{1}{2} h$.
Again half the pressure is dissipated in each zone, but the total pressure has increased (See Figure 6c).

The velocity of flow $v_1 = k_1 i_1$ etc.,

$$= \frac{3}{4} v, \text{ as before.}$$

The further case where both zones 1 and 3 are of low permeability is of definite practical interest for rich mixes are often placed at both

upstream and downstream faces, at the latter to resist weathering. The calculation is merely an extension of the above method and the resulting pressure distribution is shown in Figure 6d. In this case the flow is reduced to 3/5 of its original value.

In conclusion from the three foregoing examples,

1. A rich mix placed at the upstream end of the dam only, will reduce both pore pressure and seepage.
2. A rich mix placed at the downstream face only (or a region of low permeability caused by silting) will increase pore pressure but decrease seepage.
3. Rich mixes placed at both upstream and downstream faces will reduce seepage and reduce the higher pore pressures, but will not necessarily reduce the total uplift. In the above example the total uplift is the same as that for the homogeneous dam, though the moment centre has moved slightly downstream, reducing the overturning moment.

Initial Moisture Movement - Capillarity.

Under the heading of "permeability" the steady movement of water through a porous material of unspecified nature has been discussed. The process which leads to this steady state and the nature of the material itself, i.e. concrete, cannot be described nearly so explicitly, for some of the factors involved are abstruse and all may be subject to great variation.

The initial penetration of reservoir water into a dam appears to be affected by three things; (i) the reservoir pressure behind the water, (ii) capillarity, and (iii) the initial conditions of moisture in the concrete.

Consider first that the concrete is completely dry and that no more is known of its structure than that it is honeycombed by a maze of fine interconnecting passages. If the end of a rod or cylinder of such material

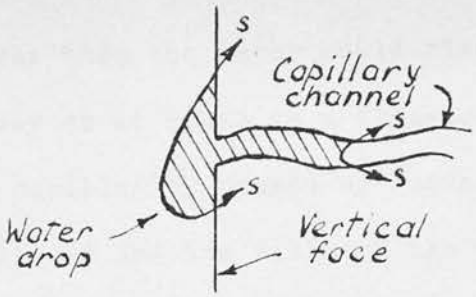

Figure 7

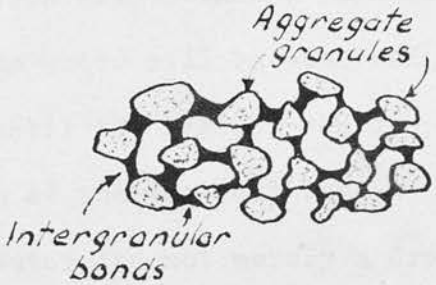

Figure 8

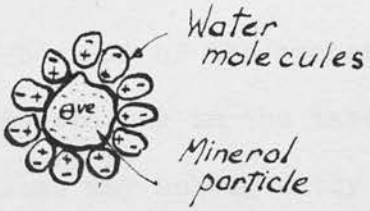

Figure 9

were immersed in water then the water would rise up the rod to some fixed height in the same way as it rises in a fine-bored tube. This is the well known phenomenon of capillarity caused by surface tension forces between the surface of the liquid and the walls of the connecting channels.

In the case of a concrete dam, the effect of capillarity is somewhat different for in the latter case flow is, on an average, horizontal and therefore uninfluenced by gravity.

Consider water applied to a vertical concrete face but, as yet, without pressure. Such a condition exists when a raindrop falls on the wall of a building (Figure 7). The water will be absorbed into the channel by the surface tension force S until the last of the drop forms another meniscus in the opposite direction at the vertical face. Alternatively, if there is a constant supply of water and not merely a drop, the penetration can go on indefinitely for there is no gravity force to arrest it.

In a dam the process of water absorption will be hastened by the pressure of the hydrostatic head which will assist in overcoming the friction forces between the water and the walls of the channels. Saturation will be hastened further by the effect of the initial moisture content.

The concrete in any massive structure will never be completely dry from the time it is first mixed because of the excess mixing water used to make it workable. This water is trapped in the interior of the concrete when it first sets, and though some may subsequently be removed by further chemical action with the cement, the concrete is only likely to dry out near faces which are exposed to a dry atmosphere. Furthermore, it is good practice to keep the concrete thoroughly damp during curing, either by sprinkling or covering with wet sacking, and this will add further to the initial moisture content.

The Internal Structure of Concrete.

Apart from the initial state of moisture, the process of moisture movement has been greatly simplified in the foregoing paragraphs. It has been assumed that the channels in the concrete are sufficiently large to allow water to flow in the manner described, and though the structure of the material is not fully understood, sufficient is known to show that this assumption is only partly correct.

On the infrequent occasions when writers express their conceptions of concrete in a pictorial manner, something like Figure 8 is usually shown. A number of solid particles are bonded together by hydrated cement which has formed a rigid framework often described as "solid gel". Running through this bonding material are the pores and channels caused by air and excess water trapped in the original mixing. These pores are generally considered to be comparable in size to the smallest aggregate particles, and this being so water movement will probably occur in the simple manner already envisaged. There is, however, evidence which shows that much smaller voids are also present. One source of such information are adsorption tests with inert gases and water vapour.

The adsorption of a fluid, as distinct from absorption by capillary action, is attributed to the presence of negative electric charges in the mineral particles of soils, rock and concrete. The negative charge attracts the positive elements of the fluid molecules which then form a layer around the particle. This is represented diagrammatically in Figure 9. If the fluid is water, the positive (hydrogen) elements of the water molecules are attracted. This attraction may extend to several layers of molecules and the total zone of influence is known as the adsorbed layer. The physical properties of the fluid in this layer are different

from those in its ordinary state, e.g. the boiling point is much higher. It may thus be necessary to heat the fluid to several times its normal boiling point to drive it away from the solid.

A theory has been devised by which it is possible to estimate the internal surface area of a granular or porous material by measuring the adsorption of a gas or vapour.[8] This is done by removing as much of the original adsorbed fluid as possible without causing any physical or chemical change in the material, then measuring the increase in weight when a fresh adsorbate is introduced. The value of such tests lies not in individual results but in the comparison of the adsorption of one material with that of another.

Preliminary attempts to relate adsorption to other physical conditions in hydrated cement paste, such as the degree, temperature and method of curing and the fineness of the cement, have met with some success; but work in this field has not been extensive. One interesting result which has come from such tests is that the surface area available to nitrogen, as determined by Blaine and Valis,[3] is much smaller than the area available to water vapour as determined previously by Powers and Brownyard.[30] The main reason for this, according to the former authors, is the difference in size between water and nitrogen molecules. Water molecules being slightly smaller, it is possible for some of the intercrystalline spaces in the cement to be penetrated by water, whereas they remain inaccessible to nitrogen. If this explanation is correct it can be logically concluded that very fine channels exist extensively within concrete, their diameters being of the same order as the diameters of water and nitrogen molecules,

viz. a few Å, sufficiently small to admit one molecule and exclude another.*

Assuming that these very fine channels do exist, they will at all times in normal circumstances be blocked with adsorbed water molecules, so that seepage through them is eliminated. Adsorbed water may also be present in channels of larger size so that the channels are not blocked but the flow merely restricted. In such a case flow may not be governed by Darcy's law if molecular forces are appreciable compared with pore pressure forces, but very little information is available on this subject.

Crystallographic Research.

The use of x-rays in determining the chemical and crystalline structure of mineral compounds has developed within the last ten years. It has provided a new method of investigating materials which defied analysis by previous methods because of the minute size of the mineral particles involved, and the complications arising when several different phases of the basic compound are present. It has thereby proved invaluable to research on cement and chemically associated compounds. The x-ray methods involve the use of elaborate and expensive electronic equipment and specialised methods of analysing test results, both quite beyond the scope of the present study; but the following short description of the principle on which the methods are based, as understood by the writer, may enable the experimental results which follow to be better appreciated.

One writer,[37] who has been largely responsible for the development of x-ray techniques, has compared the direction of a beam of x-rays on a crystal with the effect achieved in some ornate ballrooms by shining a spotlight in a rotating sphere covered with numerous small plane mirrors. In

*Å denotes Ångstrom i.e. 10^{-8} cm.

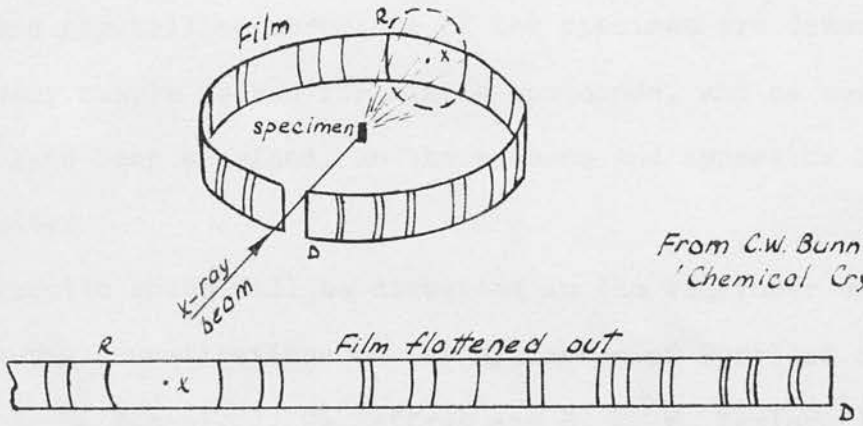
Film
R
specimen
D
X-ray beam
From C.W. Bunn's
'Chemical Crystallography'
R
Film flattened out
D

Figure 10

the former case the rays are both reflected and diffracted, and reflection occurs not from one but from all faces of the crystal. In the x-ray camera a beam of x-rays is directed on a powdered specimen prepared from or containing the mineral to be examined. A strip of film surrounds the specimen in the plane of the beam (Figure 10). The reflected beams form cones which create a pattern of slightly curved lines on the film, and it is from the spacing and width of these lines that data concerning the chemical and crystalline structure of the specimen are deduced. This is a comparatively simple method for simple compounds, and as more complex materials have been examined, so the methods and apparatus have developed in complexity.

The results which will be discussed in the remainder of this section are from x-ray investigations on the hydration of Portland cement by Professor J. D. Bernal, J. W. Jeffrey and H. F. W. Taylor.[1,2] The crystalline structure of the substances present before and after hydration has been studied, particular attention being paid to the products of hydration and the possible relation between their crystal structure and cementing properties.

It was first recognised by Le Chatelier[21] that the main cementing compound in Portland cement has the approximate formula C_3S.* It is known as alite and differs very little from pure tricalcium silicate (C_3S). It was also recognised by Le Chatelier that the main product formed by the hydration of cement must be a calcium silicate hydrate, and that this compound must be largely responsible for the development of strength. All previous

* Cement chemistry nomenclature is used here. C denotes CaO; S denotes SiO_2; H denotes H_2O. Thus e.g. C_3S denotes $3CaO.SiO_2$.

attempts to identify the hydration products yielded divergent or negative results, and the only product whose formation was definitely established was calcium hydroxide ($Ca(OH)_2$). The present investigation, however, has shown that two hydrates can be formed, calcium silicate hydrate (I) with a formula varying between CSH_x and $C_3S_2H_y$, and calcium silicate hydrate (II) whose formula is C_2SH_x. These were detected first in dilute aqueous solutions of C_3S, where the crystals quickly formed long fine fibres, and later in a hydrated paste.

Hydrated cement paste appears under a microscope to be a solid, amorphous substance devoid of any crystalline structure, thus the usual description of "solid gel" applied to the bonding matrix in concrete. The x-ray photographs have shown that in fact the products of hydration have a very strong crystalline character but that the crystals formed in a paste at room temperature are small, badly formed, and probably bemt and tangled, so that in a mass they are indistinguishable under a microscope from a homogeneous material.

Examination of the crystal structures of calcium silicate hydrates (I) and (II) shows that they are composed of layers, the interlayer spaces being filled with water molecules. There is also a marked tendancy for the crystals to grow in one direction in the plane of the layers, causing long thin fibres to be formed which are thought to be mainly responsible for the cementing properties of the material. The spacing between the layers can be varied by the entry or removal of water molecules, caused by changes in temperature, vapour pressure or by evaporation. (These spaces may well be the minute channels whose presence was suggested by the adsorption tests).

The chemical reactions which follow the hydration of alite have been studied and the following table summarizes the extent to which the various

substances could be detected at various ages in a set paste.

TABLE I

Age	C_3S	$Ca(OH)_2$	Calcium silicate hydrates (I) and (II)
10 days	Much	A little	None apparent
7 weeks	Less than before	More than before	None apparent
11 weeks	Still less	Still more	Trace
4 months	Very little	Much	Clearly present
18 months	No substantial change		

It has also been found that set pastes of alite and Portland cement show similar strengths at 28 days, the 28-day strength in each case being a large proportion of the ultimate strength. This confirms that C_3S is the main compound in cement responsible for strength particularly in the early stages, though slower acting materials such as dicalcium silicate (C_2S) may contribute towards the strength at a later stage. It is apparent then, that although the development of strength is largely complete in 28 days the chemical reaction is by no means so, and therefore only a very small amount of the calcium silicate hydrates (I) and (II) must be required to bind together the unhydrated particles and develop strength.

The cementing action of Portland cement in concrete can now be summarized as follows. Some alite in the Portland cement dissolves in the mixing water to form calcium silicate hydrates (I) and (II). These crystals grow quickly to form long fibres which bind together the unchanged cement particles and the aggregate. The practice of wet curing the concrete in the early stages facilitates the growth of crystals of calcium silicate hydrates (I) and (II) and the corresponding

development of strength.

Crystallographic research is still a very new subject and the results it has so far yielded are only a beginning towards the complete understanding of the physical and chemical structure of cement compounds and concrete. Since the work done so far indicates that the physical structure of concrete is largely of a submicroscopic nature, it appears that a complete understanding of moisture movement will depend on information from this source.

Chapter 4

THE AREA FACTOR

The area factor, sometimes called the boundary or superficial porosity, denotes the percentage area of a plane section through a porous material on which pore pressure should be assumed effective for the purpose of stress calculation. The numerical value of this factor has been in dispute since the uplift problem was first analysed at the beginning of this century, and the most recent experimental evidence contradicts what was gradually becoming a general measure of agreement.

There are two ways to approach the problem, namely by deductive reasoning and by experimental measurement. Deductive reasoning is made difficult because the structure of concrete itself is not fully understood, and also because the solution to the problem lies partly in understanding the physical significance of the term "area factor". Some experimenters have bluntly stated that any attempt to solve the problem purely by deductive reasoning is doomed to failure until the physical nature of concrete is fully understood. On the other hand, experimental workers have found it extremely difficult to reproduce in the laboratory the conditions of stress met in the saturated concrete of a dam. Most experimental methods involve the breakage of tests specimens and serious doubts have been raised as to whether the results of such tests are applicable in the case where breakage is not involved.

Originally engineers were concerned only with the uplift at the base of a dam. It was argued that in view of the high stresses at the base a

considerable amount of solid contact existed and that this contact area could not be subjected to uplift. The same apparently logical argument can be applied to any horizontal plane within the concrete. The area of such a plane intersecting voids will be about 12% as already stated in Chapter 2, and at first sight it appears to follow that the area factor is then 12%. In fact this figure of 12% is not the area factor but might be called the sectional porosity which, by Delesse's law, is equal to the volumetric porosity. The difference between the two arises because concrete, by virtue of its porosity, is not a truly isotropic material, and the term "plane section" must not be interpreted too literally when considering stresses caused by the pressure of fluid in the pores. Because the pores are connected and extensive, pore water has access to a large internal area of the concrete, so that the uplifting effect of pore pressure more nearly resembles that in a submerged granular material where the particles are completely surrounded by fluid and are therefore fully buoyant. (There may be some minute deviation from full buoyancy because of point contacts between grains, but experiments have shown this effect to be negligible). [38] In a granular material the area factor is thus considered to be 100% whereas the sectional porosity may be of the order of 25%. If one can determine the extent to which the intergranular bonds on concrete reduce the area factor from 100%, the problem will then be solved. This chapter will not provide the solution for this can only be done in the laboratory and much research remains to be carried out before the problem will be completely solved. What is attempted here is to summarize the work of previous writers, and in so doing to show clearly the meaning of the term area factor, to discuss the limitations of experimental work done so far, and finally to indicate the direction in which future research should be

directed to arrive ultimately at the solution.

Terzaghi's Experiments.

In a paper entitled "Simple Tests Determine Hydrostatic Uplift" published in 1936, Karl Terzaghi describes a number of tests carried out in his own laboratory in Vienna to determine the value of the area factor for clay, sand and concrete.[38] His conclusion for all these materials, though only the tests concerning concrete will be described here, is that the area factor is very nearly unity.

One test consists of subjecting a concrete cylinder 7 cm. in diameter and 20 cm. long to very high water pressures, and measuring its axial deformation. This was first done with a cylinder whose surfaces were sealed or "jacketed" and in whose voids the pore pressure was negligible. The cylinder was placed in a chamber filled with water and the water pressure raised to 200 Kg.per sq.cm. (28,400 lb.per sq.in.). The resulting axial compression registered 200 units on a dial gauge.

The jacket was then removed from the cylinder so that the water had free access to the voids, and after ensuring that the cylinder was fully saturated the same pressure was applied again. This time the axial compression was too small to be measured. Any compression which occurred was less than 1/200 of that for the jacketed specimen, and was at least partly due to the elastic compression of the solid material.

The significance of this result is readily seen by considering the state of stress on any horizontal section through the cylinder. On such a section, calling the area factor n, and the confining pressure p, the effective pressure applied to the section by the water in the pores is np. Since no compression is apparent, the internal stress np must almost exactly balance the external pressure p, indicating that $np = p$ or that $n = 100\%$

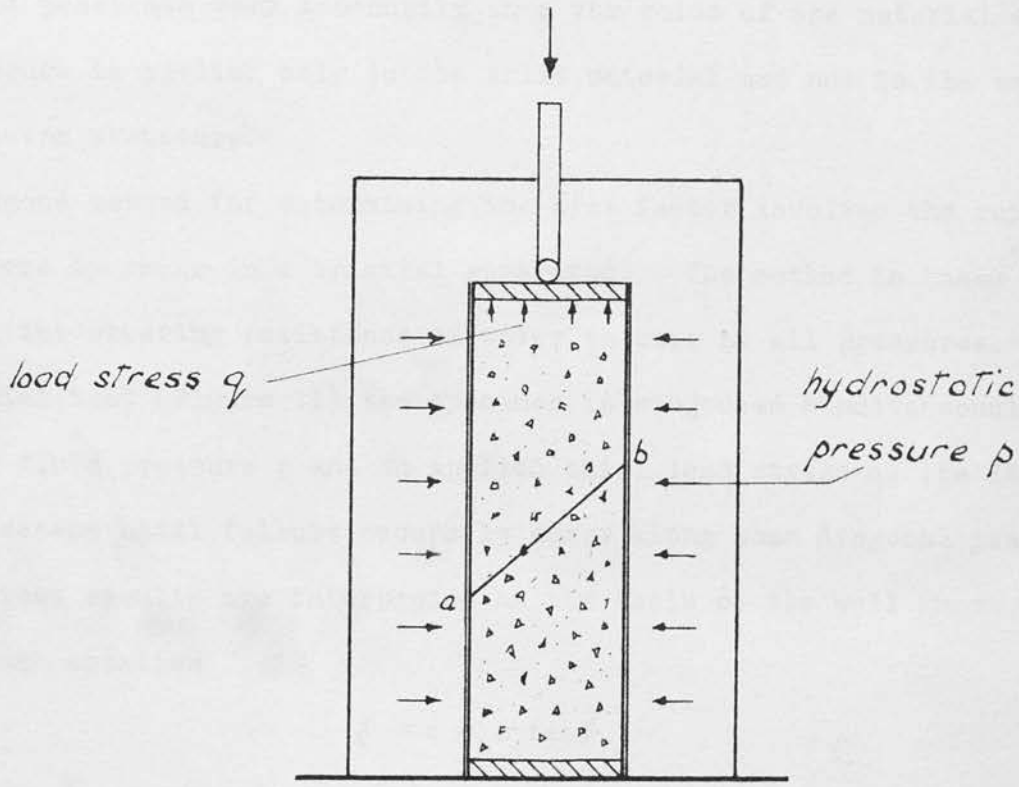

Terzoghi's test method

Figure 11

with a possible error of 1 in 200.

Because the compressibility of the concrete is much greater than the compressibility of the solid material which comprises it, any deformation must be due to a change in the shape of the pores caused by the applied load. The negligible deformation observed in the foregoing tests indicates that water must penetrate very thoroughly into the voids of the material so that pore pressure is applied only to the solid material and not to the concrete as a skeleton structure.

A second method for determining the area factor involves the rupture of cylinders by shear in a triaxial apparatus. The method is based on the fact that the shearing resistance of water is zero at all pressures. In the triaxial test (Figure 11) the specimen is subjected simultaneously to all-round fluid pressure p and an applied axial load stress q, the latter being increased until failure occurs by shear along some diagonal plane ab.

The test results are interpreted on the basis of the well known Mohr-Coulomb equation

$$\delta = c + \sigma \tan\phi$$

where δ = shearing resistance of the material per unit area,
c = cohesive strength per unit area,
ϕ = angle of internal friction,
σ = normal stress on the failure surface.

The Mohr-Coulomb equation is based on the observation that the compressive strength of many materials is greatly increased by high lateral confining pressures, and that an approximately linear relation exists between the strength and the confining pressure. It assumes that the shear resistance is composed of two parts: a constant part c independent of stress and attributed to intermolecular attraction, and a variable part $\sigma \tan\phi$ attributed to intergranular friction and dependent on the normal stress on

the failure surface. c and ϕ are empirical constants for any particular material and must be determined experimentally.

If the load q is applied to a specimen in which the pore pressure is zero, the shearing resistance is given by the above equation where σ is due to the forces applied at the boundaries of the specimen. If, however, a hydrostatic pressure p exists in the pores, the normal stress on the failure surface will be reduced by an amount np. The shear resistance will then become

$$\tau = c + (\sigma - np) \tan\phi.$$

By determining the shearing strength of specimens with and without pore pressure acting, the value of n can be found from the above two equations.

Terzaghi's tests to determine the value of n were

a) Test of a specimen with no hydrostatic pressure acting.

b) Test of a jacketed specimen (no pore pressure) with a hydrostatic pressure of 400 Kg.per sq.cm.

The application of the hydrostatic pressure in test (b) increased the axial load required for failure by 1,350 Kg.per sq.cm.

c) Tests of an unjacketed specimen with a hydrostatic pressure of 400 Kg.per sq.in.

The application of the hydrostatic pressure in test (c) caused no appreciable increase in the axial load required for failure in test (a). The effect of pore pressure was therefore to neutralise entirely the normal stress on the failure surface caused by the hydrostatic pressure in the case of the jacketed specimen. Terzaghi concludes without further calculation that an area factor very close to unity is indicated. From the data given in the paper for a small number of tests, the calculated value of n varies between 0.97 and 1.00.

A later paper by Terzaghi deals very thoroughly with the mechanism of failure in concrete and natural crystalline rocks, and the effect of pore pressure on the conditions leading to failure. [39] No new experimental data is presented but a detailed explanation is given of the observations made in his previous experimental work.

In describing or speculating on the mechanism of failure it is necessary to make some assumption about the crystalline structure of the materials. Terzaghi has assumed that for both concrete and rock, the structure consists of solid mineral grains bonded together by a cementing material in the manner illustrated in Figure 8. This figure is merely a convenient diagrammatic representation of concrete, and it will be seen that the following reasoning about the stresses does not demand that the true structure of the material should comply closely with that shown in the figure.

Terzaghi states that experience has shown the shear resistance of mineral grains at pressures of less than several hundred atmospheres to be practically independent of the normal stress on the failure surface. (References 3, 29 and 33 are given). It follows that the observed increase of shearing resistance with applied confining pressures in jacketed specimens with zero pore pressure must be due to an increase in the strength of the intergranular bonds, and that failure of the material must occur mainly through the failure of these bonds. Two reasons are given for the observed increase in strength; (a) the application of a confining pressure creates intergranular contacts which did not previously exist, thus increasing frictional resistance to shear and (b) assuming that the intergranular bonds are much smaller than the grains themselves, very high compressive stresses must be created within these bonds by relatively low confining pressures. These high stresses, normal to the failure surface,

increase the shear resistance of the bonds.

If the confining pressure fluid can penetrate into the voids, as it does in tests with unjacket specimens, the proportion of the confining pressure carried by the bonds will decrease and therefore so also will their shear resistance. Thus the shear resistance of the material as a whole will decrease. The magnitude of the decrease depends on the proportion of the failure surface in contact with the pressure fluid, and this proportion is in fact the area factor for the condition of imminent failure.

The triaxial tests already described show that the increase in shear strength caused by a confining pressure on a specimen with empty voids is almost entirely eliminated if the pressure fluid enters the voids. This shows by the above reasoning that almost the entire failure surface is in contact with the pressure fluid, or that the area factor is almost one hundred per cent.

McHenry's Experiments.

In 1948 at the Third International Congress on Large Dams, Stockholm, Sweden, Douglas McHenry described a series of tests carried out by the United States Bureau of Reclamation (U.S.B.R.) with a large triaxial testing machine.[28] These tests were identical in principle with Terzaghi's and the results were interpreted using the Mohr-Coulomb equation, assuming that the normal stress on the failure surface of an unjacketed specimen is diminished by an amount np, n being the area factor and p being the triaxial pressure.

The main difference between the two sets of tests is that Terzaghi deduced his result on the evidence of only a few measurements, whereas the U.S.B.R. experiments set out to measure the area factor or find its average value from a very large number of tests. There was also the technical

difference that whereas Terzaghi used water as the pressure fluid in all his tests, those conducted by McHenry used kerosene for the jacketed tests and nitrogen gas for the unjacketed ones. Nitrogen was used to reduce the delay which occurs in saturating the specimens when water is used. McHenry compares the respective saturation periods as about half an hour and several days. The choice of kerosene instead of water for the jacketed tests is not explained. Triaxial pressures up to 1,800 lb.per sq.in. (12.7 Kg.per sq.cm.) were employed.

The value of the area factor was determined for 337 different specimens. Values ranged from 0.78 to 1.18, the average being 1.02 with a standard deviation of 0.019. Thus a value very close to unity is indicated, confirming Terzaghi's opinion. In fact, this entire series of tests can almost be regarded as an experimental exercise to confirm Terzaghi's partly deductive conclusion, for no new principle is involved.

McHenry has pointed out that there are many possible sources of error in these tests. The specimens may not fail by pure shear, but by splitting vertically or by forming cones; the empirical values c and ϕ must vary to some extent among different specimens, and the Mohr-Coulomb equation is not strictly accurate particularly when the specimen does not fail in the desired manner. It was hoped that by carrying out a sufficiently large number of tests the effect of these sources of inaccuracy would be reduced: the fact that the scatter of results is approximately equal on either side of the average is cited as a reason for supposing that this has been achieved. It is also pointed out that the result depends to some extent on the criterion on which the statistical analysis of the test measurements is based, and that in this instance a different criterion leads to a value for n of slightly less than unity.

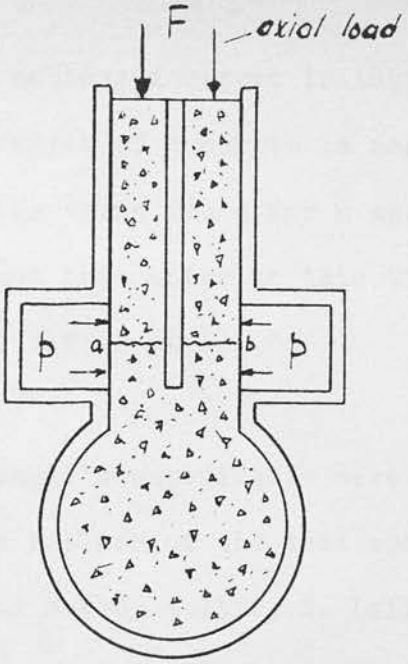

Figure 12

Leliavsky's test method

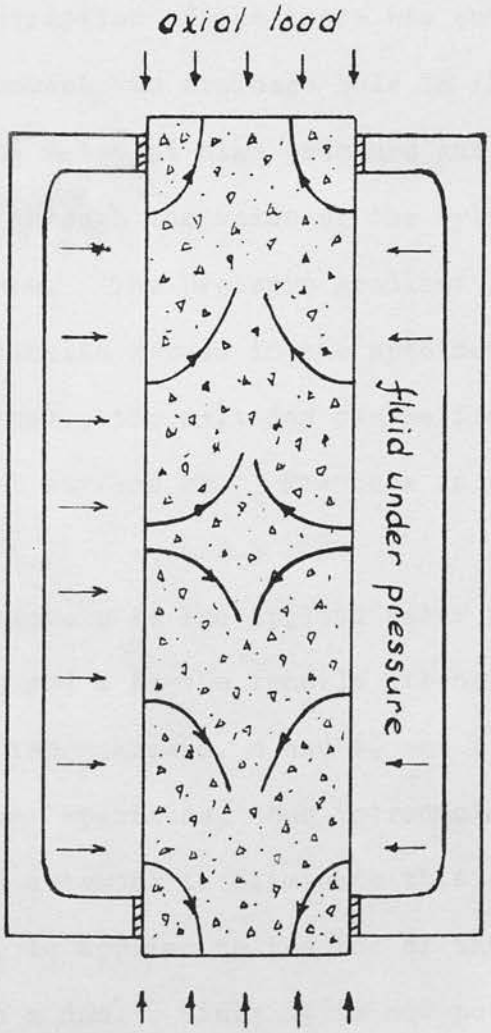

Figure 13

Serafim's test method

The main conclusion of McHenry's report is that the effect of pore pressure on the shearing strength of concrete is negligible. He draws attention to the fact that the value found for n applies to the condition immediately before failure and that prior to this time the value of the area factor might be "conceivably different".

Leliavsky's Experiments.

In the belief that Terzaghi's experiments were at variance with practical conditions because failure of the test specimens was caused by a mechanically applied load and not by uplift, S. Leliavsky devised a method in which the specimens were broken by the pressure of water in the voids. The part of the test apparatus enclosing the specimen is illustrated in Figure 12. A full description of the tests was published in 1947.[24]

Ignoring for the moment the drainage hole in the centre, it is possible, by introducing water at high pressure into the annular chamber, to cause an axial flow through the voids of the cylinder to the top which is open to the atmosphere. The pressure gradient in the direction of flow causes a longitudinal tensile stress in the specimen. By making the inlet pressure sufficiently great, the cylinder can be fractured across some approximately horizontal surface ab. Fracture is governed by the equation

$$n.A.p = z$$

where n is the area factor, p is the applied water pressure, assumed constant over the section, and z is the tensile strength of the specimen. This equation contains two unknowns, n and z, and z can only be estimated by tensile tests on other specimens, thus introducing a possibly large error.

Leliavsky's method attempts to eliminate this error in the following way. An axial load F_1 is applied to the top of the cylinder representing the vertical loading in a dam. Since it is not possible to ensure that

the applied pressure penetrates the full thickness of the concrete a central hole is made in which the pressure can be measured and in this way the pressure distribution across the cylinder can be controlled and calculated. In the tests the load F and the pressure p are applied gradually to minimise the pressure variation across the section.

The equation governing failure is now

$$n.A.p_1 = z + F_1$$

where p_1 is the average pressure across the section. By using a different value of F in a second test, the governing equation becomes

$$n.A.p_2 = z + F_2$$

assuming z to be constant. Eliminating z,

$$n = \frac{F_2 - F_1}{p_2A - p_1A} .$$

This can be done for a large number of tests so that

$$n = \frac{F_2 - F_1}{p_2A - p_1A} = \frac{F_3 - F_2}{p_3A - p_2A} \quad \text{etc.}$$

The effect of the variation in the value of z should diminish as the number of tests increases.

For a series of 95 tests the average value found for the area factor was 0.91 with a standard deviation of 0.041. These tests were divided into groups to investigate possible variations in the area factor with other physical parameters. From this latter investigation Leliavsky concludes that the area factor is independent of the stress in the material, the cement and water percentages in the mix, the temperature, rate of pressure increase, and the consecutive order of loadings and pressures applied.

Serafim's Experiments.

The desire to measure the area factor from tests not involving the

fracture of the test specimen led J. L. Serafim [34] to evolve a test method illustrated in Figure 13. A fluid under high pressure is made to flow through the test cylinder as shown, so causing an axial tension. To prevent rupture an axial compression is applied throughout the test. The area factor is calculated from the longitudinal extension of the cylinder.

By drawing a flow net Serafim has estimated that the pressure variation across sections AA, 1 cm. from the mid-section, is not more than 0.7 of one per cent. for a cylinder 5 cm. in diameter and 20 cm. in length; therefore reasonably accurate strain measurements can be made in this region. The best way to do this is to attach an electric strain gauge to the side of the cylinder, but owing to technical difficulties this could not be done when water was used as the pressure fluid. The tests were therefore done first with nitrogen gas. Further tests were done using water and measuring the total elongation of the cylinder by dial gauges placed at its extremities. With this latter method of measurement it is necessary to assume that plane transverse sections remain plane throughout the test, an assumption which is liable to error especially near the ends of the cylinder where the uneven distribution of pressure is likely to cause distortion. Thus an additional potential source of error is introduced.

A total of 103 different values was determined from the nitrogen tests and 146 from the water tests. Usually several observations were made over a period of time for each cylinder to investigate whether the area factor varied with time. The cylinders were divided into groups to investigate such variables as the age of the specimen, temperature of the pressure fluid, pressures and axial loads employed, and the method of drying in the tests with nitrogen.

The tests with nitrogen gave values for n ranging mainly between 0.80

and 1.00 with an average of 0.87. The tests with water gave values for n ranging mainly between 0.35 and 0.80 with an average of 0.43.

Serafim attributes the higher values with nitrogen to greater mobility of the nitrogen molecules when passing through dry specimens.* Most of the specimens used in the nitrogen tests were oven dried at 100°C. or 105°C. or dried under a vacuum with calcium chloride; both conditions would remove a certain amount of the adsorbed water retained from the original mixing. The specimens used in the water tests had naturally to be saturated before testing if steady flow conditions were to be achieved, so that immobile films of adsorbed water would exist within them to a greater extent than in the dried specimens. According to Serafim many pores are isolated except for minute channels whose dimensions are of the same order of magnitude as water molecules. In saturated specimens the adsorbed water in these channels would cut off the otherwise isolated pores from the pressure applied by the free water, thereby reducing the surface area available to pore pressure and consequently reducing the value of the area factor.

Serafim observed from his tests with nitrogen that the area factor increases slightly with the water-cement ratio, the value of the pore pressure and the degree of dryness of the samples. In the tests with water the lower values of the area factor were associated with lower water-cement ratios. No consistent relation was observed between the area factor and the time of testing.

Harza's Theory.

L. F. Harza has produced a simple theory which attempts to show that the area factor is exactly 100%. This theory is based on a conception

*See reference 34, Pages 207 to 208.

Figure 14

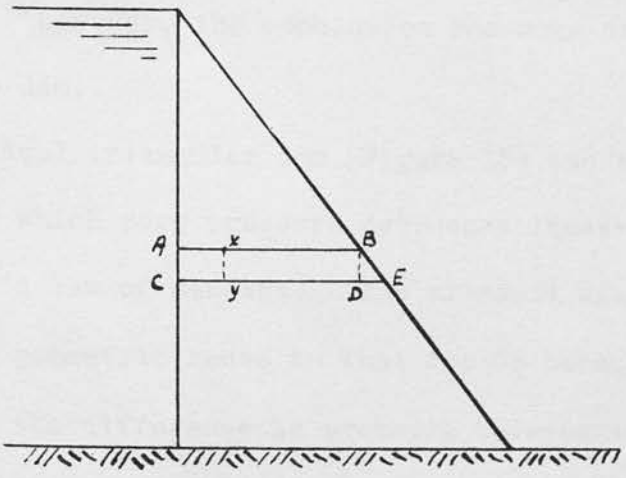

Figure 15

which he calls "internal buoyancy".[15]

Consider a block of saturated concrete immersed in water for sufficient time to allow the pressure distribution in the pores to adjust itself to a steady state. Provided all the pores are interconnected the pressure in each pore will be dependent only on its depth from the free water surface. Imagine the concrete divided into a number of elementary vertical prisms such as a-b in Figure 14, each terminated by a pore or pores. Each prism will experience an upthrust because of the difference in pressure between the pores at its extremities, and this upthrust is the same as it would experience if it could be immersed to the same depth in water. In other words the prism within the main block experiences an upthrust equal to full buoyancy. This is what Harza calls "internal buoyancy". Because all the imaginary elements of the block are fully buoyant the block itself must be fully buoyant, a conclusion which is perfectly obvious from the mere fact that it is immersed. However, the conclusion has some significance when applied to a concrete dam.

Consider in an ideal triangular dam (Figure 15) two adjacent flow lines AB and CE along which pore pressure decreases linearly, flow being assumed to obey Darcy's law of seepage. The pressure diagram for AB is similar in the strict geometric sense to that for CE because of the shape of the dam; therefore the difference in pressure between any two points x and y in the same vertical plane is the same whatever their distance from the upstream face. If x and y denote the extremities of an elementary prism then since the pressure difference between x and y is the same as that between A and C, the prism xy is fully buoyant. If pairs of flow lines such as AB and CE are taken very close together, areas such as BDE can be neglected, and the argument can be applied to the entire dam so that it

experiences internal buoyancy just as did the immersed block; that is, the dam experiences an upthrust equal to full buoyancy even though there is water only on one side of it. This is precisely the same result as if pore pressure acted over 100% of the area of a horizontal section, which is equivalent to an area factor of 100%.

The theory applies equally well to the horizontal thrust. If the cylinder in Figure 14 were encased in a horizontal tube and water under pressure applied to one end, assuming still that flow obeys Darcy's law of seepage, a uniform pressure gradient would extend from the pressure end to the outlet end. The elementary prisms which are now horizontal experience a thrust in the direction of flow because of the difference in pressure at their extremities. The total thrust, which is the integral of the body forces on each element, is equal to the applied pressure multiplied by the cross-sectional area of the cylinder. This again is equivalent to an area factor of 100%.

Discussion of Evidence.

All the foregoing experimental evidence is in agreement on at least one point, namely that the area factor is a distinctly different quantity from the sectional porosity and is much greater in magnitude. The experimental value of the area factor has varied between 0.40 and 1.00 depending on the testing method used.

The two sets of tests by Terzaghi and McHenry involving the shear failure of specimens have arrived at the same conclusion that the area factor is very nearly unity. Whatever objections may be raised to the test method because it involves fracture, the result is an important one. Throughout the literature which has been studied in the preparation of this dissertation, no instance has been cited where a gravity dam has failed by

overturning. In all cases where failure has been attributed to uplift, the dam has failed by shear across a section near the base: therefore in considering critical conditions at least, the tests of Terzaghi and McHenry may be of more value than the allegedly better methods of Leliavsky and Serafim.

Terzaghi's papers have probably been the most valuable contribution towards the solution of the problem for they provide a very plausible explanation of a high value of the area factor by showing how it is related to the structure of concrete. The fact that concrete is only statistically homogeneous and isotropic is most important in the study of pore pressure phenomena, and the earlier confusion between area factor and sectional porosity arose because this fact was ignored. However, Terzaghi's tests with jacketed and unjacketed concrete cylinders have demonstrated beyond doubt the importance of the intergranular bonds which are mainly responsible for the deformation of the material, not necessarily because they are more elastic than the mineral grains but because, owing to their relatively small cross-sectional area, the stresses accuring in them are very high. Concrete or any natural rock of similar structure can therefore be regarded as a skeleton structure comprising two types of components; (i) grains which are comparatively rigid and which maintain their shape under stresses of the order usually encountered in a dam, and (ii) intergranular bonds in which the stresses are so high that they deform under similar applied loads.

The cross-sectional area of these bonds must be very small indeed if pore pressure has access to almost the entire failure surface, but there is evidence to show that this is quite possible. It is now known from crystallographic research that the bonding material in hydrated cement is composed of needle-shaped fibres whose thickness may be as small as 50 $\mathring{A}$.

Photographs of cement paste taken with an electron microscope have shown the paste to be a mass of jagged irregular fragments joined together by minute contacts of a much smaller magnitude than the voids or solids which make up the bulk of the paste. (These photographs were taken by Professor N. Hast of the Stockholm Institute of Technology and one was shown at the Third International Congress on Large Dams, 1948).[31] The high strength that such fine bonds would require to possess can be credited by comparing them with finely drawn glass threads which have shown tensile strengths exceeding 100,000 lb.per sq.in. Their strength has been found to increase with decreasing area of cross-section, possibly because of the elimination of transverse flaws in the drawing process. It is not inconceivable that naturally grown fibre crystals would possess even greater strength.

Leliavsky's tests gave a mean value of 0.91 which is not substantially different from Terzaghi's result. In view of the fact that completely different methods were used, the results of the two experimenters are remarkably similar, and tend to support a value close to unity.

Leliavsky's lower values may perhaps be attributed to the lower pressures used, (18 kg.per sq.cm. compared with 200 Kg.per sq.cm. in Terzaghi's triaxial tests) and possibly to conditions caused by seepage; e.g. sedimentation within the concrete or the introduction of air molecules with the seeping water. If this is the case, Leliavsky's results are more representative of practical conditions than those of Terzaghi, but there is not sufficient difference to warrant the use of a factor lower than unity for design purposes.

Serafim's test method is probably the best so far used because it does not involve rupture of the test specimen. It is significant that his value for n, using water as the pressure fluid, is substantially different

from the results of all previous experimenters whose tests involve rupture, but his results are not conclusive in themselves. They represent a basic change in the present conception of the area factor and require verification by further experimental work. There is considerable scatter in the results; e.g., although the average value for n in the tests with water was 0.43, one group of five results ranged from 0.78 to 0.87 with an average of 0.82. The water-cement ratio was higher for this group than for any other, indicating a more permeable concrete and suggesting a possible relation between permeability and the area factor.

The difference between Serafim's results with water and nitrogen as the pressure fluids also requires further investigation, for no such difference occurred between the results of Terzaghi and McHenry using respectively water and nitrogen. This is a good reason for suspecting that different conditions exist before and coincidently with rupture.

Serafim himself cannot have been completely satisfied with his tests for in his concluding paragraph he states that for the present it would be prudent to employ an area factor of unity in dam design until further experimental evidence is available from tests similar to his own.* These tests might aim at more accurate measurement, greater consistency in the results, and a complete investigation of such factors as the water-cement ratio, the adsorbed water content, the applied pressure and the applied axial load. Serafim's test method is technically much more difficult than any of the previous methods because of the necessity for measuring strains; but because it apparently creates the most realistic conditions, and because of the disparity between Serafim's results and those obtained by other

*See reference 34, Page 214.

methods, there is every indication that much could be learned by developing and refining this new method.

There is no contradiction between Terzaghi's conclusion that the failure surface passes almost entirely through voids but not completely, and Harza's theory that the area factor is exactly unity. They are two different ways of looking at the problem. The fact that Terzaghi's failure surface does not pass completely through voids implies that some solid must have been intersected or the surface would have had no strength. Harza's theory of a 100% area factor does not imply, as some critics have suggested, a surface of no strength. It does not in fact necessarily involve any surface whatever, neither does it involve rupture. The conception of internal buoyancy merely requires full saturation and freedom of the water molecules to exert pressure in the minutest interstices of the concrete. The unlikelihood of such conditions ever being fully achieved in practice makes it improbable that Harza's theory could ever be fully realised.

Terzaghi must have been very close to such a condition in his tests on cylinders with only water pressure acting. (See page 29). Unfortunately his measuring gauge was not sufficiently sensitive to measure the deformation of the unjacketed cylinder, but an area factor exceeding 0.995 was indicated. However, the test conditions were especially favourable. A pressure of 400 Kg.per sq.cm. was used corresponding to a 13,000 feet head of water, 18 times the possible maximum pressure at the base of the Hoover dam, which is the highest gravity dam in the world. The method used to saturate the specimens initially is not mentioned in the paper, but in his second paper Terzaghi advocates that the cylinders for unjacketed triaxial tests should be saturated under vacuum, then subjected to a high

liquid pressure for several days. If any air is trapped inside the specimen it will gradually contract and a pressure decrease will be noted. Presumably this method was applied in his tests.

Under such favourable conditions it seems very likely that water would find access to regions of the concrete from which it would ordinarily be excluded, and so a higher value of the area factor would prevail than under the normal conditions encountered in practice where the water pressure is much lower and the presence of trapped air much more likely.

The discrepancy between Harza's theory and the true value of the area factor is the same as the discrepancy between his ideal conditions of saturation and the true conditions, much of this being due to the presence of adsorbed water and submicroscopic channels not considered by Harza.

Conclusions.

1. Concrete is a complex skeleton structure consisting of mineral grains and intergranular bonds among which exists a network of voids. The deformation of concrete under stress is mainly due to the deformation of the bonds which, because of their small cross-sectional area, carry much higher stresses than the mineral grains. The voids within the concrete are continuous, although the continuity may often be through channels whose diameters are of the same order of magnitude as water molecules. For this reason some of the voids may be permanently isolated because of the presence of immobile films of adsorbed water in the smallest channels.

2. When a pressure gradient exists within a saturated concrete body, the body experiences a force in the direction of the pressure gradient because of the differential pressure on the sides of the elements of the body, these elements being the mineral grains and intergranular bonds. This body force is comparable to the buoyancy experienced by a submerged granular

material owing to the upthrust on the individual grains. In concrete this buoyancy is less active than in a loose granular material because of the nature of the voids, some of which are isolated or blocked by adsorbed water.

3. The value of the area factor depends on the extent to which the buoyancy effect is reduced by the existence of blocked or isolated channels, created either by adsorbed water or trapped air. This reduction is dependent entirely on physical conditions such as the degree of saturation, the pore pressure, the constituents of the concrete which affect its porosity, and the degree of crystallisation in the bonding material which influences the extent to which submicroscopic channels exist. The area factor is therefore an empirical property of the concrete which is liable to variation according to the above conditions.

4. The effect of these aforementioned conditions cannot be fully understood until research has constructed a full picture of the internal structure of concrete which should include an explanation of the influence of the adsorbed water molecules. If such an understanding can be reached it will then be possible to set about measuring the area factor in a manner such as that used by Serafim, with a proper understanding of the variables involved. Any attempt to measure the area factor before this has been done might produce valuable data in the form of empirical relations between the area factor and the several variables involved. This may assist the designer by providing a more economic value of the area factor which is safe to use, but it will not by itself lead to a complete understanding of the effect of pore pressure in concrete. This can only be done with the help of the physicist by investigation along lines already begun, using crystallographic or other methods. [1, 2]

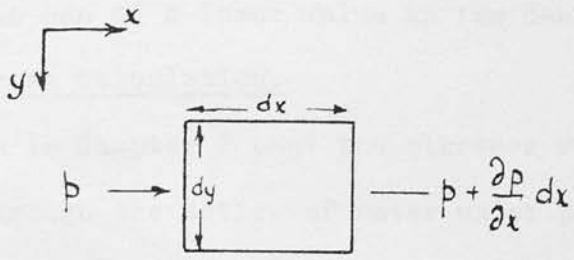

Figure 16

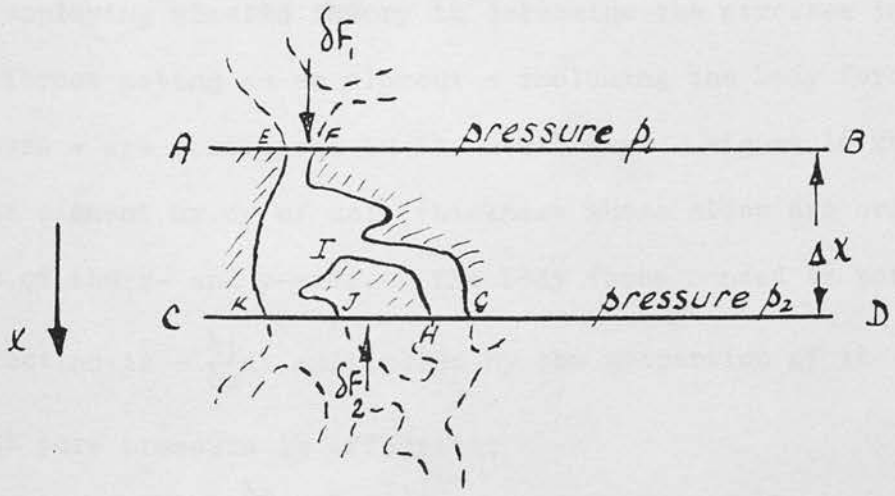

Figure 17

5. The most recent experimental evidence provided by Serafim indicates that the area factor may have a value substantially less than unity, but there is not yet sufficient evidence or sufficient knowledge of the factors involved to warrant the use of a lower value in the design of dams.

The Area Factor in Stress Calculation.

It has been shown in Chapter 2 that the stresses occurring in a porous body such as a dam, through the action of water under pressure applied at its boundaries, arise not from a thrust at the boundary but from a body force applied in the direction of the pressure gradient once water has permeated the voids. The stresses in such a body are generally calculated on the assumption that the material is homogeneous, an assumption which is not strictly correct because of the presence of voids; but provided it is remembered that the stresses found in this manner are average stresses over plane sections and not the actual stresses in the solid particles, no error is incurred.

When employing elastic theory to determine the stresses in a porous body, the forces acting on an element - including the body forces caused by pore pressure - are considered in the usual way. Figure 16 represents a rectangular element dx.dy of unit thickness whose sides are oriented in the directions of the x- and y-axes. The body force caused by pore pressure in the x-direction is $-\frac{\partial p}{\partial x}dx$ multiplied by the proportion of the area of face dy on which pore pressure is effective;

i.e. body force $= -n.\frac{\partial p}{\partial x}dx.dy$, by the definition of the area factor,

$= -n.\frac{\partial p}{\partial x}$ per unit volume.

By the same reasoning the body force in the direction of the y-axis is $-n.\frac{\partial p}{\partial y}$ per unit volume, or in general the body force per unit volume is

-n. grad p.

A recent paper dealing with stress calculation for porous bodies shows that there is still confusion in the minds of writers between the area factor and the sectional porosity. This confusion leads the author of the paper, A. Lubinski, to the conclusion that the body force is equal to -f. grad p where f is not the area factor but the sectional or volumetric porosity. Lubinski arrived at this conclusion by considering the forces acting in the pore EFGHIJKE of Figure 17 which is reproduced from his paper.[27] The bounding surfaces AB and CD are surfaces of equal pressure, and assuming that Δx is small, AB and CD are parallel. p_1 and p_2 designate the pressures at AB and CD and $p_1 > p_2$ so that the fluid flows in the direction of CD.

The forces acting on the fluid in the pore are:

1. The forces dF_1 and dF_2 caused by pressures p_1 and p_2 on faces EF and KG respectively,
2. A viscous or frictional force dF_s acting along the walls of the pore by which the pressure transmits a body force to the solid.

Since dF_1 and dF_2 are perpendicular to the constant pressure lines AB and CD, then so also must be dF_s, and for equilibrium of the element of fluid in the pore

$$dF_1 - dF_2 + dF_s = 0$$

If da_1 and da_2 designate the cross-sectional areas of the pore at AB and CD, then,

$$dF_1 = p_1\, da_1 \quad ; \quad dF_2 = p_2\, da_2 .$$

If AB and CD are taken over an area which is large compared with the area

of the pore, then $da_1 = da_2 = fa$ where f is the sectional porosity and a is the total area of the section. If F_s denotes the sum of the viscous forces between AB and CD, and $\Delta p = p_1 - p_2$, then

$$- a f \Delta p = F_s$$

or dividing by $a \Delta x$

$$\frac{F_s}{a \Delta x} = - f \frac{\Delta p}{\Delta x}$$

or in the limit,

$$N = - f \frac{\delta p}{\delta x}$$

where N is the body force per unit volume,

There is no flaw in Lubinski's reasoning after accepting the set-up illustrated in his diagram; it is in the diagram itself that the error is made because the element of the body envisaged by Lubinski is not characteristic of the material it is meant to represent.

Terzaghi showed in a convincing manner how the results of triaxial tests on jacketed and unjacketed specimens of concrete demonstrated the importance of the intergranular bonds. (See Page 32). There is in fact no other explanation of the observed increase in shear strength when the specimen is jacketed, and the absence of any such increase when it is not. In such a medium where the bonds deform and the grains are mainly passengers occupying space, a characteristic element must have similar elastic properties to the material as a whole, and therefore its sides must in general intersect bonds rather than grains. In this case the sides of the element will not be strictly straight lines, but will undulate around the grains, so that they intersect an area for greater than the sectional porosity of the material. This area, expressed as a proportion of the

total cross-sectional area, is the quantity termed the area factor. The various experimenters who have attempted to measure this quantity have at least proved that it is much greater than the sectional porosity.

Chapter 5

STRUCTURAL FEATURES AFFECTING SEEPAGE AND UPLIFT

Experience has shown that it is not possible to exclude water entirely from the interior of a dam or its foundation. Even the richest mixes of concrete exhibit permeability under high pressures of water and some degree of seepage into a rock foundation is inevitable. There are, however, various methods by which seepage can be considerably reduced or at least rendered less harmful.

A small rate of seepage through a dam or its foundation does not necessarily indicate low uplift pressures. In fact high uplift pressures could exist with no seepage whatever if water were trapped within the dam and connected through fissures or pores with the reservoir. The purpose of the "anti-seepage" devices is partly to prevent or reduce the initial development of uplift and partly to protect the structure from the erosive effects of seeping water. In some cases measures need to be taken to reduce seepage because it represents a serious loss of water, but such a condition will only arise with an unsound structure.

Grouting.

It is almost universal practice to inject grout into a rock foundation whenever possible. This both strengthens the foundation and reduces seepage. The only conditions which make grouting unfeasable are (i) where the rock fissures are too narrow to allow the penetration of grout or (ii) where the rock is soft and fissuring so extensive that the fissures cannot be filled and tightened. Both conditions are unfavourable but more so the

latter. One of the most catastrophic failures, that of the St. Francis Dam (California, U.S.A. 1928), was caused by a soft foundation which was not properly tightened, and a soluble content in the rock. Excessive uplift pressures developed soon after the first filling of the reservoir and central sections of the dam over 200 feet high slid from their foundations because of the reduced horizontal shear resistance and the lubricating effect of the water.

Where the rock fissures are too narrow to be grouted there is still the danger of high uplift pressures, for water can penetrate into much smaller openings than grout. If a structure must be built on such a foundation, adequate base width must be provided to ensure stability and efficient drainage would be a great advantage.

Most foundations can be effectively grouted, the above conditions being exceptional. Grouting operations take two forms. First, before construction begins, "blanket" grouting is carried out over the entire foundation area to a depth of 5% to 10% of the base width of the dam.

The purpose of this is to reduce seepage and to strengthen the foundation structurally. Several rows of grout holes, $1\frac{1}{2}$" or 2" in diameter, are drilled parallel to the longitudinal axis of the dam. The spacing between holes and between rows is generally of the order of 20 feet centre to centre, with extra holes in weak zones.

The second form of grouting consists of deep grouting below the upstream side of the dam to form an imprevious barrier or "curtain" to seeping water. In some cases this is also done before construction begins but in many large dams it has been done from construction galleries within the structure after the lower blocks of the dam have been laid. It is naturally preferable to have such a gallery within a dam, large enough to

accommodate drilling and grouting operations. There is then no difficulty in repairing or extending the grout curtain if necessary. A further advantage of grouting after the foundation blocks have been placed is that higher grouting pressure can be used with less danger of dislodging the rock formation. The grout curtain may be laid from one or two rows of grout holes spaced as closely together as 5 feet centre to centre. The depth of the grout curtain has varied considerably as practices have changed, but it is not generally greater than 25% of the height of the dam. For the exceptionally high Hoover Dam, the grout curtain was extended to a depth of 41% of the height of the dam.

At one time it was the practice to provide a cut-off at the downstream end of the structure either as an alternative or in addition to the cut-off at the upstream end. The purpose of this was to reduce seepage by lengthening the seepage path. This device is no longer used because it tends to increase uplift pressures, particularly in the downstream region of the base of the dam. Modern practice is to provide pressure relief points immediately downstream from the grout curtain and to drain away water which succeeds in seeping through.

Drainage.

In many of the large dams now existing, a system of drainholes or a "drainage curtain" is situated a short distance behind the grout curtain at the upstream end of the dam. A typical system consists of holes 6 inches in diameter spaced at 10 feet centre to centre and extending to one third of the depth of the grout curtain. The drainholes are generally connected with a larger drain or gallery running the entire length of the dam from which the water collected is discharged through further drains to the downstream side.

Much cruder forms of drainage are sometimes employed such as gravel-filled trenches crossing the foundation. Probably the earliest such attempt at drainage was in the Vyrnwy Dam of the Liverpool water system in 1882, where a complete system of rock drains was installed.

Uplift measuring systems have frequently proved the efficiency of drainage but nevertheless it is not universally favoured. At the Third International Congress on Large Dams, Stockholm, 1948, delegates from India[20] and Sweden[31] told of the difficulties experienced in their countries with drainage in dam foundations. It was found that drains were difficult to clean and their functioning could not be relied upon when making uplift assumptions. Indeed, the practice of foundation drainage has now been completely abandoned in Sweden. It is considered that even when the drain is functioning properly the resulting increase in the volume and velocity of seepage is highly detrimental to the grout curtain.

In the U.S.A. where many large dams have been built in the last few decades, the attitude towards drainage is quite different. Nearly all large projects have an extensive system of drainholes leading into a transverse gallery within the dam. These drains run vertically into the foundation in the centre sections of the dam and fan outwards at the abutments. Drainage difficulties, such as choked drains, have either not been encountered or have been overcome in many cases by suitable design. The chief causes of choking drains appear to be (i) the deposition in the drainholes of solid matter carried by the seeping water, (ii) solids carried by the seeping water may be deposited within the concrete near the surface of the hole because of the drop in pressure in approaching the drain, (iii) the evaporation of water containing dissolved salts so leaving a coating of lime or other compound on the surface of the hole, (iv) bad

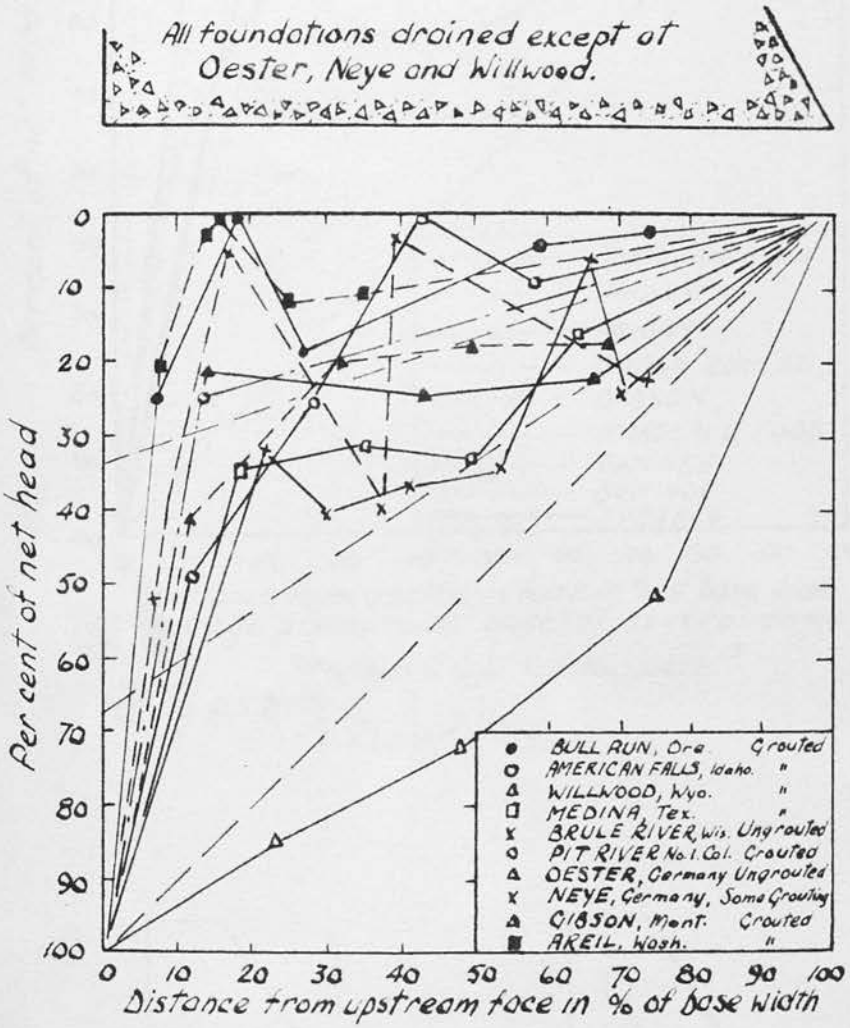

Max. pressures under dams on rock foundations [18]

Figure 18

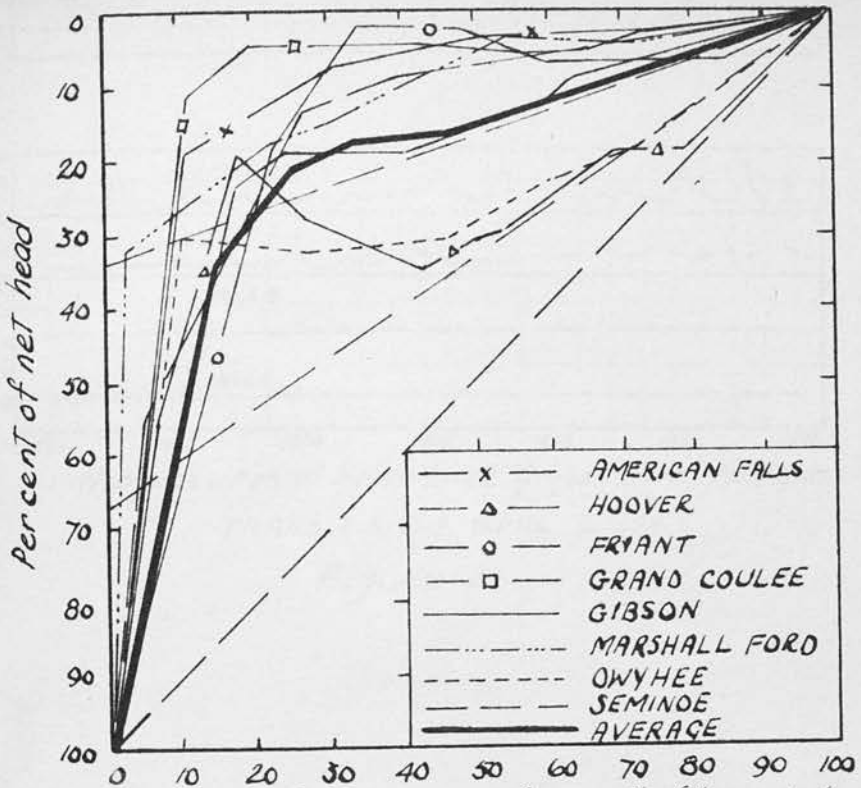

Distance from upstream face in % of base width
Average pressure of base of several dams
TRANS. A.S.C.E. Vol. 116, p. 1228.[19]

Figure 19

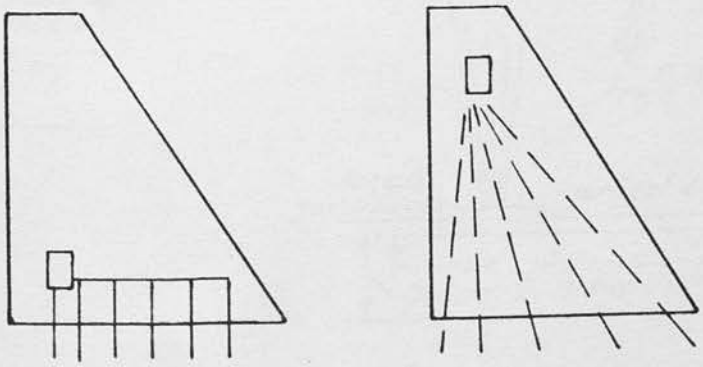

Uplift measuring pipes

Figure 20

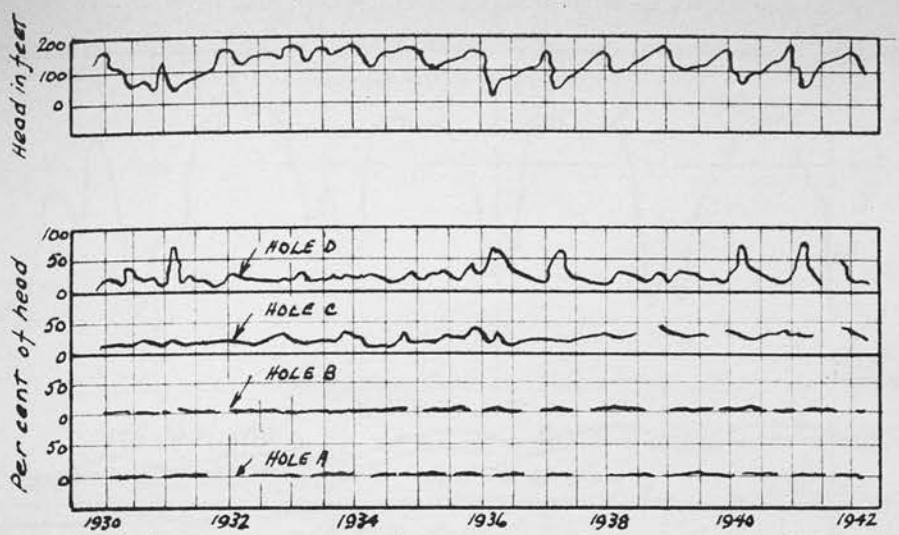

Uplift pressures at base: line 2 Gibson Dam, Montana

TRANS. A.S.C.E. Vol. 116, p. 1224 [19]

Figure 21

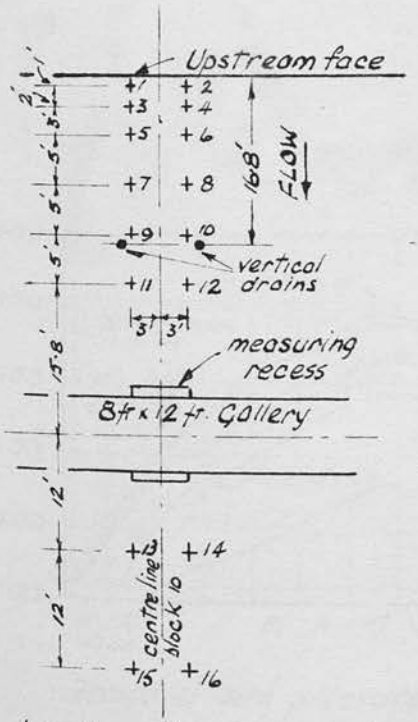

Location of pressure cells
Hiwassee Dam
TRANS. A.S.C.E. Vol. 116, p1039 [19]

Figure 22

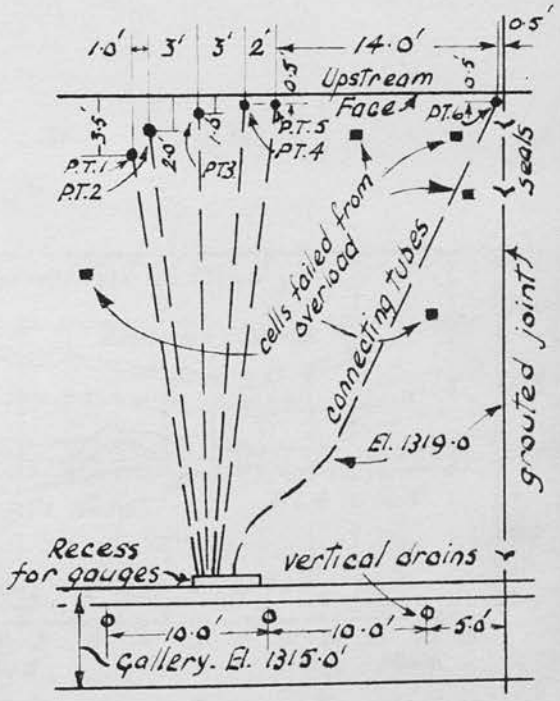

Location of piezometric tips
Fontana Dam.
TRANS. A.S.C.E. Vol. 116, p1241. [19]

Figure 24

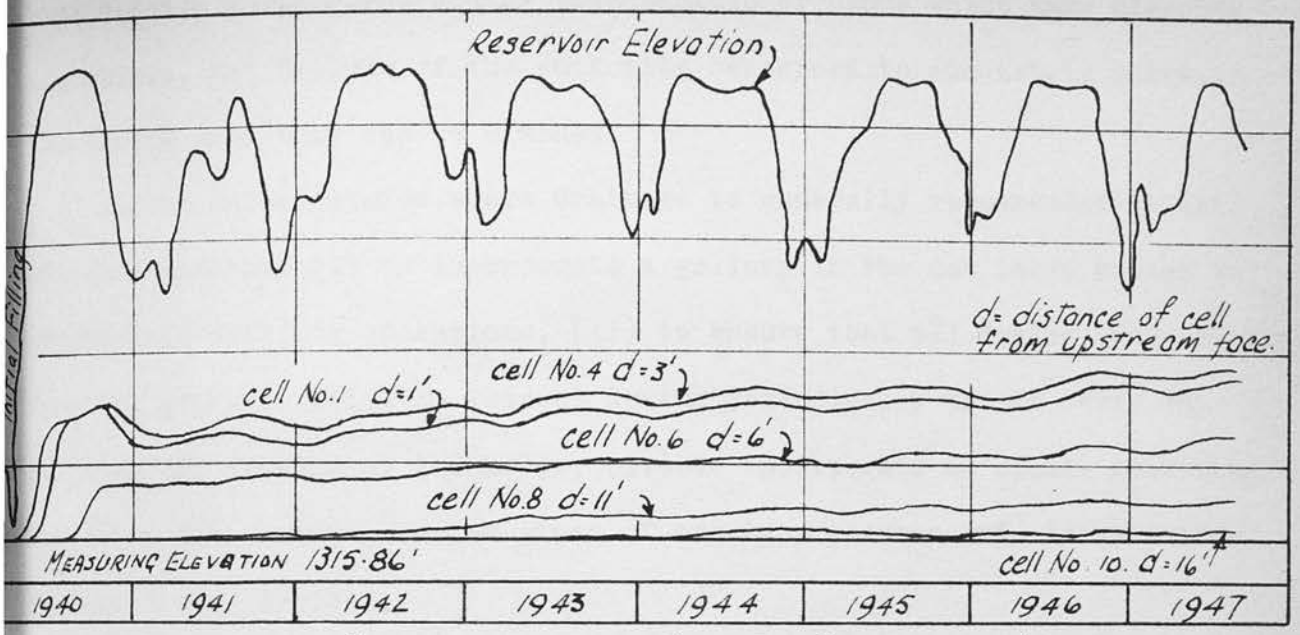

Pore pressure at Hiwassee Dam, N. Carolina

Figure 23

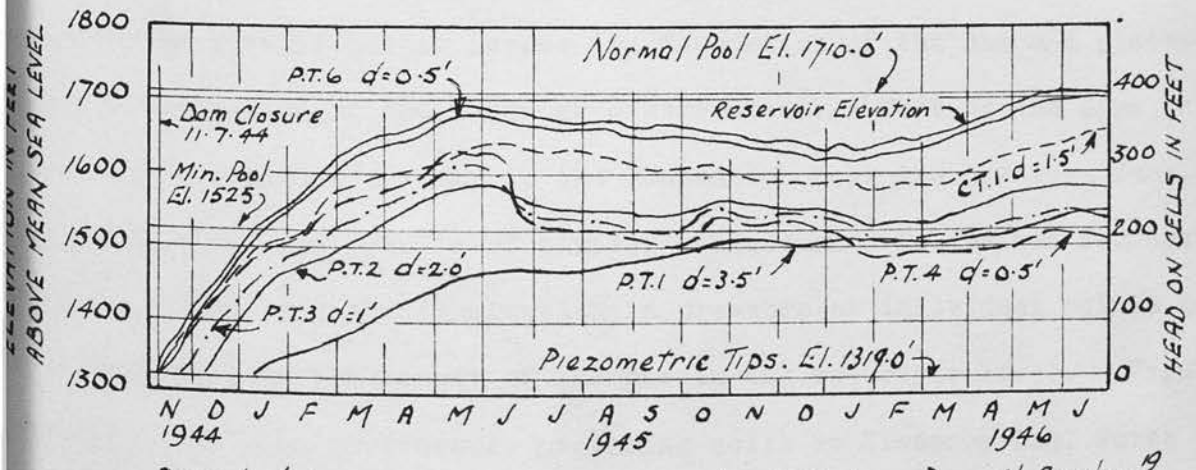

Record of pore pressure measurements at Fontana Dam, N. Carolina[19]

Figure 25

construction which makes drains inaccessible or bends which make cleaning impossible, (v) failure of the authority concerned to adequately maintain the drains when they can be cleaned.

In the United States where drainage is generally recommended it is standard practice (i) to incorporate a gallery in the dam large enough to accommodate drilling operations, (ii) to ensure that all drains run straight from the gallery, (iii) to inspect drains periodically and to carry out scraping and reaming of the holes, (iv) to incorporate an uplift measuring system so that warning can be given of excess pressures and, if necessary, further drains drilled.

Evidence shows that with effective grouting and drainage of a foundation, pressure drops rapidly from the upstream face to the drainage line, and that in normal conditions high pressures are not likely to develop downstream of the drains. Figure 18 shows some of the first published data and is typical of the results subsequently obtained in the same manner at many other dams. Using pipe systems as shown in Figure 20 uplift has been measured at several points across the foundation of the dam and plotted to give an indication of the pressure distribution. Most of the dams represented have drainage systems in the foundation near the upstream face. Figure 19 shows the results of similar measurements in drained foundations. Figure 21 indicates the fluctuation in pressure at individual points in a dam foundation as the result of changes in the reservoir level. Figure 22 indicates the plan of pressure measuring cells at Hiwassee Dam, North Carolina, and the results in Figure 23 show a decided drop in pressure from the upstream face to the drains. No appreciable pressure has been measured downstream from the drains up to the time of publication of these results, seven years after the initial filling of the reservoir.

Similar measurements carried out at Fontana Dam,

North Carolina, (Figures 24 and 25) again show the effect of drainage. The pressures recorded are a much higher proportion of the static head then at Hiwassee indicating a more permeable concrete, but the drop again is quite distinct.

Grouting and Drainage as Remedial Measures.

It is sometimes the case that uplift pressure beneath and within a structure develops in excess of that assumed for design purposes and so endangers the stability of the dam. Warning of such a condition would be given by an uplift measuring system but in the absence of this various other indications might be given e.g., excessive discharge from drains, visible seepage through the structure or foundation, or possibly in an old dam, the realisation in the light of up-to-date knowledge that the original uplift provisions were inadequate. Whatever the warning might be, such a condition demands immediate investigation and a remedy must be provided.

If uplift pressures are found to be truly dangerous the reservoir surface can be lowered as an immediate measure while contemplating further action. This, however, may waste valuable storage water and it is unlikely that a condition sufficiently grave to warrant this measure would develop without previous warning. In some instances (as described in the following section) it has been felt necessary to empty the reservoir and build a protective screen in front of the dam. No case, however, is known to the writer where this has been done for a dam much more than 100 feet in height. For a very large dam the cost of such a screen would be very great.

The most usual method for reducing uplift pressures is to tighten the grout curtain by additional grouting and provide additional drainage. To illustrate the use and effectiveness of such methods two outstanding

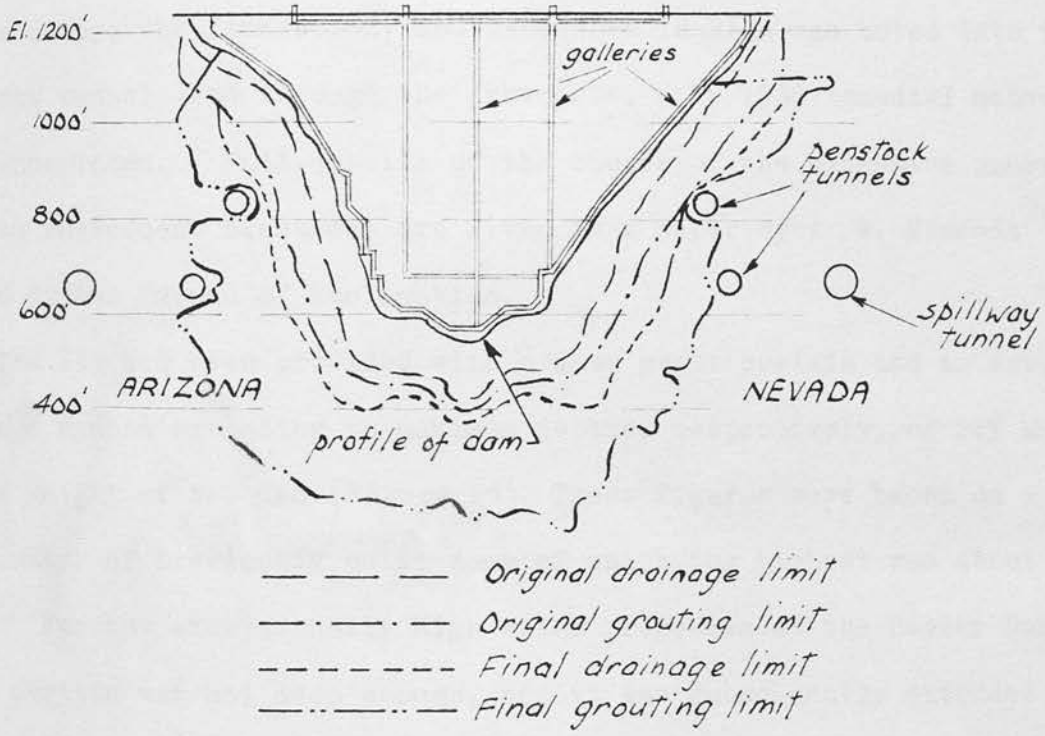

Grouting and drainage at Hoover Dam
(compiled from figures 2, 3, 9 and 12, Ref. 19)

Figure 26

examples will be discussed.

The first is the famous Hoover Dam (previously called the Boulder Dam) on the Colorado River in the U.S.A. The dam, the highest gravity structure in the world, (726 feet maximum height above foundation) was completed in 1934. During the following five years while the reservoir was filling, high pressures were recorded by the uplift measuring system at various points across the foundation, and excessive leakage was noted into the penstock tunnels and through the abutments. In 1939 remedial measures were undertaken. Full details of the causes of the excessive pressures and the subsequent treatment are given in a paper by A. W. Simonds[36] of the United States Bureau of Reclamation.

The dam had been provided with a deep grout curtain and an extensive drainage system extending to maximum depths, respectively, of 21% and 14% of the height of the dam (Figure 26). These figures were based on a survey of a number of previously built dams of which the highest was about 400 feet. For the exceptionally high water pressures at the Hoover Dam this grout curtain was not deep enough, and it was subsequently extended to 41% of the height of the dam.

Besides the high head of water, the high uplift pressures were partly attributed to the presence of warm alkaline springs in the foundation beneath the structure. The initial grouting treatment had not sealed these springs effectively for, as it was subsequently found, a flash set occurred when the Portland cement grout came in contact with the warm alkaline water. Whether this was due to the heat or to the alkalinity was never clearly established. To deal with the problem a suitable cement containing a retarder was eventually found, which had been developed for use in oil mining.

The leakage of reservoir water at the abutments and penstocks, and to some extent the uplift pressures, were caused by the necessity for abandoning some of the original curtain grouting. A special rock-concrete joint had been provided at the abutments, which was left open prior to filling the reservoir to allow for the free deflection of the dam under load. A system of grout holes had been made to grout up the joint at a future date. However, some of the grout from the grout curtain was found to leak into the abutment joint, and so grouting in this area was abandoned rather than foul the grouting system for the joint.

The remedial grouting was effected by using the drainholes of the original drainage system as grout holes, and a new drainage line was made. The grouting and drainage operations had to be carried out simultaneously and great care taken that the uplift pressures were not substantially increased by the closing of drainholes. This generally meant that only a few holes could be treated at one time, and since many holes took several thousand bags of cement the process was a very slow one. It was, however, effective and successful. Uplift pressures dropped to tolerable magnitudes, leakage in the abutments and penstocks was substantially reduced, inspection galleries became dry, and drains showed greatly reduced discharges.

The maintenance of the penstocks was a major item of expenditure before the remedial measures were carried out and the following figures testify to their effectiveness;

Year	1939	1946
Repainting of Penstocks	$29,979	$5,894
Pumping from Penstocks	$11,270	$5,861

A further reduction is reported since 1946.

The total cost of grouting and drainage operations at Hoover Dam was

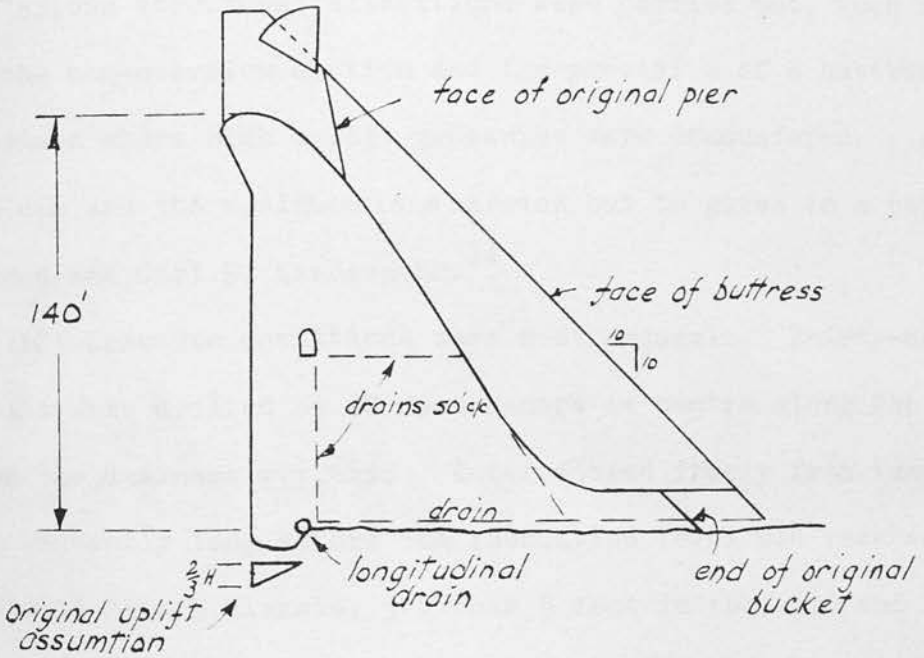

Bartlett's Ferry Dam

Figure 27

$1,840,000 or 2.3% of the total cost of the dam.

The second outstanding example of remedial work is the Bartlett's Ferry Dam on the Chattahoochee River, Georgia, U.S.A., built in 1925. An investigation into the stability of the dam was prompted in 1946 when certain maximum flood and rainfall data became available for the first time. The low uplift design assumption (see Figure 27) must also have caused anxiety. Various structural alterations were carried out, such as the raising of the non-overflow section and the provision of a buttress for the spillway section where high uplift pressures were encountered. A description of the dam and the modifications carried out is given in a paper by E. S. Harrison and Carl E. Kindsvater.[14]

The uplift pressure conditions were most unusual. Thirty-one 3 inches diameter holes were drilled at 20 feet centre to centre along the spillway section from the drainage gallery. Water flowed freely from twenty-six of these holes generally long before the foundation level was reached. From one hole a solid 3-inch diameter jet rose 5 feet in the air, and sixteen other holes produced spouting flows, the total estimated flow from all holes being 3,400 gallons per minute.

High pressure grouting was used to seal the holes and, as was the case at the Hoover Dam, a considerable amount of cement was used. The holes were then redrilled and carried down into the bedrock. Greatly improved conditions were revealed, none of the holes showing excessive leakage. The pressures at the foundation were measured by sounding in the holes. Only one showed a pressure exceeding half of full headwater and five had pressures exceeding one third of full headwater.

It is interesting that in this dam the main discharge of water came from within the concrete rather than from the foundations which was gener-

ally only reached at the second drilling.

Table II taken from the aforementioned paper by A. W. Simonds,[36] gives an interesting comparison of the cost of grouting and drainage operations at various dams in the U.S.A. It is noteworthy that only in one case does the cost of these extremely important operations exceed 2½% of the total cost of the main structure.

TABLE II
COST IN DOLLARS OF FOUNDATION GROUTING AND DRAINAGE OF CONCRETE DAMS CONSTRUCTED BY THE UNITED STATES BUREAU OF RECLAMATION BETWEEN 1927 AND 1947

Dam and State	Total cost of dam ($)	Volume of concrete Cubic Yards	Foundation grouting and drainage		Date of cost report
			Cost ($)	% of total	
Gibson, Montana	2,388,000	161,173	29,000	1.21	April, 1931
Deadwood, Idaho	1,359,000	55,463	13,000	0.96	June, 1931
Owyhee, Oregon	6,728,000	488,113	334,000	4.97	May, 1938
Seminoe, Wyoming	7,083,000	173,127	138,000	1.95	Aug., 1941
Parker, Ariz.-Nev.	4,695,000	290,640	48,000	1.03	Nov., 1942
Grand Coulee, Wash.	112,990,000	10,181,742	1,460,000	1.29	Dec., 1942
Marshall Ford, Tex.	23,395,000	1,838,167	572,000	2.46	May, 1947
Shasta, California	74,567,000	6,353,227	676,000	0.91	May, 1947
Hoover, Ariz.-Nev.	77,549,000	3,251,137	1,840,000	2.38	July, 1947
Friant, California	18,636,000	2,030,736	267,000	1.43	Dec., 1947

Protective Screens.

The use of screens to protect dams from seepage and uplift forces has been extremely varied in both design and intent. The screen may merely be meant as a precautionary measure to give additional safety or it may be an integral part of the structure designed to give complete protection from seepage and uplift. Screens have sometimes been erected after a dam has been in service in order to reduce excessive uplift or leakage, and some

screens appear to have been built because of uncertainty of the nature and magnitude of uplift forces.

The types of screen can be divided into two broad categories; (i) "plain" screens which consist of a covering on the face of the dam which is made as impermeable as possible and (ii) "hollow" screens which consist of a guard wall built in front of the dam and supported against the main structure with an air space between the two.

The plain screen has several forms varying from thin layers of cement to sheet metal armour. In the former case a layer of neat cement approximately 1 inch thick and sometimes reinforced with a metal grillage is sprayed on the upstream face. This is intended to form an impermeable membrane but its effectiveness is questionable. The possibility of temperature and shrinkage cracking is considerable, and whether or not cracks form, no known cement is waterproof especially under the high pressure encountered near the base of a dam. At best this device will reduce the permeability of some areas of the upstream face, but water has only to enter a crack at one level to decrease the stability of the entire structure above that level. The practice of using a richer concrete near the upstream face is much simpler and probably much more effective.

A more robust device employed on some French dams consists of covering the thin cement layer with a strongly reinforced concrete slab or alternatively to place the cement layer within the slab, coinciding with its neutal axis. These methods are probably better than the external layer but they are complicated and costly.

On two Italian dams, the Diavolo and the Gabiet, the upstream faces were covered with sheet iron 0.2 and 0.5 cm. thick in respective cases, to reduce excessive leakage. Horizontal joints in the sheets were welded and

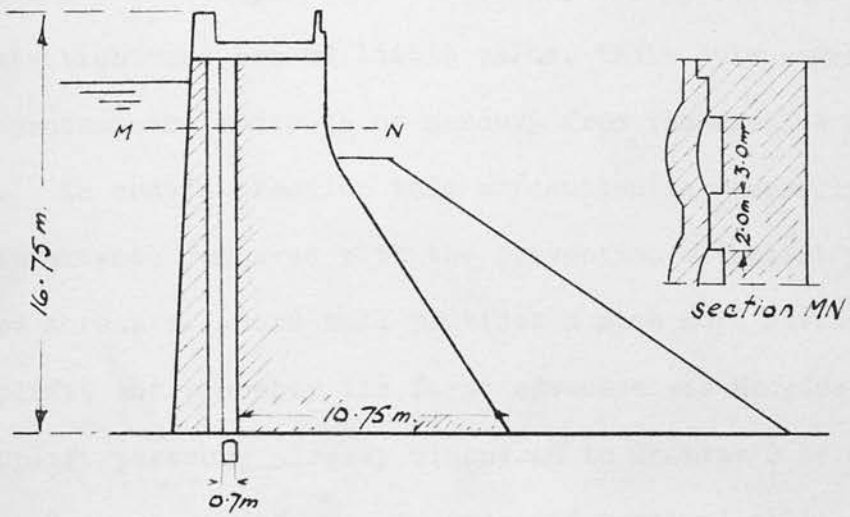

Diagrammatic section through the Bouillouse Dam showing heavy type of hollow screen

From 'The Engineer' 18th March, 1949.[23]

Figure 28

vertical watertight expansion joints provided at frequent intervals. At the base of the dam the sheets were embedded in a trench of rich concrete and tarred rope. This method was reported successful in reducing leakage, but there was some doubt as to whether or not uplift pressure was relieved. Indeed the fundamental weakness of all plain screen methods seems to be the provision of an adequate cut-off; for no matter how imprevious the upper structure of the dam is made, if uplift develops along the base the efforts at securing watertightness are of little value, their only remaining function being to protect the concrete or masonry from the erosive effects of seeping water. In modern practice this precaution is generally considered of secondary importance compared with the prevention of uplift forces.

The hollow screen or guard wall provides a much more satisfactory means of reducing uplift, and probably its first advocate was Maurice Levy. In his paper on uplift pressure already discussed in Chapter 2 he outlines his proposals for a "mur de garde".[25] A series of vertical pillars 2 metres square and spaced 2 metres apart were to be built against the upstream face of the dam. Against these pillars a heavy wall would be constructed running parallel to the face of the dam and of the same height. Thus, a series of wells 2 metres square would be formed between the guard wall and the dam. The corners of the wells would be rounded off to increase their strength. Water seeping through the wall would be collected in the wells and drained off to the downstream face leaving the main structure dry and free from uplift. The simple principle of this device has been employed in dams up to the present time.

The heavy type of hollow screen proposed by Levy has been used in several French dams, e.g. the Bouillouse Dam illustrated in Figure 28. The segmental arches rest against the counterforts which are part of the

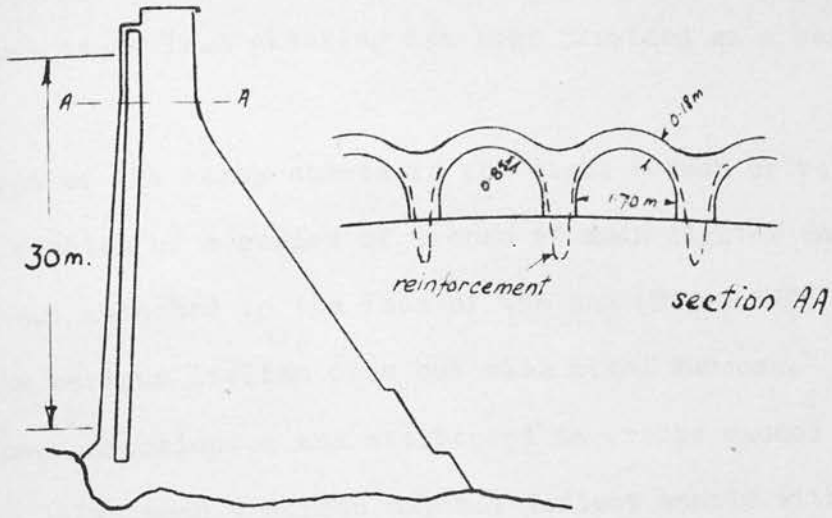

Section through dam with light revetement

From 'The Engineer' 18th March, 1949.[23]

Figure 29

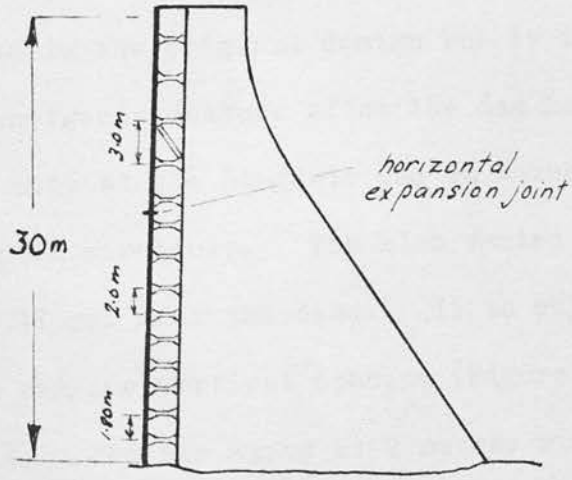

Screen at Ringedals Dam

from 'The Engineer' 18th March 1949[23]

Figure 30

main structure, but can expand and contract independently with temperature change. In some cases lead sheeting has been provided as a bearing for the movement.

A refinement of the heavy screen is the light screen or revetment. This may again consist of a series of arches of much lighter and more graceful form, but attached to the face of the dam (Figure 29). The device has been used on various Italian dams but with mixed success. Heavy leakage has often been experienced and attributed to cracks caused by temperature movement. Also such a screen may not deflect easily with the dam because of its large horizontal moment of inertia. This type of screen should make the dam safe from uplift but the loss of water through leakage may be a serious consideration.

From the point of view of elasticity a reinforced concrete slab (as in Figure 30) will give a much better performance than the arched revetment. It can be incorporated in the original design but it is also comparatively easy to erect as an emergency measure after the dam has been in operation. Such an erection was made at the Ringdals dam in Norway to stop excessive leakage through the main structure. The slab varied in thickness from 20 cm. at the top to 47 cm. near the base. It is supported by reinforced concrete struts with varying vertical spacing (Figure 30) and a horizontal spacing of 2.5 metres. The air space is 2 metres wide allowing adequate room for inspection. This type of screen is also favoured in Sweden and was proposed as an alternative to drainage within the main structure at the Third International Congress on Large Dams.[31]

The great advantage of the hollow screen is that it provides a definite pressure relief point which should attract a large proportion of the water which would normally seep through the foundation and the main structure of

the dam itself. A grout curtain beneath the screen will give further protection and drainholes drilled vertically at the foot of the air space will improve the water-trapping efficiency of the screen.

With the slab type of hollow screen it is now the practice to assume that the main structure is free from uplift. There has been no evidence to show that this assumption is not justified. If the main structure is free from uplift a lower proportion of cement can be used in building it and this saving will partly off-set the additional cost of the screen.

The use of a screen rather than a system of pipe drains is, with smaller dams at least, a matter of choice, but the former appears to be favoured in European countries and the latter in the United States of America. The writer has found no case where a screen was built for a dam of much more than 100 feet in height, probably because in very large structures the cost of incorporating a screen would be excessive.

Contraction Joints.

In addition to the above methods designed to prevent or reduce uplift, further relief is given where the vertical contraction joints in a dam are left open. This is done to allow the individual blocks of the dam to adjust themselves to the peculiarities of the foundation without throwing part of their load on adjacent blocks. Duplicate metal seals placed at the upstream end prevent leakage. The practice is not universal for in many cases the joints are grouted up after the concrete has been cured and shrinkage has ceased. In cases where the joints are left open, the possibility of high uplift pressures developing within the main structure is considerably reduced without the provision of actual drainholes within the dam.

The decision whether to have open or grouted joints will be influenced

to some extent by the distance which the dam has to span. For example the Hoover Dam situated in a narrow valley has a comparatively short span in relation to its height (see Figure 26). The contraction joints in this case were grouted up to give a completely monolithic structure. This also increases the stability of the dam by ensuring an arch action against the abutments. Geological investigation of the foundation showed that the site of the dam was a solid block of rock lying between two major faults, so that the chances of relative settlement in the foundation were not great. If a dam has to be built in a wide valley where foundation conditions are liable to vary, the possibility of relative settlement is increased and the provision of free joints would be a safeguard.

Uplift Measuring Devices.

Devices for measuring foundation uplift have varied very little since the practice first began. A row of pipes, usually between five and ten, joins points along the base of a section with an inspection gallery in either of the manners shown in Figure 20. The internal diameter of the pipes varies from 1 inch to 3 inches. Uplift head is measured either with a pressure gauge attached to the top of the pipe or by sounding if the water has not reached that level. Although this method is often very effective it has several disadvantages and it is very crude.

In the case of a dam founded on a gravel or sand bed, there will be a large quantity of seepage water present beneath the structure soon after the first filling of the reservoir. Provided the pipe has access to this supply, a head of water can be measured in it corresponding to the uplift at the base. However, for a dam set on a tightly grouted rock foundation, the discharge beneath it will be comparatively small because of the low permeability; and for a structure like the Hoover Dam where some measuring

pipes are over 100 feet long and contain many gallons of water, it might require many years before sufficient water is discharged into the pipe to give a true measure of the pressure at its base.

The same criticism applies to the so-called "pressure cells" installed to measure pressure in the lift joints. These cells consist of sacks of gravel connected by pipes to pressure gauges in an inspection gallery. Once again the time required to fill these cells must be considered in estimating their value. Such installations were made at Gibson, Owyhee and Hoover Dams in the U.S.A.[19] At the Gibson Dam observations were discontinued when no sign of pressure was apparent after 12 years. At Owyhee, observations from 1934 to 1951 showed no signs of pressure. At the Hoover Dam no pressure was recorded during observations made between 1935 and 1951.

The practice of using large bore pipes is not without value, but the results may be misleading or entirely erroneous; e.g. if the pipe becomes blocked and cannot be cleaned or, contrarily, has access to a water bearing fissure. Only when a distinct relation is established between fluctuations in level in the reservoir and the measuring pipe can the observations so made be accepted as valid. For example, on a chart showing reservoir level and pipe level plotted against time, the peaks and troughs of the reservoir graph should be followed by corresponding peaks and troughs in the measuring pipe graph with a time lag (usually of several months) allowing for the pressure change to reach the measuring point. Such graphs from measurements made at the Gibson Dam are shown in Figure 21. The trough-peak relation is recognisable at least in the first two graphs, showing that this system has been working efficiently.

With more accurate devices, pore pressure has been measured in the body of the dam between lift joints, and some data have been published.

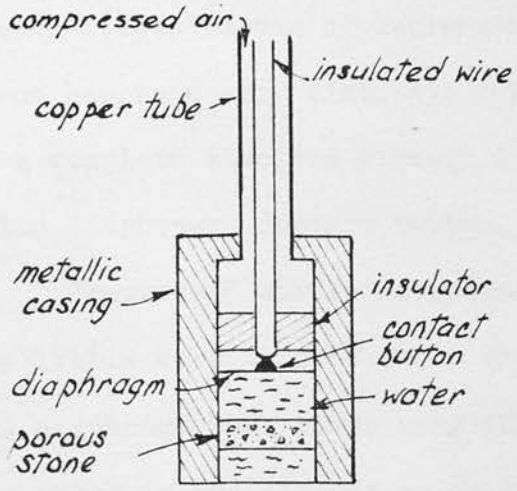

Pressure Cell used at Hiwassee[4]

Figure 31

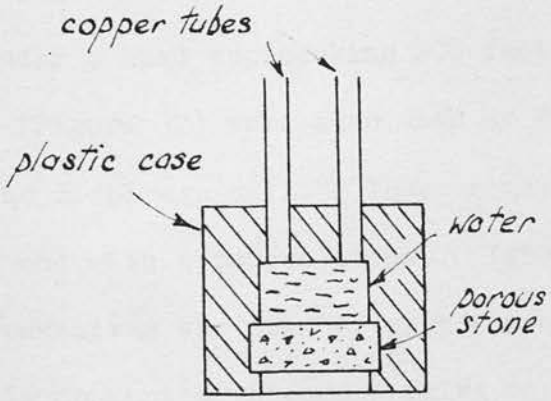

Piezometer Tip used at Fontana Dam[4]

Figure 32

At Hiwassee and Fontana Dams in North Carolina, a pressure cell containing a diaphragm was used. (This cell and the Piezometric tips described below were developed by the United States Bureau of Reclamation (U.S.B.R.)[4] and their use up to the present has been very limited). A diagram of the cell is shown in Figure 31. A complete electric circuit is made by the copper tube, cell casing, metallic diaphragm, contact button, insulated wire, battery and galvanometer. Compressed air is introduced through the copper tube until air pressure a little more than balances the water pressure. The contact button on the diaphragm then moves away from its contact with the insulated wire. The break in the circuit is recorded by the galvanometer and a pressure reading taken. In this way only a very small volume of seepage water is required to measure the pressure and there is no drainage effect to upset the flow pattern and give a misleading local result. Unfortunately these cells can only be used safely with a head of up to 200 feet. Those installed at Fontana worked normally for some time but subsequently failed under a head approaching 400 feet.

Piezometric tips (Figure 32) were also used at Fontana to give results similar to those of the diaphragm cell. These consist of a small plastic chamber closed at one end with a porous stone. Into the other end run two $\frac{1}{4}$ inch copper tubes connecting the chamber with the observation point. One tube is permanently connected through a valve to a Bourdon pressure gauge. The other tube, also provided with a valve, is used to fill the system with water before observations begin. In this way the necessity for a large volume of seepage water is again obviated.

One further instrument, a Carlson-Terzaghi cell, was installed in the Fontana Dam at the same elevation as the piezometric tips. The record of this instrument as shown in Figure 25 is quite consistent with those of the

piezometric tips. The device is an adaptation from the Carlson strain meter and was developed by Professors Carlson and Terzaghi for measuring pore pressure in earth dams. . It consists of a pressure diaphragm attached to a strain gauge so that the deflection of the diaphragm under pressure can be measured by the gauge. This cell and the piezometric tips do not appear to have any practical limitation such as the pressure cell described above.

A great deal could be learned about the rate of development and magnitude of pore pressure if sensitive pressure cells entirely replaced the large bore pipe systems used up to the present. These cells, arranged in a regular pattern across the foundation and lower levels of the dam where pore pressures are highest, would enable an accurate check to be kept on uplift at all times. A comparison could be made of the effectiveness of uplift reducing methods, warning would immediately be given of high pressures, and accurate comparisons could be made between actual uplift and the uplift allowances made in design. The present evidence indicates that pore pressure seldom develops downstream of a well built drainage screen; if this could be confirmed by more accurate measurements it could lead eventually to a substantial reduction in the size and cost of dams.

Many cases have occurred where remedial measures have been carried out to reduce leakage, but owing to the absence of an uplift measuring system it was not known whether uplift had also been reduced, or whether it had been or still was endangering the stability of the structure. Such a system should be a feature of every new dam, for the value of the information it provides and the reassurance it can give to the owner of the dam will by far outweigh the cost of its installation.

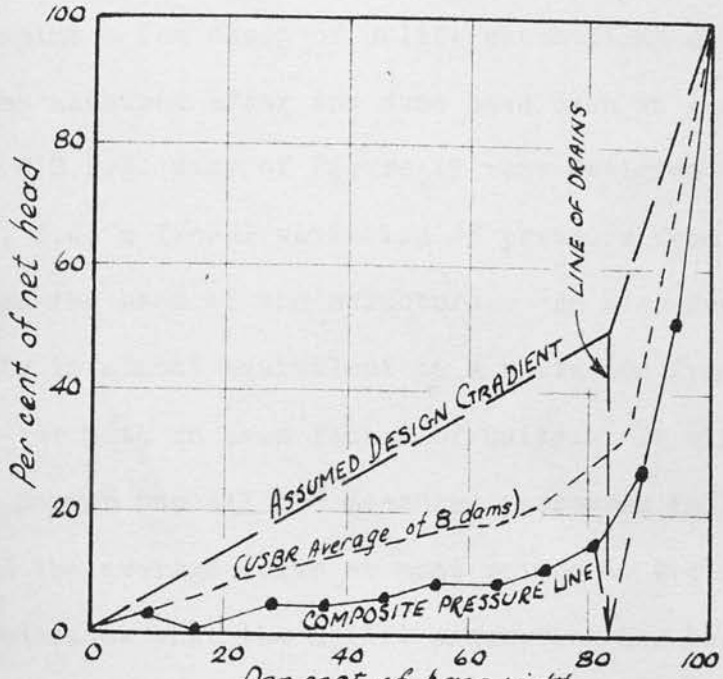

Composite uplift pressure curve for four dams of the T.V.A.

(TRANS. A.S.C.E. Vol. 116, p. 1239)[19]

Figure 33

Design Assumptions.

No positive rules can be laid down about uplift assumptions. They will vary from job to job and will rest in the last resort with the designer. They will be based on standard recommendations, on precedent and on his own judgement, taking into consideration the peculiarities of the site on which any particular dam has to be built. It is interesting, however, to examine a few cases of uplift assumptions and compare them with actual pressures measured after the dams have been in service.

The eight U.S.B.R. dams of Figure 19 were designed on the assumption of full uplift, i.e. a linear variation of pressure from headwater to tailwater across the base of the structure. An area factor of two-thirds was used. This is almost equivalent to a variation from two-thirds headwater to tailwater with an area factor of unity. It will be observed that apart from the Hoover Dam all the measured pressures fall within the two-thirds line and the average curve at most points is within the one-third line. This indicates that the uplift assumption has been adequate if not excessive. The measurements were made before remedial measures were carried out at the Hoover Dam, thus the high pressures in this one case.

Figure 33 shows a composite or average pressure line for four large dams of the Tennessee Valley Authority (T.V.A.). It is seen to be well within the non-linear design assumption also shown in the figure, even allowing that for three of the dams, Douglas, Hiwassee and Cherokee, an area factor of two-thirds was used. At the fourth dam, Fontana, the area factor was taken to be unity. It will also be noticed that the average curve from Figure 19 falls within the non-linear design gradient even when the area factor of two-thirds is considered.

When effective drainage is installed, a non-linear design assumption

is more logical than the linear assumptions generally used in the past with low area factors. There is at present no justification for employing an area factor of less than unity, and the continued stability of structures where low area factors have been used is probably largely due to the fact that uplift pressure seldom develops to the magnitude assumed in design.

Chapter 6

THE EFFECT OF PORE PRESSURE ON THE DISTRIBUTION OF STRESS IN GRAVITY DAMS

A great many works have been written on the various aspects of the uplift problem but not many of these have included other than approximate deductions about the stresses caused by pore pressure. In many cases these deductions have not been supported by mathematical proof. A few writers, however, have tackled the problem by exact analysis and this section is devoted to a summary and study of such work, including some recent work in which the writer has assisted.

It has been necessary to simplify the problem since the elastic analysis of a gravity dam of conventional shape with foundation restraint, even treated as a two-dimensional problem, involves difficult and lengthy mathematical work which has no direct bearing on the problem of pore pressure. It has therefore been expedient to idealise the problem and deal with triangular profiles of great or infinite height with the reservoir reaching the level of the apex of the dam. This simplification is not unreasonable, for various investigators have shown that the resulting stresses correspond closely to those found for practical profiles for sections not immediately adjacent to the foundation.[41,42,5]

Elastic analysis shows that for an impermeable dam of great or infinite height, assuming two-dimensional plane strain conditions, a linear stress distribution exists on plane sections. Maurice Levy was the first to publish the proof of this in 1898.[26] How the stress distribution is altered by the presence of pore pressure is not generally known except in

the very simple case where pore pressure varies linearly from the upstream end to the downstream end of horizontal sections. However, work has recently been done which makes possible the calculation of stresses whatever the distribution of pore pressure may be, provided the pressure can be defined in explicit mathematical terms.

Assumptions.

The usual assumptions are made that the dam is elastically isotropic and of uniform density throughout. These conditions are only approximated to in practice because of the inevitable variation in the quality of different batches of concrete, and the well-known creep characteristics of the material, but such assumptions are necessary or the problem becomes impossibly difficult.

The assumption that concrete is a homogeneous material is not strictly correct because of the presence of pores, but the pores are so minute that the assumption is sufficiently good for all practical purposes. One writer, whose work is discussed in Appendix B has attempted to deal with both the elastic constants of concrete as a homogeneous material, and the elastic constants of the interpore material. In so doing he finds a basis for a useful method of solving pore-pressure problems by analogy with thermal problems: but the solutions thus derived are shown to be identical with those found without considering interpore material at all.

I. Work of J. H. A. Brahtz

A general treatment of the influence of pore water pressure on the stresses in hydraulic structures was presented by Brahtz at the Second International Congress on Large Dams, Washington, D.C. 1936.[5] The following conclusions (i) and (ii) are of particular importance:

i) For the steady, continuous, laminar flow of an incompressible fluid through a porous medium, the distribution of fluid pressure is governed by the Laplace equation:

$$\nabla^2 p = 0$$

i.e. when the seepage obeys Darcy's law the pressure function p is harmonic. The percolation of water through concrete is assumed to resemble closely the above conditions.

ii) The stresses determined by the boundary and body forces in the absence of pore pressure must be decreased by an amount np if internal liquid pressure is also present.

n is the area factor.

The proof of this latter conclusion will be shown in detail for it is the subject of further examination in the next chapter. The proof applies only to simply-connected bodies for reasons which are set out in Chapter 7.

Proof.

The state of stress at a point (x, y) in a stressed body can be represented as shown in Figure 34, irrespective of whether or not the body is subjected to internal pore pressure. (The term "stress" is understood to mean the average stress on plane sections intersecting voids and solids, and not the stress in the interpore material). Arrows denote the positive directions of the stress components and gravity is assumed to act downwards in the direction of the y axis.

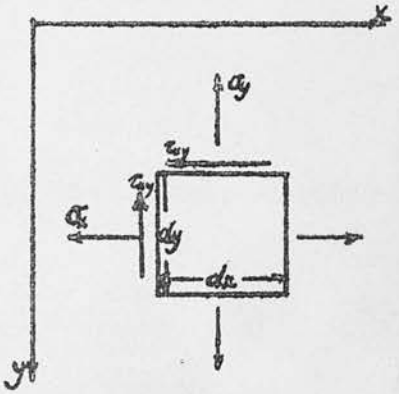

Figure 34

When a water pressure p acts in the pores of the body, a body force of magnitude $-n.\,grad\,p$ per unit volume of the body exists. The

equations of equilibrium of an element are then

$$\frac{\partial \sigma_x}{\partial x} + \frac{\partial \tau_{xy}}{\partial y} - n\frac{\partial p}{\partial x} = 0$$
$$\frac{\partial \sigma_y}{\partial y} + \frac{\partial \tau_{xy}}{\partial x} - n\frac{\partial p}{\partial y} + w_s = 0 \qquad (1)$$

where w_s represents the weight per unit volume of the body, and in the case of a porous body, its saturated weight.

The equations of equilibrium are automatically satisfied if the stresses are defined in terms of a stress function ϕ in the following manner:

$$\sigma_x = \frac{\partial^2 \phi}{\partial y^2} - w_s y + np \qquad (2a)$$

$$\sigma_y = \frac{\partial^2 \phi}{\partial x^2} - w_s y + np \qquad (2b)$$

$$\tau_{xy} = -\frac{\partial^2 \phi}{\partial x \partial y} \qquad (2c)$$

In the case of a non-porous body the terms involving p disappear from equations (1) and (2).

For a unique solution the stress function must also satisfy the condition for compatibility of strains which, in a two-dimensional plane-strain problem, is

$$\nabla^2(\sigma_x + \sigma_y) = \frac{1}{(1-\nu)}\nabla^2 V \qquad (3)$$

where V is a potential function representing all body forces.

For a non-porous body, if weight is the only body force,

$$V = -w_s y$$

and

$$\nabla^2 V = 0 \qquad (4)$$

Substituting (2) and (4) into expression (3), the governing

equation becomes:

$$\nabla^4 \phi = 0 \qquad (5)$$

For a porous body having a pressure gradient in the pores:

$$V = n p - w_s y$$

so that:

$$\nabla^2 V = n \nabla^2 p$$

and the governing equation (3) becomes:

$$\nabla^4 \phi = n \frac{(1-2\nu)}{(1-\nu)} \nabla^2 p \qquad (6)$$

However, in regions of continuous flow, $\nabla^2 p = 0$ from Brahtz' conclusion (i) so that (6) becomes:

$$\nabla^4 \phi = 0 \qquad (7)$$

Thus the governing equations (5) and (7) are identical in the cases of porous and non-porous bodies.

The arbitrary constants in the general solution of (5) or (7) must be determined from the boundary conditions. In the cases of porous and non-porous bodies these vary only with the normal forces at the boundary where fluid pressure is applied, for example the upstream face of a dam. It will be supposed for convenience that this boundary coincides with the y-axis, then considering the boundary conditions;

at $x = 0$ let the applied pressure be p_0.

For a non-porous body, from equation (2a)

$$\underset{(x=0)}{\sigma_x} = -p_0 = \frac{\partial^2 \phi}{\partial y^2} - w_s y$$

or

$$\frac{\partial^2 \phi}{\partial y^2} = w_s y - p_0 \qquad (8)$$

For a porous body, from equation (2a)

Figure (35a)

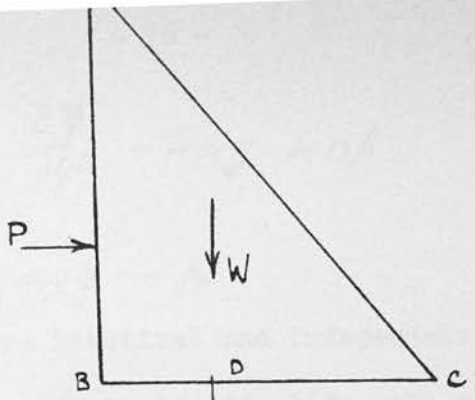

(b)

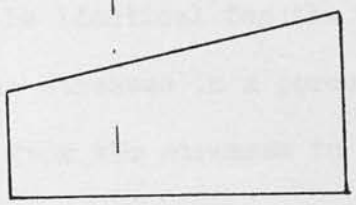

(c)

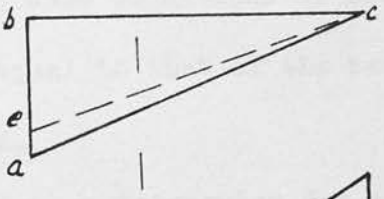

compression plotted above axis

(d)

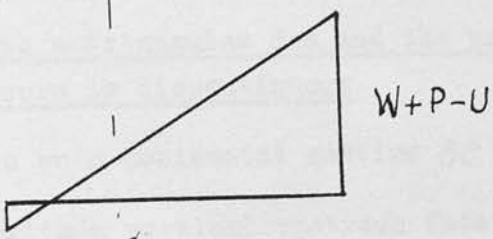

(e)

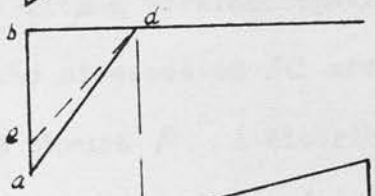

(f)

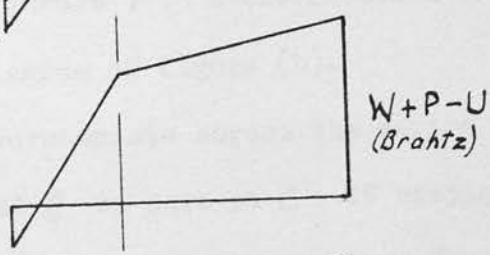

(g)

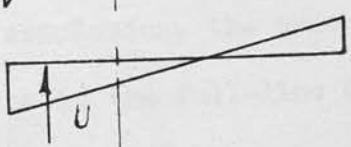

(h)

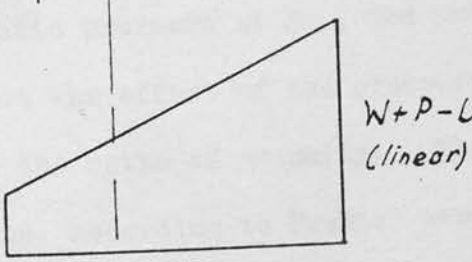

$$\underset{(x=0)}{\sigma_x} = -p_0(1-n) = \frac{\partial^2\phi}{\partial y^2} - w_s y + np$$

or

$$\frac{\partial^2\phi}{\partial y^2} = w_s y - p_0 \qquad (9)$$

The results (8) and (9) are identical and independent of the area factor, therefore, the stress function ϕ is identical for the two cases. It follows from equations (2) that the stresses in a porous body can be found simply by deducting an amount np from the stresses in a geometrically similar non-porous body under the same conditions of external loading, whose weight per unit volume is equal to that of the saturated porous body. This is Brahtz' second conclusion.

II. Brahtz' conclusions applied to a triangular dam and the problem when the pressure is discontinuous

Consider the vertical stresses on a horizontal section BC of a triangular dam of infinite height with a vertical upstream face (Figure 35). In the absence of pore pressure the stresses on BC are caused by the weight of the dam W and the hydrostatic thrust P. A distribution of stress will exist as shown in the full-line diagram of figure (b).

Supposing now that pore pressure exists across the entire section, varying from full reservoir head at B to zero at C; if seepage obeys Darcy's law then, by Brahtz first conclusion, the pressure function p will be represented by a straight line as in the full-line diagram of figure (c). If ab represents the full hydrostatic pressure at B, the influence of the area factor n will be to reduce the effect of the pressure at B to some value eb where $eb:ab$ is in the ratio of n :unity. The stress distribution on BC is then obtained, according to Brahtz' second conclusion, by subtracting the area ebc from the stress diagram of figure (b). The

resulting stress distribution is shown in figure (d).

The case is now considered where a system of effective drainage within the dam creates a drainage plane at an angle β to the upstream face, intersecting BC at D. * The pressure distribution on BC for this is shown in figure (e) and the pressure function ϕ has now two gradients. On either side of D the expression $\nabla^2\phi = 0$ holds good, but at the point D, $\nabla^2\phi$ is equal to infinity, a contingency for which Brahtz' theory does not provide.

In estimating the resulting stress distribution one might either assume that Brahtz' theory is still applicable and so deduct the area of figure (e) from figure (b) to give the stress distribution in figure (f), or consider the pore pressure as a resultant force U causing a linear distribution of stress as in figure (g); then subtracting figure (g) from figure (b), the resulting stress distribution is shown in figure (h). There is no fully logical reason for adopting either course, although the second is more in keeping with the general practice of stress calculation. The correct solution can only be found by analysing the problem from first

---

* Drainage within a dam is likely to be caused either by a series of vertical drains situated at intervals along the face of the dam, or by a drainage gallery running at right-angles to a transverse section, or perhaps to a combination of both these and other small drains. The free water surface within the dam will vary with the orientation of the various drains and it is liable to have some arbitrary shape not easily expressed in mathematical terms. The assumption of a drainage plane passing through the apex seems a reasonable idealisation which at the same time, is easily expressible in mathematical terms for the analysis which follows.

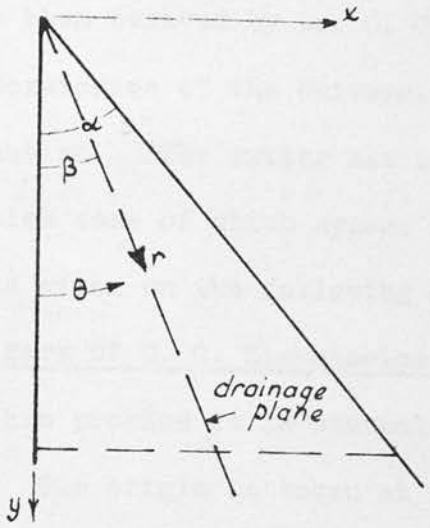

Figure 36

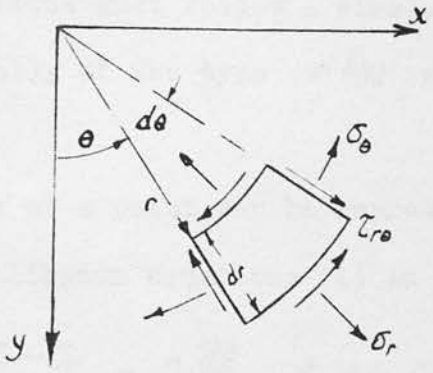

Figure 37

principles and this solution is not generally known. A reference was made to the problem by L. Gherardelli in 1951 but no solution was offered.[11] The solution has recently been derived by Dr. O. C. Zienkiewicz at the Sanderson Engineering Laboratories of the University of Edinburgh, and is at present pending publication. The writer has assisted in this work and worked out numerous examples some of which appear later in the text. An outline of the solution is given on the following section.

III. Work of O. C. Zienkiewicz

In the analysis of this problem it is convenient to use polar co-ordinates r and ϕ. The origin is taken at the apex of the dam, and θ is assumed positive in the anticlockwise direction measured from the upstream face (Figure 36). The apex angle is α and the drainage plane makes an angle β with the upstream face.

Stress-Strain Relations and the Governing Equation.

From consideration of symmetry the distribution of stress and of pore pressure on similar sections must follow a similar pattern. It follows that stresses are generally of the type $r f(\theta)$ where $f(\theta)$ is a function of θ only.

The state of stress at a point can be represented as shown in Figure 37. Rewriting the equilibrium equations (1) in polar co-ordinates:

$$\frac{\partial \sigma_r}{\partial r} + \frac{1}{r}\frac{\partial \tau_{r\theta}}{\partial \theta} + \frac{\sigma_r - \sigma_\theta}{r} - n\frac{\partial p}{\partial r} + w_s \cos\theta = 0$$

$$\frac{1}{r}\frac{\partial \sigma_\theta}{\partial \theta} + \frac{\partial \tau_{r\theta}}{\partial r} + \frac{2\tau_{r\theta}}{r} - \frac{n}{r}\frac{\partial p}{\partial \theta} - w_s \sin\theta = 0 \qquad (10)$$

Equations (10) are automatically satisfied if the stress components are defined in terms of a stress function ϕ in the following manner:

$$\sigma_r = \frac{1}{r}\frac{\partial \phi}{\partial r} + \frac{1}{r^2}\frac{\partial^2 \phi}{\partial \theta^2} + np - \omega_s r\cos\theta$$

$$\sigma_\theta = \frac{\partial^2 \phi}{\partial r^2} + np - \omega_s r\cos\theta \qquad (11)$$

$$\tau_{r\theta} = \frac{1}{r^2}\frac{\partial \phi}{\partial \theta} - \frac{1}{r}\frac{\partial^2 \phi}{\partial r \partial \theta}$$

must also satisfy the condition of compatibility:

$$\nabla^4 \phi = \frac{n(1-2\nu)}{(1-\nu)} \qquad (6)$$

which holds both for Cartesian and polar co-ordinates.

In order to satisfy equations (11) it is sufficient that the stress function ϕ should have the form:

$$\phi = r^3 f(\theta)$$

where $f(\theta)$ is a function of (θ) only.

The distribution of pore pressure can in general be defined in the form:

$$p = r.\psi(\theta)$$

where $\psi(\theta)$ is a function of (θ) only. Provided p can be defined explicitly in the above form, there is no limitation on its form of distribution.

The substitution of p and ϕ in equation (6) gives the following ordinary linear differential equation:

$$\frac{d^4 f}{d\theta^4} + 10\frac{d^2 f}{d\theta^2} + 9f = -nk\left(\psi + \frac{d^2\psi}{d\theta^2}\right) \qquad (12)$$

where f denotes $f(\theta)$, ψ denotes $\psi(\theta)$ and k is equal to $\frac{(1-2\nu)}{(1-\nu)}$

Solution of the Governing Equation.

The general solution of equation (12) has the form:

$$f = A\cos\theta + B\sin\theta + C\cos 3\theta + D\sin 3\theta + \text{Particular integral} \qquad (13)$$

A, B, C and D are arbitrary constants which must be determined from the

boundary conditions, namely:

$$\begin{aligned} \sigma_\theta &= -p_0(1-n) && \text{at } \theta = 0 \\ \sigma_\theta &= 0 && \text{at } \theta = \alpha \\ \tau_{r\theta} &= 0 && \text{at } \theta = 0 \\ \tau_{r\theta} &= 0 && \text{at } \theta = \alpha \end{aligned} \qquad (14)$$

where p_0 is the hydrostatic pressure in the reservoir.

The value of the particular integral depends on the form of the pressure distribution. For the particular case where p is reduced to zero at the radial drainage plane, the pressure distribution shown in Figure 35(e) can be defined as follows: recalling that p has the form $p = r\psi$,

$$\begin{aligned} \psi &= \frac{w \sin(\beta-\theta)}{\sin\beta} && \text{for } 0 < \theta < \beta \\ \psi &= 0 && \text{for } \beta < \theta < \alpha \end{aligned} \qquad (15)$$

where w is the unit weight of water.

The term $\left(\psi + \frac{d^2\psi}{d\theta^2}\right)$ in equation (12) is equal to zero except when $\theta = \beta$ when it becomes infinite. It is convenient to represent this term by the Dirac 'delta' function $\delta(\theta-\beta)$ which is defined as follows:[6]

$$\delta(\theta-\beta) = \infty \quad \text{for } \theta = \beta$$

$$\delta(\theta-\beta) = 0 \quad \text{for } \theta \neq \beta$$

$$\int_{-\infty}^{+\infty} \delta(\theta-\beta)\,d\theta = 1 \text{ (unity)}.$$

Substituting the delta function in equation (12) gives:

$$\frac{d^4f}{d\theta^4} + 10\frac{d^2f}{d\theta^2} + 9f = -K\delta(\theta-\beta) \qquad (16)$$

where

$$K\delta(\theta-\beta) = nk\left(\psi + \frac{d^2\psi}{d\theta^2}\right) \qquad (17)$$

K, which is a constant, can be found by integrating both sides of equation (17) over any range of θ from $0<\theta<\beta$ to $\beta<\theta<\alpha$. For the distribution of pressure defined in equation (15), K has the value $\frac{nk\omega}{\sin\beta}$. (See equation 24). Equation (16) can then be solved by the Laplace transformation method in a manner similar to that shown in Appendix Cor D. The resulting form of f is then:

$$f = A\cos\theta + B\sin\theta + C\cos 3\theta + D\sin 3\theta + \frac{K}{24}\left[\sin 3(\theta-\beta) - 3\sin(\theta-\beta)\right] H(\theta-\beta) \qquad (18)$$

where

$$H(\theta-\beta) = 0 \quad \text{for} \quad \theta<\beta$$

$$H(\theta-\beta) = 1 \quad \text{for} \quad \theta>\beta$$

Evaluation of the Constants.

By applying the boundary conditions (14) to equations (11) it is found that

$$\begin{aligned} A &= \tfrac{1}{16}\left[3(\omega_s-\omega) + 2f_0''\right] \\ B &= \tfrac{1}{8} f_0''' \\ C &= -\tfrac{1}{48}\left[(\omega_s-\omega) + 6f_0''\right] \\ D &= -\tfrac{1}{24} f_0''' \end{aligned} \qquad (19)$$

where $f_0'' = \left(\frac{d^2 f}{d\theta^2}\right)$ at $\theta = 0$

and $f_0''' = \left(\frac{d^3 f}{d\theta^3}\right)$ at $\theta = 0$

Substituting (19) in (18) gives:

$$f_0'' = \left[\frac{\omega(1+\cos^2\alpha)}{2\sin^2\alpha} - \frac{\omega_s}{2}\right] - K\frac{\sin^2(\alpha-\beta)\sin\beta}{\sin^2\alpha}$$

and

$$f_0''' = \omega_s \cot^2\alpha - 2\omega\cot^2\alpha + \frac{K\sin^2(\alpha-\beta)}{\sin^3\alpha}\left[\cos\beta\sin\alpha + 2\sin\beta\cos\alpha\right]$$

The Stress Components.

By expressing $\phi = r^3 f$ in Cartesian co-ordinates, the stress components σ_x, σ_y & τ_{xy} are readily found. They have the form:

$$\sigma_x = -wy - K(x\cos\beta - y\sin\beta)\sin^2\beta\ H(\theta-\beta) + np$$

$$\sigma_y = x f_0''' + y\left[f_0'' - \frac{w_s+w}{2}\right] - K(x\cos\beta - y\sin\beta)\cos^2\beta\ H(\theta-\beta) + np$$

$$\tau_{xy} = -x\left[\frac{w_s-w}{2} + f_0''\right] - K(x\cos\beta - y\sin\beta)\sin\beta\cos\beta\ H(\theta-\beta) \qquad (20)$$

Equations (20) show that the distribution of stress is linear in all cases with a change of gradient where a section intersects the drainage plane. At this point the term involving the step function $H(\theta-\beta)$ increases from zero as θ becomes greater than β. The distribution of stress on any plane section is known therefore if the stresses at the end of the section $(\theta = 0)$ and $(\theta = \alpha)$ and at the drainage plane $(\theta = \beta)$ are calculated.

The stresses which most interest the designer are the vertical and shear stresses on horizontal sections. The expressions for these stresses, determined from equations (20) are as follows: γ represents the ratio w_s/w

Vertical Stress.

At $\theta = 0$ $(x = 0)$,

$$\sigma_y = \frac{wy}{\sin^2\alpha}\left[\cos^2\alpha + n\sin^2\alpha - \gamma\sin^2\alpha - nk\sin^2(\alpha-\beta)\right]. \qquad (21a)$$

At $\theta = \beta$ $(x = y\tan\beta)$,

$$\sigma_y = wy\left[\gamma\left(\frac{\tan\beta}{\tan\alpha} - 1\right) + 2nk\,\frac{\sin^2(\alpha-\beta)}{\sin^2\alpha}\,\frac{\tan\beta}{\tan\alpha} - \frac{2\tan\beta}{\tan^2\alpha} + \cot^2\alpha\right] \qquad (21b)$$

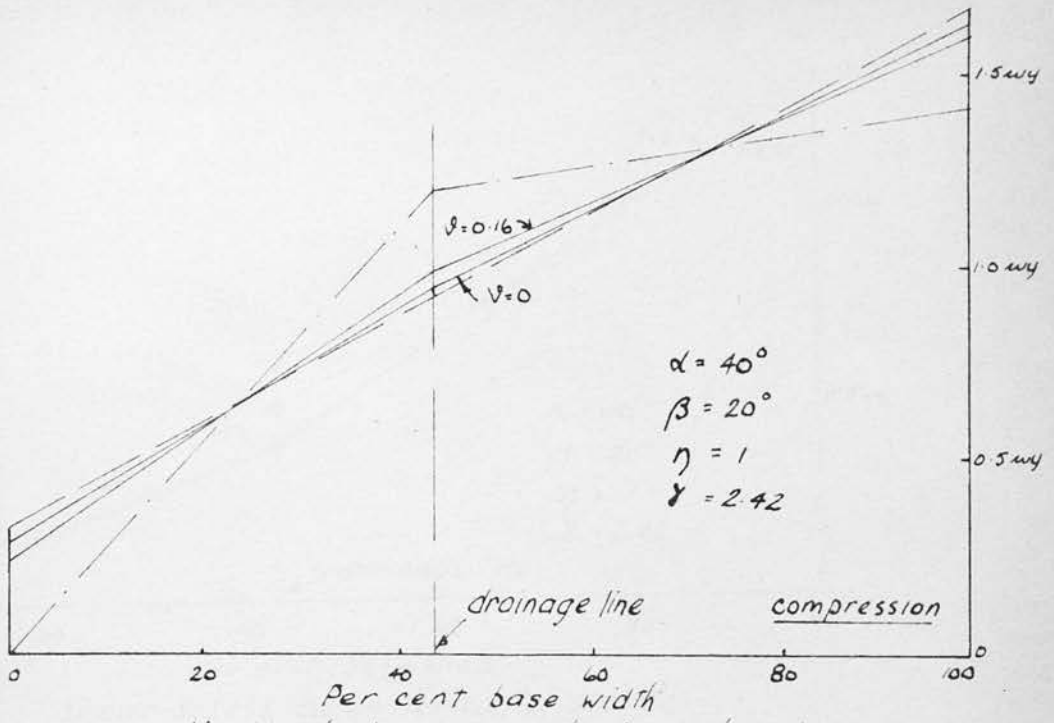

Vertical stress σ_y on horizontal sections

Figure 38

——— True stress distribution

—·—· Stress distribution by extension of Brahtz theory

— — — Stress distribution by straight-line assumption

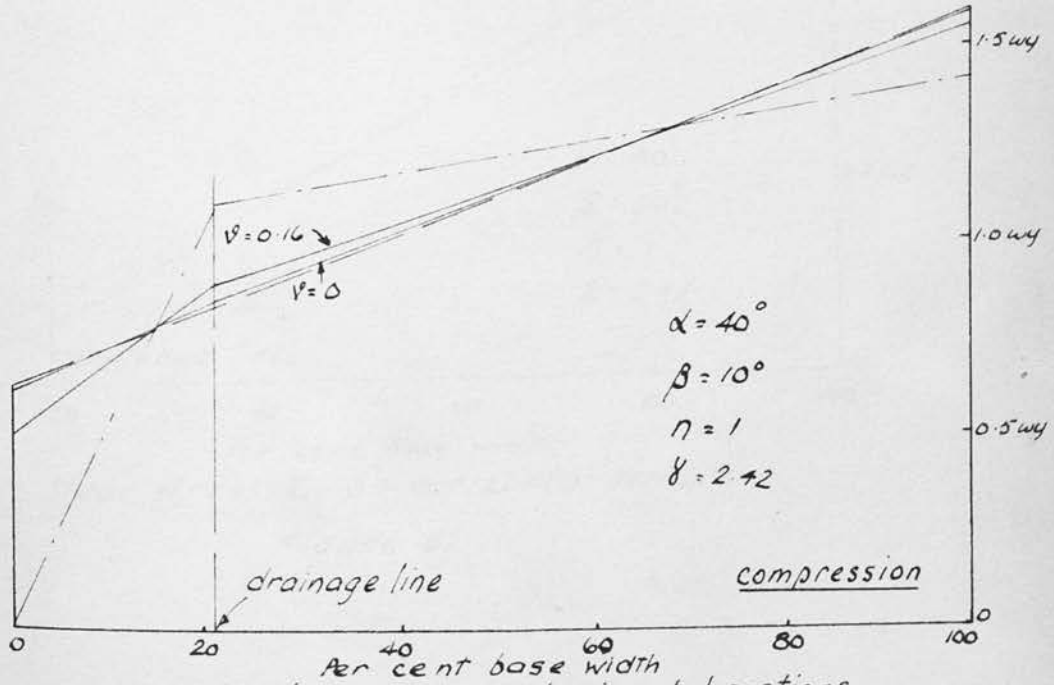

Vertical stress σ_y on horizontal sections

Figure 39

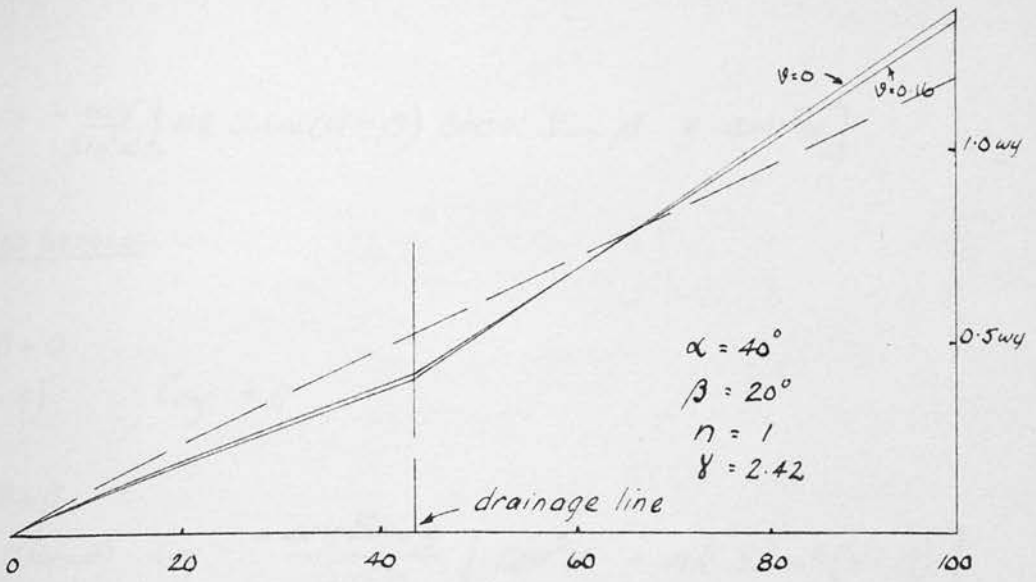

Shear stress τ_{xy} on horizontal sections

Figure 40

—— True stress distribution

— — - Straight-line assumption

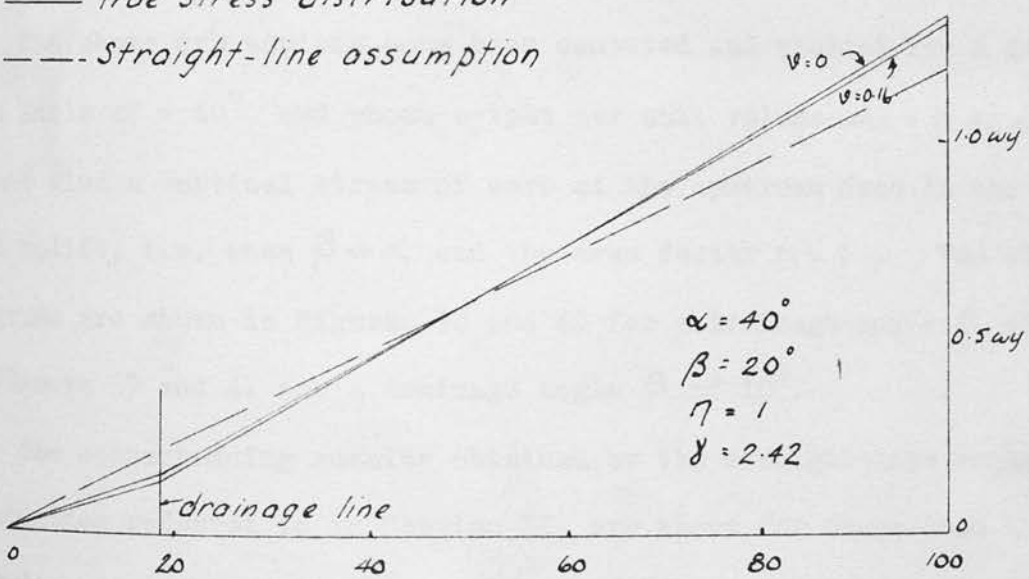

Shear stress τ_{xy} on horizontal sections

Figure 41

At $\theta = \alpha$ $(x = y \tan \alpha)$

$$\sigma_y = -\frac{wy}{\sin^2\alpha}\left[nk \sin(\alpha-\beta)\cos\alpha \sin\beta + \cos^2\alpha\right] \qquad (21c)$$

Shear Stress.

At $\theta = 0$

$(x = 0)$ $\qquad \tau_{xy} = 0 \qquad (22a)$

At $\theta = \beta$

$(x = y\tan\beta)$ $\qquad \tau_{xy} = -\frac{wy\tan\beta}{\sin^2\alpha}\left[\cos^2\alpha - nk\sin^2(\alpha-\beta)\right] \qquad (22b)$

At $\theta = \alpha$

$(x = y\tan\alpha)$ $\qquad \tau_{xy} = -wy\cot\alpha - nkwy\frac{\sin(\alpha-\beta)\sin\beta}{\sin\alpha} \qquad (22c)$

The above expressions have been computed and plotted for a dam with apex angle $\alpha = 40^\circ$, and whose weight per unit volume $w_s = 2{\cdot}42\,w$. These values give a vertical stress of zero at the upstream face in the case of full uplift, i.e. when $\beta = \alpha$ and the area factor $n = 1$. The stress diagrams are shown in Figures 38 and 40 for a drainage angle β of 20°, and in Figures 39 and 41 for a drainage angle β of 10°.

The corresponding results obtained by the straight-line method of stress calculation referred to in Section II, are shown for comparison by the dash-line diagrams in the same figures. The distribution of vertical stress, found by extending Brahtz' theory to this case, is also shown in Figures 38 and 39.

The area factor has been taken as unity in all computations. Values of zero and 0.16 have been used for Poisson's ratio.

There has been considerable uncertainty in the past about the value of Poisson's ratio and it is known to vary with time because of creep. Values ranging between zero and 0.2 have been used, and recently published work gives an average experimental value of 0.16. It has been shown in tests that although the value is of this order on immediate loading, the effect of creep is to decrease the ratio to a much smaller value with time. It has therefore been suggested that to assume a value of zero in the first instance will give just as realistic an answer as to assume a value of 0.15 to 0.20, and at the same time will simplify calculations.[43] This is obviously a question which requires fuller investigation before any logical ruling can be adopted, and it is of secondary importance to the present calculations. However, to illustrate the effect of Poisson's ratio, values of zero and 0.16 have been used in the calculations of Figures 38 to 41. In all subsequent calculations a value of zero only is used.

IV. Problem when pressure is not reduced to zero at the drainage line

In the case where drainage is not fully effective, the pore pressure at the drainage line may be supposed to drop to some fraction λ of the full reservoir head. This is the case with the non-linear design assumption shown in Figure 33. It is a straightforward matter to extend Zienkiewicz' method to meet this case.

The distribution of pore pressure defined in the previous case by equations (15) now becomes:

$$\psi = w\left(\cos\theta + \frac{(\lambda-1)\sin\theta\cos\beta}{\sin\beta}\right) \qquad \text{for } 0 < \theta < \beta$$

$$\psi = \frac{w\lambda\cos\beta\sin(\alpha-\theta)}{\sin(\alpha-\beta)} \qquad \text{for } \beta < \theta < \alpha$$

The quantity $\psi + \frac{d^2\psi}{d\theta^2}$ arising in equation (12) is again equal to zero for $\theta \neq \beta$ and equal to infinity for $\theta = \beta$. It can therefore be represented by the delta function $\delta(\theta-\beta)$ such that:

$$K\,\delta(\theta-\beta) = nk\left(\psi + \frac{d^2\psi}{d\theta^2}\right)$$ as in equation (17).

In this case, however, the value of K, obtained by integrating both sides of the latter equation, is different from the previous case. It is obtained as follows.

Since both sides of the equation have the value zero except at $\theta = \beta$ it follows that integration over the range $-\infty$ to $+\infty$ will give the same result as integration over the range $\beta-\epsilon$ to $\beta+\epsilon$, where ϵ is any small angle.

Therefore

$$K\int_{\beta-\epsilon}^{\beta+\epsilon} \delta(\theta-\beta)\,d\theta = K$$ (by definition of 1" the delta function)

and

$$K = nk\int_{\beta-\epsilon}^{\beta+\epsilon} \left(\psi + \frac{d^2\psi}{d\theta^2}\right) d\theta$$

$$= nk\int_{\beta-\epsilon}^{\beta+\epsilon} \psi\,d\theta + nk\left|\frac{d\psi}{d\theta}\right|_{\beta-\epsilon}^{\beta+\epsilon}$$

$$= 1-$$

$$= nkw \left[\frac{\lambda \cos\beta \cos(\alpha-\beta-\epsilon)}{\sin(\alpha-\beta)} - \frac{\lambda \cos\beta \cos(\alpha-\beta)}{\sin(\alpha-\beta)} + \sin\beta \right.$$

$$+ \frac{(\lambda-1)\cos^2\beta}{\sin\beta} - \sin(\beta-\epsilon) + \frac{(\lambda-1)\cos(\beta-\epsilon)\cos\beta}{\sin\beta}$$

$$\left. - \frac{\lambda \cos\beta \cos(\alpha-\beta-\epsilon)}{\sin(\alpha-\beta)} + \sin(\beta-\epsilon) - \frac{(\lambda-1)\cos\beta\cos(\beta-\epsilon)}{\sin\beta} \right]$$

$$= nkw \left[\frac{1-\lambda\cos^2\beta}{\sin\beta} - \frac{\lambda\cos\beta\cos(\alpha-\beta)}{\sin(\alpha-\beta)} \right] \qquad (24)$$

(The value of K when pore pressure is zero at the drains is simply obtained by putting $\lambda = 0$ in expression (24)).

By substituting expressions (24) in equations (20), the following values for the stress components have been obtained, corresponding to expressions (21) and (22).

Vertical Stress.

At $\theta = 0$, $(x = 0)$:

$$\sigma_y = \frac{wy}{\sin^2\alpha}\left[\cos^2\alpha + n\sin^2\alpha - \gamma\sin^2\alpha - nk\sin(\alpha-\beta)[\sin(\alpha-\beta) - \lambda\sin\alpha\cos\beta]\right]$$

At $\theta = \beta$, $(x = y\tan\beta)$:

$$\sigma_y = \frac{wy}{\sin^2\alpha}\left[\cos^2\alpha\left(1 - \frac{2\tan\beta}{\tan\alpha}\right) - \gamma\sin^2\alpha\left(1 - \frac{\tan\beta}{\tan\alpha}\right) + n\lambda\sin^2\alpha \right.$$

$$\left. + 2nk\sin(\alpha-\beta)[\sin(\alpha-\beta) - \lambda\sin\alpha\cos\beta]\frac{\tan\beta}{\tan\alpha}\right] \qquad (25)$$

At $\theta = \alpha$, $(x = y\tan\alpha)$:

$$\sigma_y = \frac{wy}{\sin^2\alpha}\left[-\cos^2\alpha - nk\sin(\alpha-\beta)\cos\alpha\sin\beta + nk\lambda\sin\alpha\cos\alpha\sin\beta\cos\beta\right]$$

Shear Stress.

At $\theta = 0$, $(x = 0)$:

$$\tau_{xy} = 0.$$

At $\theta = \beta$, $(x = y \tan\beta)$

$$\tau_{xy} = \frac{-wy\tan\beta}{\sin^2\alpha}\left[\cos^2\alpha - nk\sin^2(\alpha-\beta)(1-\lambda\cos^2\beta) + nk\lambda\sin\beta\cdot\cos\beta\sin(\alpha-\beta)\cos(\alpha-\beta)\right]$$

At $\theta = \alpha$, $(x = y\tan\alpha)$

$$\tau_{xy} = -wy\cot\alpha - \frac{nk\,wy\sin(\alpha-\beta)\sin^2\beta}{\sin\alpha}\left[\frac{1-\lambda\cos^2\beta}{\sin\beta} - \frac{\lambda\cos\beta\cos(\alpha-\beta)}{\sin(\alpha-\beta)}\right]$$

The stress diagrams computed from expressions (25) and (26) are shown in Figures 42 and 43. β has been taken as 20°, λ as 50% and Poisson's ratio ν as zero.

V. Parabolic distribution of pressure

The case is now considered where, because of some peculiarity of the concrete or owing to the effect of drainage, the pressure distribution is non-linear and can be expressed by a cubic parabola, thus:

$$p = \frac{r\,w(\alpha-\theta)^3}{\alpha^3} \qquad (27)$$

The pressure distribution is shown in Figure 44a.

Substituting this value of p into the governing equation (6) gives:

$$\frac{d^4f}{d\theta^4} + 10\frac{d^2f}{d\theta^2} + 9f = -\frac{k\,w}{\alpha^3}\left[(\alpha-\theta)^3 - 6(\alpha-\theta)\right]$$

Solving for f by the method of inverse differential operators:

$$f = A\cos\theta + B\sin\theta + C\cos 3\theta + D\sin 3\theta - \frac{k\,w}{9\alpha^3}\left[(\alpha-\theta)^3 - \tfrac{2}{3}(\alpha-\theta)\right] \qquad (28)$$

The constants A, B, C and D must be found from the boundary conditions as before. The stress function ϕ can now be expressed in the form:

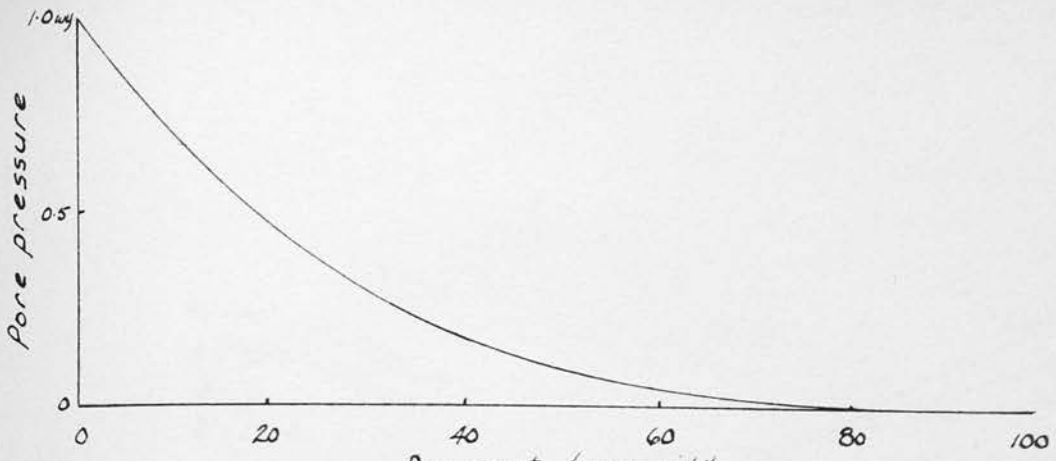

Parabolic pressure distribution

Figure 44a

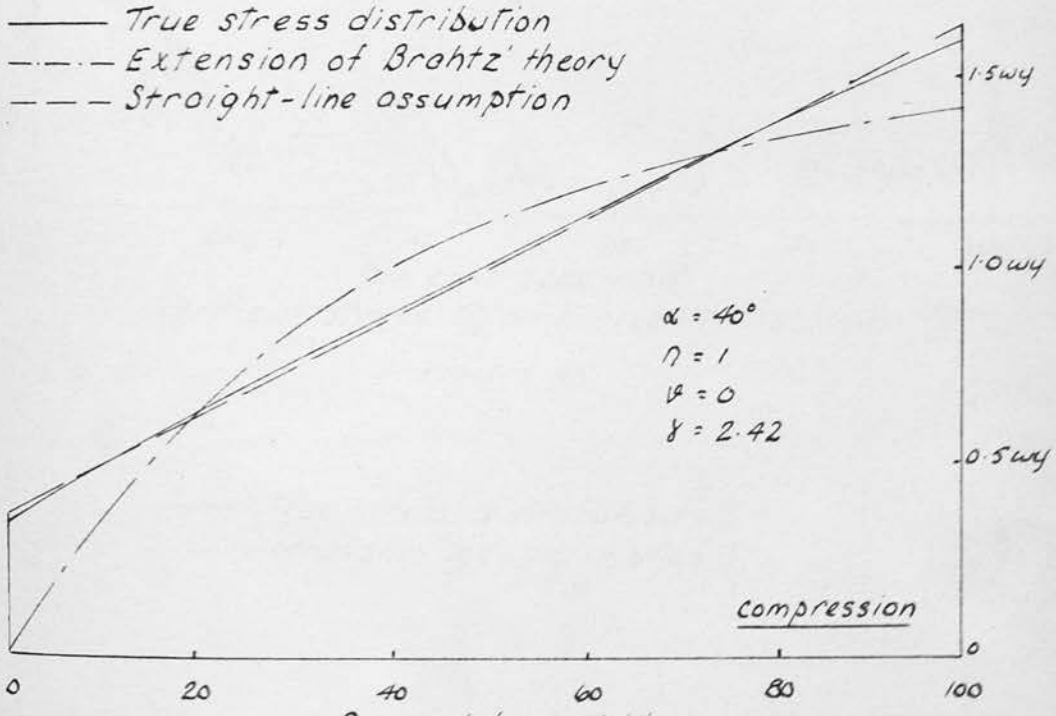

Vertical stress σ_y on horizontal sections

Figure 44b

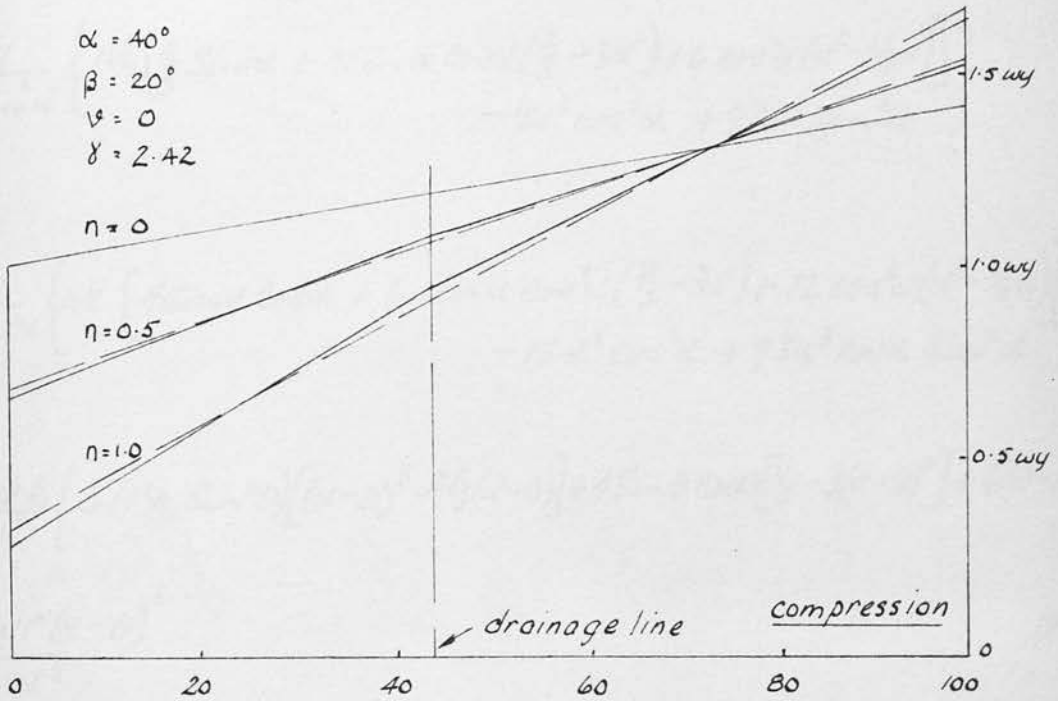

Vertical stress σ_y on horizontal sections

Figure 45

——— True stress distribution

— — — Straight-line assumption

$$\phi = Ay(x^2+y^2) + Bx(x^2+y^2) + C(y^3-3x^2y) + D(3xy^2-x^3) - \frac{r^3 w k}{9\alpha^3}\left[(\alpha-\theta)^3 - \tfrac{2}{3}(\alpha-\theta)\right]$$

Substituting expression (29) into equation (2b), the vertical stress σ_y is found to be:

$$\sigma_y = \frac{-wy}{9\alpha^3\sin^2\alpha}\left\{nk\left[\tfrac{4}{3}\sin\alpha + 4\sin\alpha\cos\alpha\left(\tfrac{2}{3}-3\alpha^2\right) + 6\cos^2\alpha\left(\alpha^3-\tfrac{2}{3}\alpha\right)\right] - 9\alpha^3\cos^2\alpha + 98\alpha^3\sin^2\alpha\right\}$$

$$\frac{+wx}{9\alpha^3\sin^3\alpha}\left\{nk\left[4\sin\alpha\cos\alpha + 6\sin\alpha\cos^2\alpha\left(\tfrac{2}{3}-3\alpha^2\right) + 12\cos^3\alpha\left(\alpha^3-\tfrac{2}{3}\alpha\right)\right] - 18\alpha^3\cos^3\alpha + 98\alpha^3\cos\alpha\sin^2\alpha\right\}$$

$$-\frac{nwrk}{9\alpha^3}\left\{3(1+\sin^2\theta)\left[(\alpha-\theta)^3-\tfrac{2}{3}(\alpha-\theta)\right] + 4\sin\theta\cos\theta\left[\tfrac{2}{3}-3(\alpha-\theta)^2\right] + 6(\alpha-\theta)\cos^2\alpha\right\}$$

$$+\frac{nwr(\alpha-\theta)^3}{\alpha^3} \qquad (29)$$

Equation (29) has been plotted for a horizontal section of the dam. The stress distribution is shown in the full line diagram of Figure 44b. The dash-line diagram shows the corresponding straight-line distribution.

VI. <u>The effect of the area factor n</u>

The effect of the value of the area factor n is illustrated in Figure 45. The vertical stress σ_y on horizontal sections is plotted for a dam with apex angle $\alpha = 40^\circ$; drainage angle $\beta = 20^\circ$; and values for n of zero, 0.5, and 1.0. Both the correct theoretical distribution and the approximate straight-line distribution are shown.

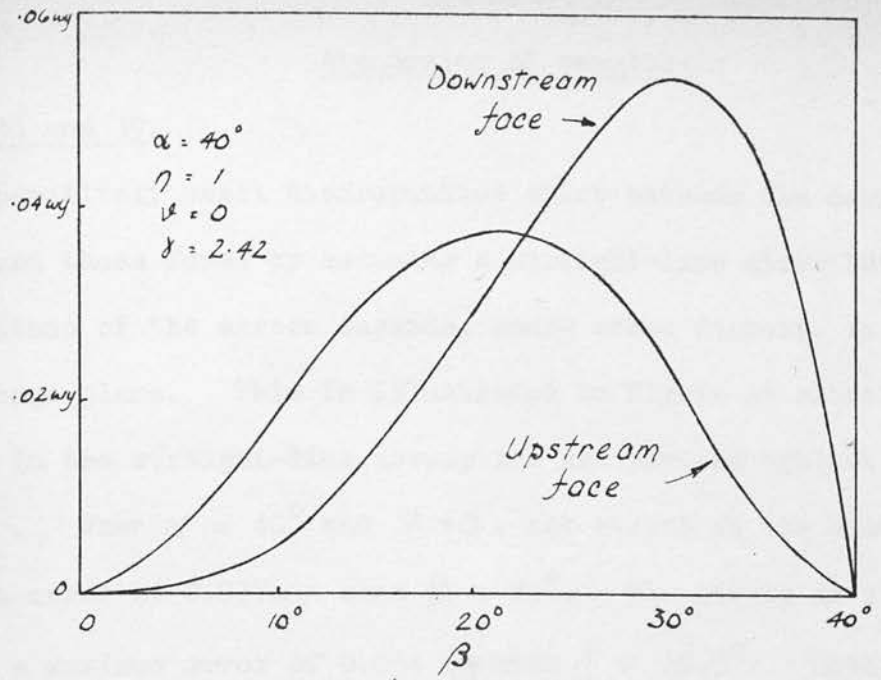

Errors incurred by straight-line assumption

Figure 46

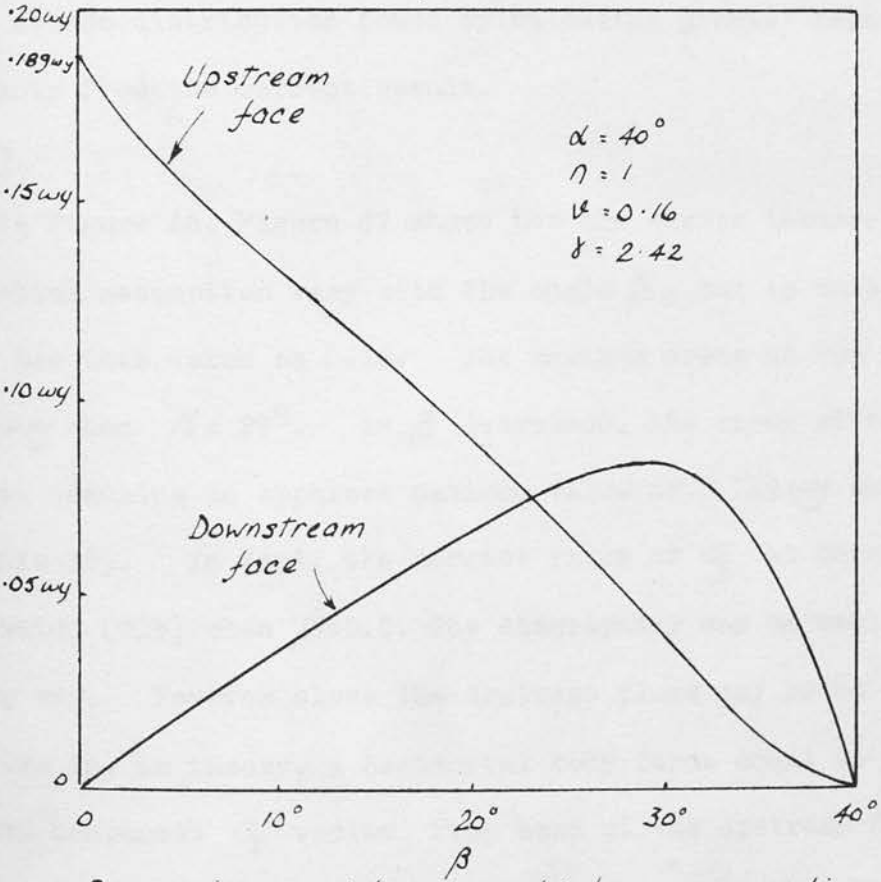

Errors incurred by straight-line assumption

Figure 47

VII. Discussion of results

Figures 38 and 39.

Comparatively small discrepancies exist between the correct theoretical results and those found by assuming a straight-line distribution of stress. The magnitude of the errors depends, among other factors, on the position of the drainage plane. This is illustrated in Figure 46 where the errors involved in the straight-line assumption are plotted against values of the angle β. When $\alpha = 40^\circ$ and $\nu = 0$, the stress at the upstream face has a maximum error of $0.037 wy$ when $\beta = 21^\circ$. The stress at the downstream face has a maximum error of $0.054\ wy$ when $\beta = 30.5^\circ$. Greater errors are incurred with increasing values of Poisson's ratio.

The stress distribution found by extending Brahtz' theory diverges considerably from the correct result.

Figure 47.

As in Figure 46, Figure 47 shows how the errors incurred by the straight-line assumption vary with the angle β, but in this case Poisson's ratio ν has been taken as 0.16. The maximum error at the downstream face is $0.085\ wy$ when $\beta = 29^\circ$. As β decreases, the error at the upstream face increases, reaching an apparent maximum value of $0.189\ wy$ when $\beta = 0^\circ$. (See Figure 48). In fact, the correct value of σ_y at this point is given by expression (21b) when $\beta = 0.0$. The discrepancy can be explained in the following way. However close the drainage plane may be to the upstream face, there is, in theory, a horizontal body force equal to $-n\beta$. If $n = 1$, the stress component σ_x varies from zero at the upstream face to $-\beta$ at the drainage plane an infinitesimal distance away. This discontinuity in horizontal stress creates a discontinuity of vertical stress if Poisson's

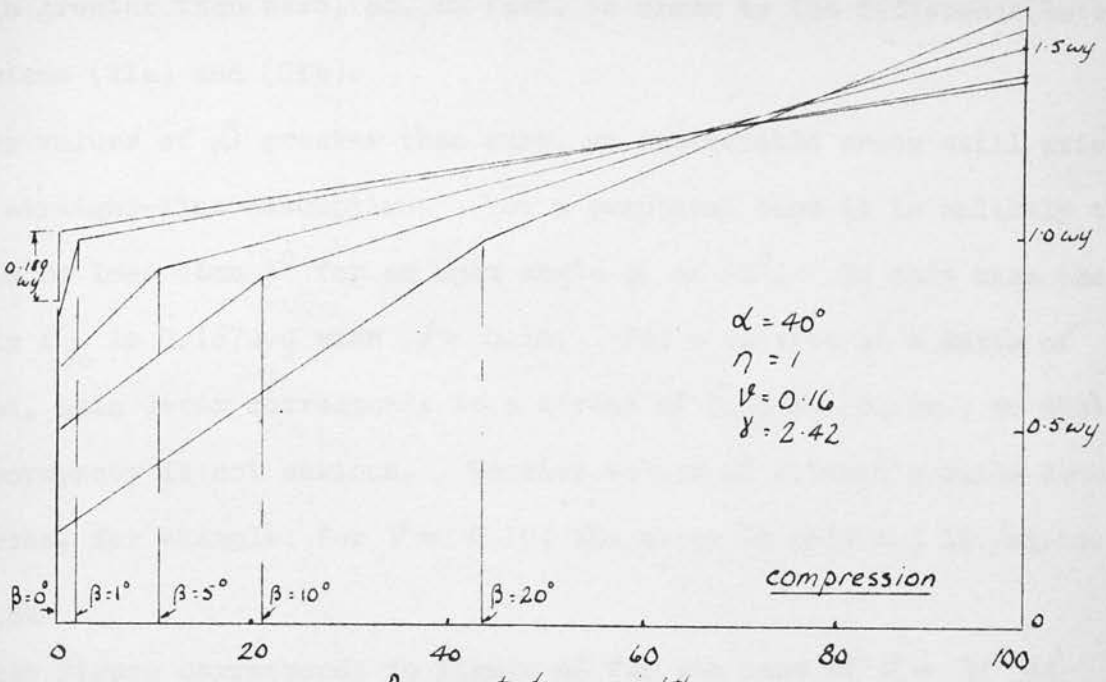

Vertical stress σ_y for various positions of the drainage plane

Figure 48

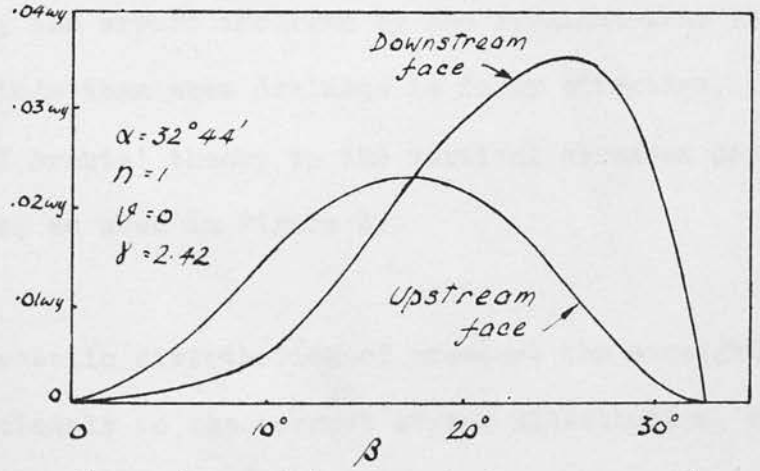

Errors incurred by straight-line assumption

Figure 49

ratio is greater than zero, as, in fact, is shown by the difference between expressions (21a) and (21b).

For values of β greater than zero, an appreciable error still exists in the straight-line assumption. For a practical case it is unlikely that β would be less than 5° for an apex angle α of 40°. In this case the error in σ_{y_0} is $0.167 \omega y$ when $\nu = 0.16$. For a section at a depth of 100 feet, this error corresponds to a stress of 7.25 lb./sq.in., so that the discrepancy is not serious. Smaller values of Poisson's ratio decrease this error, for example, for $\nu = 0.10$, the error is only 4.3 lb./sq.in.

Figure 49.

This figure corresponds to Figure 46 for the case of $\alpha = 32^\circ 44'$ a value which gives zero stress at the downstream face when there is no uplift. The errors incurred by the straight-line assumption are appreciably smaller than those occuring with the larger apex angle.

Figures 42 and 43.

In the case where the pore pressure is reduced by only 50% at the drainage line, the errors incurred by the straight-line theory are of smaller magnitude than when drainage is fully effective. In this case the application of Brahtz' theory to the vertical stresses does not lead to serious errors, as seen in Figure 42.

Figure 44b.

For a parabolic distribution of pressure the straight-line method approximates closely to the correct stress distribution, but the use of Brahtz' theory incurs considerable errors.

Figures 40, 41 and 43.

With shear stresses the errors incurred by the straight-line assumption are of greater magnitude than in the case of vertical stresses. The error

is greatest when $\beta = \frac{1}{2}\alpha$ and when Poisson's ratio $\nu = 0$. The maximum error at the downstream face for the case shown in Figure 40 is $0.18\omega y$, i.e. the straight-line method underestimates the stress by 13%. If drainage is not fully effective as in Figure 43, a decrease is noted in the magnitude of the errors. A variation in Poisson's ratio causes less variation in the stresses than in the case of vertical stresses.

Figure 45.

Different values of the area factor n lead to considerably different stress distributions. If the value of n is overestimated the section will be excessively safe from tension at the upstream face.

The error incurred by the straight-line assumption decreases with decreasing values of n.

VIII. Conclusions

1. Vertical Stress on Horizontal Sections.

In general the assumption of a straight-line stress distribution gives a good approximation to the correct vertical stresses. The true stresses at the upstream and downstream faces are more tensile than those indicated by the straight-line theory. Discrepancies between the two methods are increased with:

i) Increasing values of Poission's ratio ν.

ii) Increasing values of the apex angle α.

iii) Increasing reduction of pressure at the drainage line.

iv) Increasing values of the area factor n.

When $\nu \neq 0$, the error at the upstream face increases with decreasing values of β. Otherwise, discrepancies vary with β, having a maximum at some optimum value of β.

2. Vertical Stress - Brahtz' Theory.

In general, large errors are incurred by the extension of Brahtz' theory to cases where internal drainage exists. The use of Brahtz' theory in design would lead to a section excessively safe from tension at the upstream face. The compressive stress at the downstream face would be underestimated. Only in cases where drainage is not very effective, or where the drainage plane is close to the downstream face, i.e. in cases approaching full uplift, does Brahtz' theory give fairly accurate results. Otherwise it cannot be extended beyond the limits of its strict applicability viz. where the pressure function is harmonic throughout the entire region.

3. Shear Stress on Horizontal Sections.

The assumption of a straight-line distribution of shear stress will underestimate the maximum shear at the downstream face. The error is greatest when $\beta = \frac{1}{2}\alpha$, and decreases to zero as $\beta \to 0$ or as $\beta \to \alpha$. The error decreases with increasing values of Poisson's ratio. The straight-line assumption cannot be said in general to give good results in the case of shear stresses.

4. The Area Factor.

A knowledge of the correct value of the area factor is extremely important in designing an economical section.

Chapter 7

THE DISTRIBUTION OF STRESS IN THICK POROUS CYLINDERS DUE TO PORE-WATER PRESSURE

The solution to the problem of the distribution of stress in a thick, circular cylinder of solid material due to internal or external fluid pressure, can be found in almost any text-book on "Strength of Materials" or the "Theory of Elasticity". However, if the cylinder is made of a material such as concrete containing continuous voids, a body force will exist arising from the presence of water under pressure in the pores of the material. The resulting distribution of stress in not generally known. In a paper published in 1954, Gherardelli assumed that Brahtz' theory of pore pressure was applicable, and therefore subtracted the pore pressure at very point from the normal stress in a cylinder of solid material.[11] The analysis in the following chapter and in Appendix A shows that Brahtz' theory is not applicable in a region of multiple connection, and that the stress distribution in a porous cylinder must be deduced from first principles.

Solutions are also given for other problems of a similar but more complex nature; viz. (a) the effect of reducing the pore-pressure by drainage before the percolating water reaches the free boundary, and (b) the effect of an impermeable boundary within the material.

Assumptions and Conventions.

The material of the cylinders is assumed to be perfectly elastic, homogeneous and isotropic.

The problem is treated as a case of plane strain and the effect of

gravity forces is not included.

The stress components are defined in Figure 37.

I. The distribution of stress in a thick porous cylinder subjected to internal pressure p_a and external pressure p_b

Stresses in a Non-Porous Cylinder.

If a pressure p_a is applied to the internal boundary $(r = a)$, and a pressure p_b applied to the external boundary $(r = b)$ of a non-porous cylinder, the radial and tangential stress components σ_r and σ_θ are:*

$$\sigma_r = \frac{(p_b - p_a)\,a^2 b^2}{(b^2 - a^2)r^2} + \frac{p_a a^2 - p_b b^2}{(b^2 - a^2)}$$

$$\sigma_\theta = -\frac{(p_b - p_a)a^2 b^2}{(b^2 - a^2)r^2} + \frac{p_a a^2 - p_b b^2}{(b^2 - a^2)} \qquad (30)$$

If the external pressure p_b is equal to zero, equations (30) reduce to:

$$\sigma_r = \frac{p_a a^2}{b^2 - a^2}\left(1 - \frac{b^2}{r^2}\right)$$

$$\sigma_\theta = \frac{p_a a^2}{b^2 - a^2}\left(1 + \frac{b^2}{r^2}\right) \qquad (31)$$

It is required to find how the above expressions are affected, in the case of a porous cylinder, by the addition of a body force due to the radial percolation of water.

Distribution of Pore Pressure.

Assuming that the percolation of water through the cylinder obeys Darcy's law of seepage, from Brahtz' first conclusion (see Page 73) the pressure function p obeys the Laplace equation which, in polar co-ordinates, omitting expressions involving because of symmetry, is:

$$\frac{d^2p}{dr^2} + \frac{1}{r}\frac{dp}{dr} = 0$$

* See for example reference 40, Chapter 4, equations 45.

or: $$\frac{1}{r}\frac{d}{dr}\left(r\frac{dp}{dr}\right) = 0$$

therefore: $$r\frac{dp}{dr} = \text{a constant}$$

Solving for p and imposing the boundary conditions:

$$p = p_a \quad at \quad r = a$$
$$p = p_b \quad at \quad r = b$$

the distribution of pore pressure is given by:

$$p = p_a - (p_a - p_b)\frac{\log r/a}{\log b/a} \tag{32}$$

Again if $p_b = 0$, equation (32) reduces to:

$$p = p_a \frac{\log b/r}{\log b/a} \tag{33}$$

Gherardelli's Expressions for the Stress Distribution.

In the paper mentioned in the introduction to this chapter, Gherardelli stated that because the pore pressure p was harmonic, Brahtz' results were applicable.[11] Thus in the simple case where $p_b = 0$, he simply added expression (33) above to the normal stress components (31) for the section of a non-porous cylinder. The resulting expressions, inserting the area factor n, were:

$$\sigma_r = \frac{p_a a^2}{b^2 - a^2}\left(1 - \frac{b^2}{r^2}\right) + n p_a \frac{\log b/r}{\log b/a}$$
$$\sigma_\theta = \frac{p_a a^2}{b^2 - a^2}\left(1 + \frac{b^2}{r^2}\right) + n p_a \frac{\log b/r}{\log b/a} \tag{34}$$

However, when the writer worked out the problem from first principles and included pore pressure terms in the governing equation, it was found that (34) were not the correct expressions for stress, and this lead to a

re-examination of Brahtz' results (Chapter 6, Section I) as applied to multiply-connected bodies.

Brahtz' Conclusions and Multiply-Connected Bodies.

The essence of Brahtz' proof for singly-connected bodies, given in Section I of Chapter 6, was:

i) That the governing equations (5) and (7), and thus the general forms of that stress function ϕ, were indentical for porous and non-porous bodies, and

ii) That the arbitrary constants in the general solution of (5) or (7), which were determined from the boundary conditions, were also identical.

Then from equations (2), it was seen that the stress components differed only by an amount $n\rho$.

The first of the above steps applies to any section whether singly-connected or multiply-connected, for up to that point the boundaries of the section have not been considered. Therefore again, the equation $\nabla^4\phi = 0$ .... (5) and (7), holds good. The general solution of this equation in polar co-ordinates, for a radially symmetrical case, is:

$$\phi = A\log r + Br^2\log r + Cr^2 + D \qquad (35)$$

The stress components (2), rewritten in polar co-ordinates and assuming pore pressure to be the only body force, are, in the case of axial symmetry:

$$\sigma_r = \frac{1}{r}\frac{d\phi}{dr} + n\rho$$

$$\sigma_\theta = \frac{d^2\phi}{dr^2} + n\rho \qquad (36)$$

Considering now the second step of Brahtz' proof, the stress components (36) contain the three arbitrary constants A, B and C in the general expression (35) for ϕ, yet for the section of a cylinder there are only

two boundary conditions, namely the conditions of normal stress at the inner and outer boundaries. Thus the constants cannot be determined from the boundary conditions alone and it is necessary to consider displacements, imposing the conditions that they must single valued functions only. No such conditions are considered in Brahtz' proof.

Substituting the general expression for ϕ , the stress components (36) become:

$$\sigma_r = \frac{A}{r^2} + B(3 + 2\log r) + 2C + n\beta$$

$$\sigma_\theta = -\frac{A}{r^2} + B(3 + 2\log r) + 2C + n\beta \qquad (37)$$

It is shown in Appendix A that the constant B must have a value of zero in the case of a non-porous section, in order to fulfil the condition of single-valued displacements. The remaining constants A and C can be found from the boundary conditions. But in the case of a porous section where pore pressure creates a body force and additional terms are involved in the expressions for displacements, to fulfil the condition of single-valued displacements the constant B has a value greater than zero and so tha values of constants A and C also differ from those for a non-porous section.

It has thus been illustrated that Brahtz' proof is only sufficient for singly-connected sections where the stresses can be determined from the boundary conditions alone. In the case of a multiply-connected section, the additional condition which it is necessary to impose leads to a different particular value of the stress function, so that Brahtz' result is no longer applicable.

The Governing Equation for the Section of a Cylinder.

The equilibrium equation in polar co-ordinates for a symmetrical system is:

$$\frac{d\sigma_r}{dr} + \frac{\sigma_r - \sigma_\theta}{r} + R = 0$$

R is the body force per unit volume of the body, and in this case, due to the presence of water in the pores, is equal to $-n\frac{dp}{dr}$. The equilibrium equation can then be written:

$$\frac{d}{dr}(r\sigma_r) - \sigma_\theta - nr\frac{dp}{dr} = 0 \qquad (38)$$

Equation (38) is automatically satisfied by a stress function F if the stress components are defined in the following manner:

$$\sigma_r = \frac{F}{r}$$
$$\sigma_\theta = \frac{dF}{dr} - nr\frac{dp}{dr} \qquad (39)$$

In the case of complete symmetry, the radial and tangential strain components, ϵ_r and ϵ_θ respectively, expressed in terms of the radial displacement u, are equal to:

$$\epsilon_r = \frac{du}{dr}$$
$$\epsilon_\theta = \frac{u}{r} \qquad (40)$$

Eliminating u between equations (40) gives:

$$\epsilon_\theta - \epsilon_r + r\frac{d\epsilon_\theta}{dr} = 0 \qquad (41)$$

which is the condition for compatibility of strain.

Substituting the plane strain relations:

$$\epsilon_r = \frac{1}{E}\left[(1-\nu^2)\sigma_r - \nu(1+\nu)\sigma_\theta\right]$$
$$\epsilon_\theta = \frac{1}{E}\left[(1-\nu^2)\sigma_\theta - \nu(1+\nu)\sigma_r\right] \qquad (42)$$

in equation (41), and expressing the stress components in terms of the stress function F (equation (39)), the governing equation becomes:

$$r\frac{d^2F}{dr^2} + \frac{dF}{dr} - \frac{F}{r} = \frac{n}{(1-\nu)} r \frac{dp}{dr} + nr\nabla^2 p \qquad (43)$$

Equation (43) is the general equation for any distribution of stress in an axially symmetrical system. In general the solution entails the substitution $r = ae^t$ where a is the radius of the inner boundary and e is the base of natural logarithms.

The Stress Compnents σ_r and σ_θ.

It has been assumed that the pressure function p is harmonic, i.e. $\nabla^2 p = 0$. The governing equation (43) becomes then:

$$r\frac{d^2F}{dr^2} + \frac{dF}{dr} - \frac{F}{r} = \frac{n}{(1-\nu)} r \frac{dp}{dr}$$

Substituting $r = ae^t$

$$\frac{d^2F}{dt^2} - F = \frac{n}{1-\nu} r^2 \frac{dp}{dr} = Qae^t \qquad (44)$$

where Q is a constant and equal to $\frac{nr\frac{dp}{dr}}{1-\nu} = \frac{n(p_a - p_b)}{(1-\nu)\log a/b}$ (from equation 32)

Equation (44) is readily solved to give:

$$F = c_1 r + c_2 \frac{1}{r} + \frac{Q}{2} r \log r \qquad (45)$$

c_1 and c_2 being constants, which must be evaluated from the boundary conditions, viz.

$$\begin{aligned} \sigma_r &= -p_a(1-n) \quad \text{at} \quad r = a \\ \sigma_\theta &= -p_b(1-n) \quad \text{at} \quad r = b \end{aligned} \qquad (46)$$

From equation (45) and (39)

$$\begin{aligned} \sigma_r &= c_1 + \frac{c_2}{r^2} + \frac{Q\log r}{2} \\ \sigma_\theta &= c_1 - \frac{c_2}{r^2} + \frac{Q}{2}(1+\log r) - nr\frac{dp}{dr} \end{aligned} \qquad (47)$$

Thus, imposing the boundary conditions:

$$C_1 + \frac{C_2}{a^2} + \frac{Q \log a}{2} = -p_a(1-n)$$
$$C_1 + \frac{C_2}{b^2} + \frac{Q \log b}{2} = -p_b(1-n) \qquad (48)$$

therefore:

$$C_1 = \frac{(p_a - p_b)a^2}{b^2 - a^2}\left[\frac{n}{2(1-\nu)} + 1 - n\right] - \frac{n(p_a - p_b)}{2(1-\nu)} \frac{\log b}{\log a/b} - p_b(1-n)$$
$$C_2 = -\frac{(p_a - p_b)a^2 b^2}{b^2 - a^2}\left[\frac{n}{2(1-\nu)} + 1 - n\right] \qquad (49)$$

Substituting expressions (49) in (47), the stress components are found to be:

$$\sigma_r = \frac{(p_a - p_b)a^2}{(b^2 - a^2)}\left(1 - \frac{b^2}{r^2}\right)\left[\frac{n}{2(1-\nu)} + 1 - n\right] + \frac{n(p_a - p_b)}{2(1-\nu)} \frac{\log b/r}{\log b/a} - p_b(1-n)$$
$$\sigma_\theta = \frac{(p_a - p_b)a^2}{b^2 - a^2}\left(1 + \frac{b^2}{r^2}\right)\left[\frac{n}{2(1-\nu)} + 1 - n\right] + \frac{n(p_a - p_b)(1 - \log r/b)}{2(1-\nu)\log a/b} + \frac{n(p_a - p_b)}{\log b/a} - p_b(1-n) \qquad (50)$$

When $p_b = 0$ equations (50) reduce to:

$$\sigma_r = \frac{p_a a^2}{(b^2 - a^2)}\left(1 - \frac{b^2}{r^2}\right)\left[\frac{n}{2(1-\nu)} + 1 - n\right] + \frac{n p_a}{2(1-\nu)} \frac{\log b/r}{\log b/a}$$
$$\sigma_\theta = \frac{p_a a^2}{b^2 - a^2}\left(1 + \frac{b^2}{r^2}\right)\left[\frac{n}{2(1-\nu)} + 1 - n\right] + \frac{n p_a}{2(1-\nu)} \frac{\log b/r}{\log b/a} + \frac{n p_a}{2 \log b/a} \frac{(1-2\nu)}{(1-\nu)} \qquad (51)$$

A comparison of equations (51) and (34) will illustrate the fallacy in applying Brahtz' results to multiply-connected sections.

By manipulating the terms in expressions (50) the stress components can be written in the manner shown below (equations (52)). This is done for ease of comparison with the work of A. Lubinski which is discussed in Appendix B.

$$\sigma_r = \frac{n(1-2\nu)}{1-\nu}\frac{p_a - p_b}{2}\left[\frac{\log r/a}{\log b/a} - \frac{b^2(r^2-a^2)}{r^2(b^2-a^2)}\right] - \frac{a^2b^2(p_a-p_b)}{r^2(b^2-a^2)}$$

$$+ \frac{a^2p_a - b^2p_b}{(b^2-a^2)} + n\left[p_a - (p_a-p_b)\frac{\log r/a}{\log b/a}\right] \qquad (52)$$

$$\sigma_\theta = \frac{n(1-2\nu)}{(1-\nu)}\frac{p_a-p_b}{2}\left[\frac{1+\log r/a}{\log b/a} - \frac{b^2(r^2+a^2)}{r^2(b^2-a^2)}\right] + \frac{a^2b^2(p_a-p_b)}{r^2(b^2-a^2)}$$

$$+ \frac{a^2p_a - b^2p_b}{b^2-a^2} + n\left[p_a - (p_a-p_b)\frac{\log r/a}{\log b/a}\right]$$

II. The effect of complete drainage at radius c where $a < c < b$.

The problem is now considered where a concentric drainage ring at radius c reduces the pore pressure from p_a at $r = a$ to zero at $r = c$. The distribution of pressure which can be deduced from equations (33) is given by:

$$p = p_a \frac{\log c/r}{\log c/a} \quad \text{in the region} \quad a < r < c$$

$$p = 0 \quad \text{in the region} \quad c < r < b \qquad (53)$$

The two regions will be referred to as "wet" and "dry" respectively.

The general equation (43), which is applicable for any distribution of pressure, is:

$$r\frac{d^2F}{dr^2} + \frac{dF}{dr} - \frac{F}{r} = \frac{n}{1-\nu} r \frac{dp}{dr} + nr\nabla^2 p \qquad (43)$$

Substituting $r = ae^t$, $\nabla^2 p$ becomes:

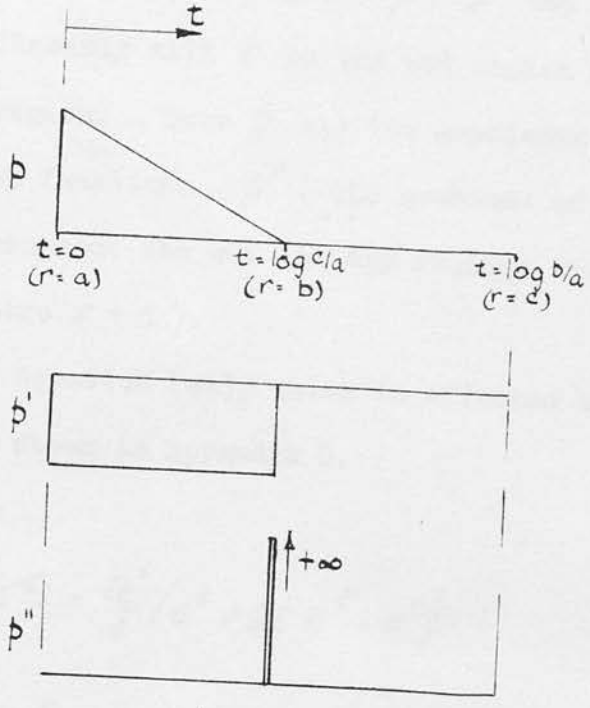

Figure 50

and equation (43) becomes:

$$\frac{d^2F}{dt^2} - F = \frac{\eta}{1-\nu} a e^t \rho' + n a e^t \rho'' \qquad (54)$$

where ρ' denotes $\frac{d\rho}{dt}$ and ρ'' denotes $\frac{d^2\rho}{dt^2}$

Figure 50 shows diagrammatically how ρ, ρ' and ρ'' vary with respect to t. ρ varies linearly with t in the wet ragion and is equal to zero throughout the dry region. Thus ρ has two gradients with respect to t so that ρ' is a step function. ρ'', the gradient of ρ' with respect to t is equal to zero throughout the wet and dry regions, but equal to $\neq \infty$ at $t = \log c/a$ (or where $r = c$).

The solution of equation (44), which is effected by the Laplace transformation method, is shown in Appendix C.

From Appendix C:

$$F = Ae^t + Be^{-t} - \frac{Q'}{4}(e^t + 2t e^t - e^t)$$

$$+ Q'\frac{(1-\nu)}{4}\frac{c}{a}\Big[(1-k')e^{t-\log c/a} + 2(1+k')(t-\log c/a)e^{t-\log c/a} - (1-k')e^{-(t-\log c/a)}\Big]H(t-\log c/a)$$

where $Q' = \frac{n a \rho_a}{(1-\nu)\log c/a}$, $k' = \frac{\nu}{1-\nu}$ and $H(t-\log c/a) = 0$ for $t < \log c/a$, $H(t-\log c/a) = 1$ for $t \geq \log c/a$.

Substituting $r = ae^t$, in equation (45)

$$F = A\frac{c}{a} + B\frac{a}{r} - \frac{Q'}{4}\left(\frac{a}{r} + 2\frac{c}{a}\log\frac{r}{a} - \frac{r}{a}\right)$$

$$+ Q'\frac{(1-\nu)}{4}\frac{c}{a}\left[(1-k')\frac{r}{c} + 2\frac{r}{c}(k'+1)\log\frac{r}{c} - (1-k')\frac{c}{r}\right]H(r-c) \qquad (55)$$

Thus from equation (39):

$$\sigma_r = \frac{A}{a} + \frac{Ba}{r^2} - \frac{Q'}{4a}\left[\frac{a^2}{r^2} + 2\log\frac{r}{a} - 1\right]$$

$$+ Q'\frac{(1-\nu)}{4a}\left[(1-k') + 2(1+k')\log r/c - (1-k')\frac{c^2}{r^2}\right] H(r-c) \qquad (56a)$$

$$*\sigma_\theta = \frac{A}{a} - \frac{Ba}{r^2} - \frac{Q'}{4a}\left[-\frac{a^2}{r^2} + 2\log\frac{r}{a} + 1\right]$$

$$+ Q'\frac{(1-\nu)}{4a}\left[(1-k') + 2(1+k')(1+\log r/c) + (1+k')\frac{c^2}{r^2}\right] H(r-c) - nr\frac{dp}{dr} \qquad (56b)$$

Applying the boundary conditions

$$\sigma_r = -pa(1-n) \quad \text{at } r = a$$

$$\sigma_r = 0 \quad \text{at } r = b$$

to equation (46);

$$-pa(1-n) = \frac{A}{a} + \frac{B}{a}$$

$$0 = \frac{A}{a} + \frac{Ba}{b^2} - \frac{Q'}{4a}\left(\frac{a^2}{b^2} + 2\log b/a - 1\right)$$

$$+ Q'\frac{(1-\nu)}{4a}\left[(1-k') + 2(1+k')\log b/c - (1-k')\frac{c^2}{b^2}\right]$$

Thus, solving for A and B,

---

* For a completely rigorous expression of σ_θ the step function $H(r-c)$ should be differentiated and the term:

$$Q'\frac{(1-\nu)}{4a}\left[(1-k')r + 2r(1+k')\log r/c - (1-k')\frac{c^2}{r}\right]\frac{d}{dr}\left[H(r-c)\right] \qquad (57)$$

added to the equation (56b). However, $\frac{d}{dr}\left[H(r-c)\right]$, being the derivative of a step function, is equal to zero at all points except at $r = c$ where it is infinite. At this point the remainder of expression (57) is zero, so that expression (57) is equal to zero for all values of .

$$B = \frac{ab^2}{b^2-a^2}\left[-p_a(1-n) - \frac{Q'}{4a}\left(\frac{a^2}{b^2} + 2\log\frac{b}{a} - 1\right)\right.$$

$$\left. + \frac{Q'(1-\nu)}{4a}\left[(1-k') + 2(1+k')\log b/c - (1-k')\frac{c^2}{b^2}\right]\right]$$

$$A = \frac{Q'}{4a}\left(\frac{a^2}{b^2} + 2\log\frac{b}{a} - 1\right) - \frac{Q'(1-\nu)}{4a}\left[(1-k') + 2(1+k')\log b/c - (1-k')\frac{c^2}{b^2}\right] - B\frac{a^2}{b^2}$$

Inserting the values for A, B, Q' and k' in equations (46), the stress components are found to be:

$$\sigma_r = \frac{p_a a^2}{(b^2-a^2)}\left(1 - \frac{b^2}{r^2}\right)\left[1 - n + \frac{n}{2(1-\nu)} - \frac{n(1-2\nu)(1-c^2/b^2)}{4(1-\nu)\log c/a}\right]$$

$$+ \frac{n p_a}{4(1-\nu)\log c/a}\left[2\log c/r - (1-2\nu)(1-c^2/b^2)\right]$$

$$+ \frac{n p_a}{4(1-\nu)\log c/a}\left[2\log r/c + (1-2\nu)(1-\frac{c^2}{r^2})\right] H(r-c) \qquad (58a)$$

$$\sigma_\theta = \frac{p_a a^2}{b^2-a^2}\left(1 + \frac{b^2}{r^2}\right)\left[1 - n + \frac{n}{2(1-\nu)} - \frac{n(1-2\nu)(1-\frac{c^2}{b^2})}{4(1-\nu)\log c/a}\right]$$

$$+ \frac{n p_a}{4(1-\nu)\log c/a}\left[2(\log c/r - 1) - (1-2\nu)(1-\frac{c^2}{b^2})\right]$$

$$+ \frac{n p_a}{4(1-\nu)\log c/a}\left[2(\log r/c + 1) + (1-2\nu)(1+\frac{c^2}{r^2})\right] H(r-c) - nr\frac{dp}{dr} \qquad (58b)$$

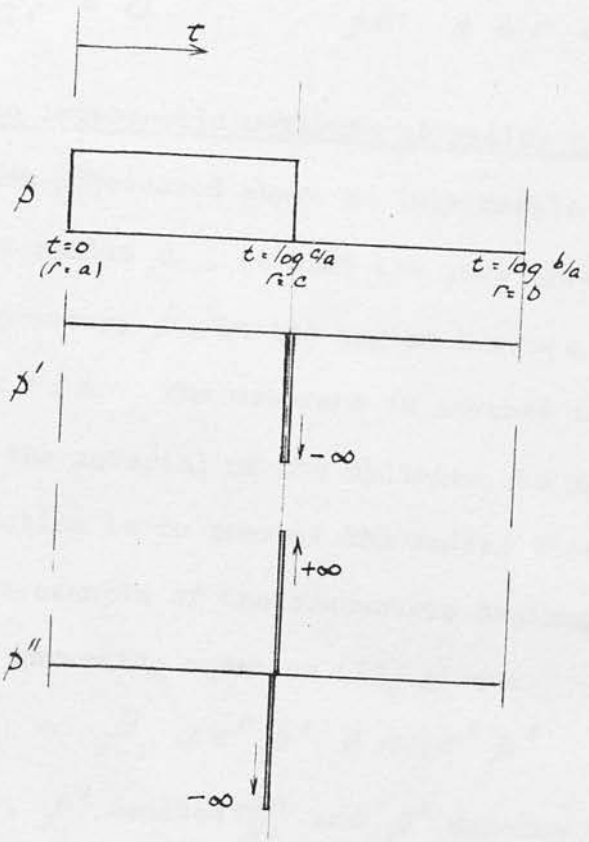

Figure 51

where, from equation (53)

$$nr\frac{dp}{dr} = -\frac{np_o}{\log c/a} \qquad \text{for } a < r < c$$

$$nr\frac{dp}{dr} = 0 \qquad \text{for } c < r < b.$$

III. <u>The effect of an impermeable membrane at radius c where $a < c < b$.</u>

The problem is now considered where an impermeable membrane exists within the cylinder at radius c, so that the pore pressure p is equal to the internal applied pressure p_a in the region $a < r < c$, and is equal to zero in the region $c < r < b$. The membrane is assumed to be sufficiently elastic compared with the material of the cylinder, to have no constraining effect. Its sole function is to prevent the radial flow of water.

As in the previous example of the concentric drainage ring, the substitution $r = ae^t$ in the governing equation (43) gives:

$$F'' - F = \frac{n}{1-\nu} ae^t p' + nae^t p'' \qquad (54)$$

where F'' denotes $\frac{d^2F}{dt^2}$, p' denotes $\frac{dp}{dt}$ and p'' denotes $\frac{d^2p}{dt^2}$

The pressure function has been defined as:

$$\begin{aligned} p &= p_a \quad \text{in the region} \quad a < r < c \\ p &= 0 \quad \text{in the region} \quad c < r < b \end{aligned} \qquad (59)$$

Figure 51 shows diagrammatically how p, p', and p'' vary with respect to t. Since p is a step function p' is equal to zero throughout the wet and dry regions, but is infinite at $r = c$. p'' is also zero throughout both regions but at $r = c$ it tends to minus infinity on the side $r < c$ and to plus infinity on the side $r > c$.

The solution to equation (54) for the particular values of p (59), is again effected by the Laplace transformation method and is shown in

Appendix D.

From Appendix D, the value of F is found to be:

$$F = Ae^{t} + Be^{-t} - n\frac{\rho_a}{2}c\left[(1+k')e^{t-\log c/a} + (1-k')e^{-(t-\log c/a)}\right] H(t-\log c/a) \qquad (60)$$

where, as before A and B are arbitrary constants,

Substituting $r = ae^{t}$ in equation (60):

$$F = A\frac{r}{a} + B\frac{a}{r} - n\frac{\rho_a}{2}r\left[(1+k') + (1-k')\frac{c^2}{r^2}\right] H(r-c) \qquad (61)$$

Substituting equation (61) in equations (39), the stress components become:

$$\sigma_r = \frac{A}{a} + \frac{Ba}{r^2} - n\frac{\rho_a}{2}\left[(1+k') + (1-k')\frac{c^2}{r^2}\right] H(r-c) \qquad (62a)$$

$$\sigma_\theta = \frac{A}{a} - \frac{Ba}{r^2} - n\frac{\rho_a}{2}\left[(1+k') - (1-k')\frac{c^2}{r^2}\right] H(r-c)$$
$$- n\frac{\rho_a}{2}r\left[(1+k') + (1-k')\frac{c^2}{r^2}\right]\frac{d}{dr}\left[H(r-c)\right] - nr\frac{dp}{dr} \qquad (62b)$$

The last two terms of expression (62b) are equal to zero throughout the wet and dry regions, and at $r = c$ they are equal respectively to plus infinity and minus infinity. It is shown in Appendix E that the integrals of these two terms are equal in magnitude but opposite in sign so that they cancel out.

Applying the boundary conditions:

$$\sigma_r = -\rho_a(1-n) \quad \text{at} \quad r = a$$

$$\sigma_r = 0 \quad \text{at} \quad r = b$$

to expression (62a), the arbitrary constants are found to be:

$$B = -\frac{\rho_a a b^2}{(b^2-a^2)}\left[(1-n) + \frac{n}{2}\left(1+k' + (1-k')\frac{c^2}{b^2}\right)\right]$$

$$A = n\frac{\rho_a}{2}a\left[1+k' + (1-k')\frac{c^2}{b^2}\right] - B\frac{a^2}{b^2} \qquad (63)$$

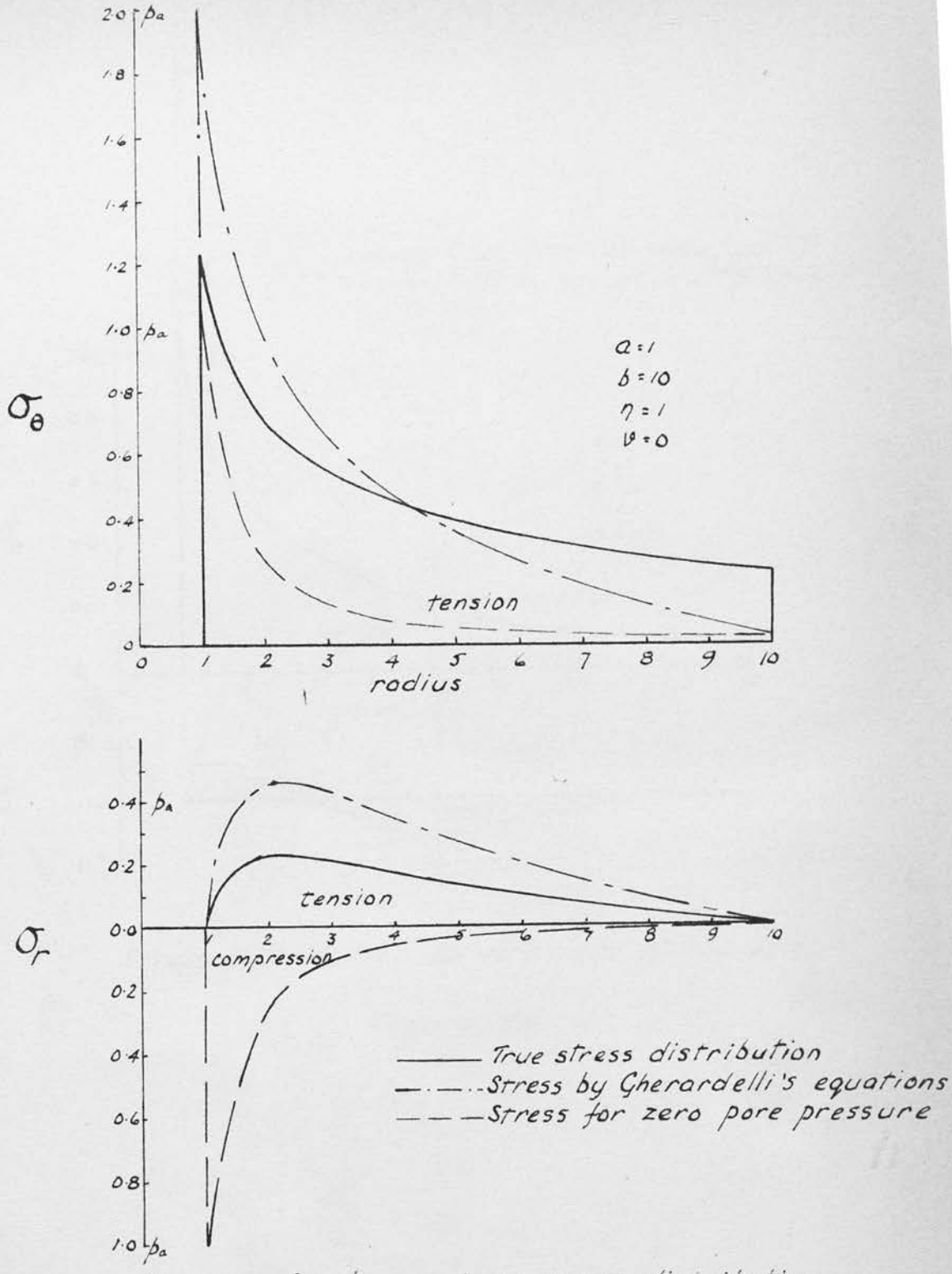

Stresses for harmonic pressure distribution

Figure 53

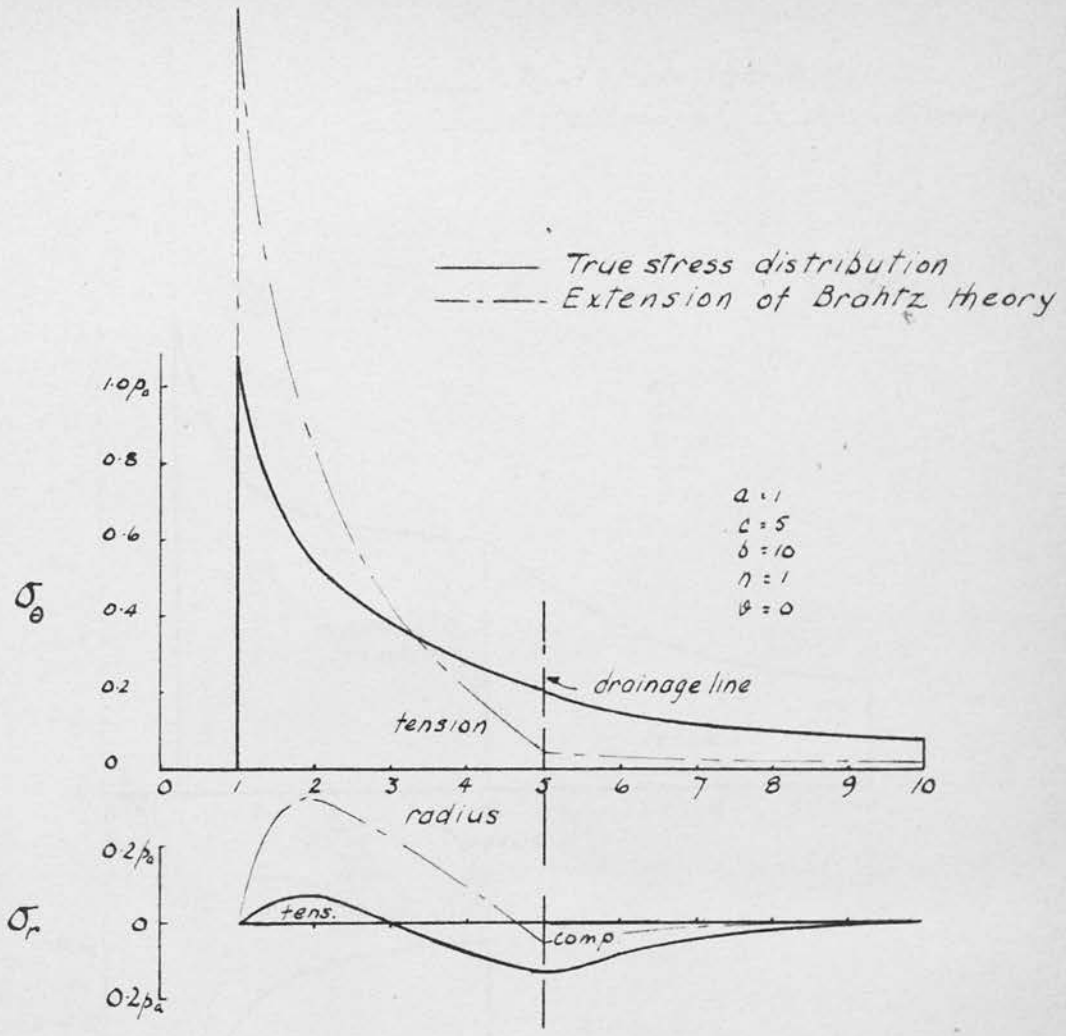

Stress distribution for drainage of radius c.

Figure 54

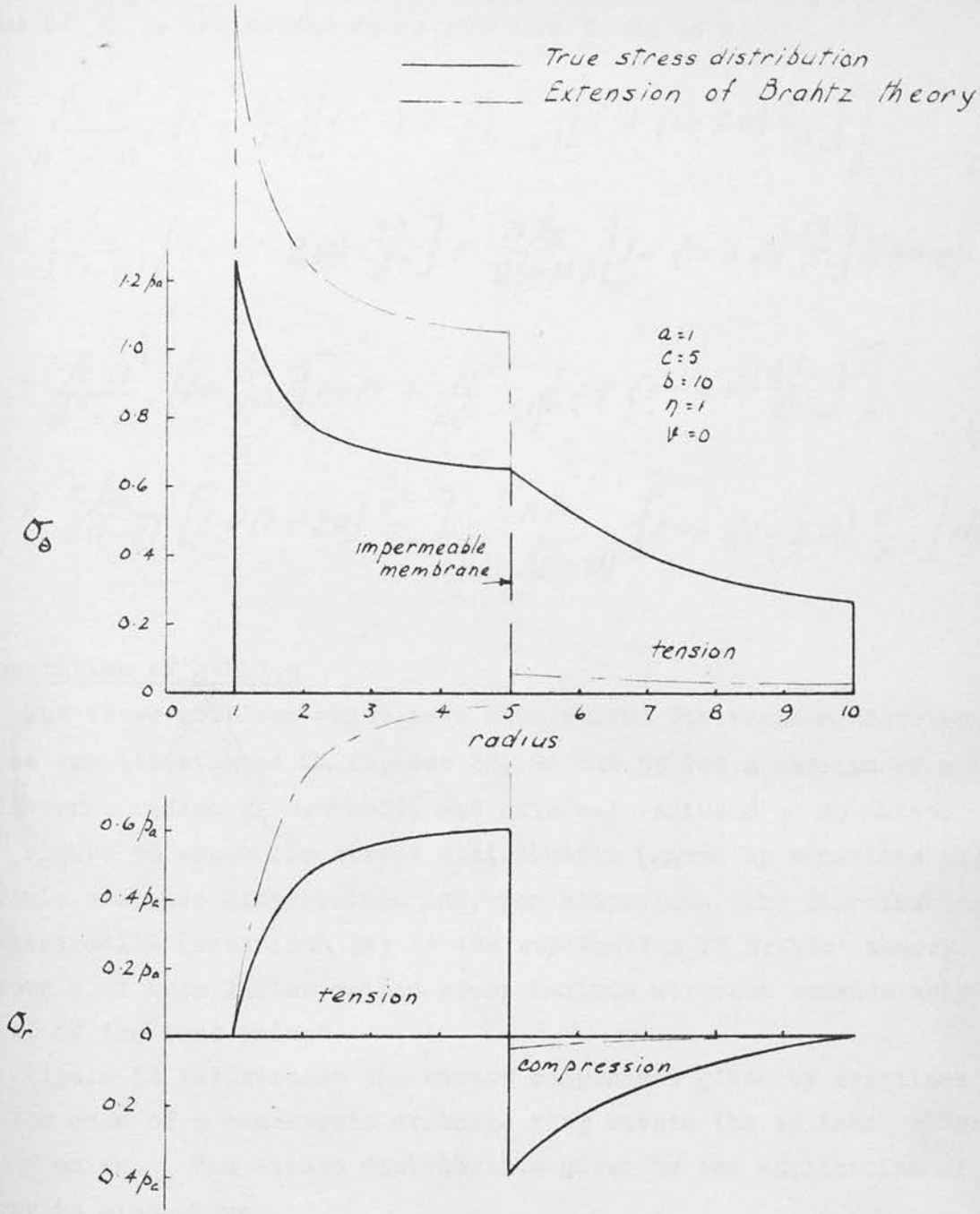

Stress distribution for membrane at radius c

Figure 55

Substituting the values for A and B (expressions 63) and inserting the value of k', the stress components are found to be:

$$\sigma_r = \frac{p_a a^2}{b^2 - a^2}\left(1 - \frac{b^2}{r^2}\right)\left[1 - n + \frac{n}{2(1-\nu)}\left[1 + (1-2\nu)\frac{c^2}{b^2}\right]\right] \qquad (64a)$$

$$+ \frac{n p_a}{2(1-\nu)}\left[1 + (1-2\nu)\frac{c^2}{b^2}\right] + \frac{n p_a}{2(1-\nu)}\left[1 - (1-2\nu)\frac{c^2}{r^2}\right] H(r-c)$$

$$\sigma_\theta = \frac{p_a a^2}{b^2 - a^2}\left(1 + \frac{b^2}{r^2}\right)\left[1 - n + \frac{n}{2(1-\nu)}\left[1 + (1-2\nu)\frac{c^2}{b^2}\right]\right] \qquad (64b)$$

$$+ \frac{n p_a}{2(1-\nu)}\left[1 + (1-2\nu)\frac{c^2}{b^2}\right] - \frac{n p_a}{2(1-\nu)}\left[1 - (1-2\nu)\frac{c^2}{r^2}\right] H(r-c)$$

Illustration of Results.

The three problems which have been solved for various distributions of stress are illustrated in Figures 53, 54 and 55 for a section of a cylinder of internal radius $a = 1$ unit, and external radius $b = 10$ units.

Figure 53 shows the stress distribution (given by equations 51) for a harmonic pressure distribution and, for comparison, the distribution given by Gherardelli (equations 34) by the application of Brahtz' theory. It is seen that this latter method gives maximum stresses considerably in excess of the true values.

Figure 54 illustrates the stress components given by equations (58) for the case of a concentric drainage ring within the cylinder at radius $c = 5$ units. The stress distribution given by the application of Brahtz' theory is also shown.

Figure 55 illustrates the stress components given by equations (64) for the case of an impermeable membrane within the cylinder at radius $c = 5$ units. The stress distribution given by the application of Brahtz' theory is also shown.

Restating the conclusions of Chapters 6 and 7 regarding Brahtz' theory, its applicability is confined to simply-connected bodies in regions of harmonic pressure distribution.

APPENDIX A
EVALUATION OF THE CONSTANTS A, B AND C IN EQUATION (37) BY CONSIDERATION OF DISPLACEMENTS*

The radial and tangential displacements, u and v respectively, must be expressed in terms of r, θ and the arbitrary constants A, B and C.

The components of radial, tangential and shear strain (respectively) can be expressed in terms of the radial and tangential displacements, u and v, as follows:

$$\epsilon_r = \frac{\partial u}{\partial r} \qquad \text{(ia)}$$

$$\epsilon_\theta = \frac{u}{r} + \frac{1}{r}\frac{\partial v}{\partial \theta} \qquad \text{(ib)}$$

$$\gamma_{r\theta} = \frac{1}{r}\frac{\partial u}{\partial \theta} + \frac{\partial v}{\partial r} - \frac{v}{r} \qquad \text{(ic)}$$

Using Hooke's law, the strain components can also be expressed in terms of the stress components:

$$\epsilon_r = \frac{1}{E}\left[(1-\nu^2)\sigma_r - \nu(1+\nu)\sigma_\theta\right] \qquad \text{(iia)}$$

$$\epsilon_\theta = \frac{1}{E}\left[(1-\nu^2)\sigma_\theta - \nu(1+\nu)\sigma_r\right] \qquad \text{(iib)}$$

$$\gamma_{r\theta} = \frac{2(1+\nu)}{E}\tau_{r\theta} \qquad \text{(iic)}$$

From (ia) and (iia), substituting the expression (37)

---

* The analysis is derived from that given by Timoshenko and Goodier (Theory of Elasticity, Second Edition, Chapter 4, Section 29) for non-porous rings or curved bars with symmetrical stress distribution.

$$\frac{\partial u}{\partial r} = \frac{1}{E}\left[\frac{A}{r^2}(1+\nu) + B(1-3\nu-4\nu^2) + 2B\log r(1-\nu-2\nu^2)\right.$$
$$\left. + 2C(1-\nu-2\nu^2) + n(1-\nu-2\nu^2)p\right]$$

and integrating with respect to r,

$$u = \frac{1}{E}\left[-\frac{A}{r}(1+\nu) - Br(1+\nu) + 2Br\log r(1-\nu-2\nu^2)\right.$$
$$\left. + 2Cr(1-\nu-2\nu^2) + n(1-\nu-2\nu^2)\int p\,dr\right] + f(\theta) \qquad \text{(iii)}$$

where $f(\theta)$ is a function of θ only.

From (ib) and (iib)

$$\frac{\partial v}{\partial \theta} = r\epsilon_\theta - u$$
$$= \frac{r}{E}\left[(1-\nu^2)\sigma_\theta - \nu(1+\nu)\sigma_r\right] - u$$

and substituting from (37) and (iii)

$$= \frac{1}{E}\left[4Br(1-\nu^2) + n(1-\nu-2\nu^2)[pr - \int p\,dr]\right] - f(\theta)$$

Integrating with respect to θ,

$$v = \frac{1}{E}\left[4Br(1-\nu^2)\theta + n(1-\nu-2\nu^2)[pr - \int p\,dr]\theta\right] - \int f(\theta)\,d\theta + f(r) \qquad \text{(iv)}$$

where $f(r)$ is a function of (r) only.

For a system of symmetrical stress distribution the shear stress $\tau_{r\theta}$ is zero, therefore, $\gamma_{r\theta}$ is also zero. Thus, substituting (iii) and (iv) in (ic)

$$\frac{1}{r}\frac{df(\theta)}{d\theta} + \frac{df(r)}{dr} + \frac{1}{r}\int f(\theta)\,d\theta - \frac{1}{r}f(r) = 0$$

from which, by separating functions of r and θ,

$$f(r) = F_1 r + F_2 \quad : \quad f(\theta) = F_3 \sin\theta + F_4 \cos\theta \qquad \text{(v)}$$

F_1, F_2, F_3 and F_4 being constants.

Substituting expressions (v) in (iii) and (iv)

$$u = \left[-\frac{A}{r}(1+\nu) - Br(1+\nu) + 2Br\log r(1-\nu-2\nu^2) + 2Cr(1-\nu-2\nu^2) + n(1-\nu-2\nu^2)\int p\,dr \right] + F_3 \sin\theta + F_4 \cos\theta \qquad \text{(vi)}$$

$$v = 4\frac{Br(1-\nu^2)}{E}\theta + \frac{n}{E}(1-\nu-2\nu^2)\left[pr - \int p\,dr\right]\theta + F_3\cos\theta - F_4 \sin\theta + F_1 r + F_2 \qquad \text{(vii)}$$

Considering now the section of a cylinder, from symmetry displacements can occur only in radial planes. v must therefore be zero for all values of θ.

It follows from (vii) that

$$4\frac{Br(1-\nu^2)}{E} + \frac{n}{E}(1-\nu-2\nu^2)\left[pr - \int p\,dr\right] = 0$$

$$F_1 = 0$$

$$F_2 = 0$$

$$F_3 = 0$$

$$F_4 = 0$$

For a non-porous body, the pore-pressure terms involving p must vanish and so $B = 0$

However, where pore pressure exists:

$$B = -\frac{n}{4}\frac{(1-2\nu)}{(1-\nu)}\frac{1}{r}\left[pr - \int p\,dr\right]$$

$$= -\frac{n(1-2\nu)}{4(1-\nu)}\frac{1}{r}\left[pr - \int p_a \frac{\log b/r}{\log b/a}\,dr\right]$$

$$= \frac{n(1-2\nu)}{4(1-\nu)}\frac{p_a}{\log b/a}$$

The two remaining constants A and C must now be determined from the boundary conditions.

APPENDIX B

THE THERMAL ANALOGY METHOD OF ARTHUR LUBINSKI

Lubinski's work has been published in the Proceedings of the Second U.S. National Congress of Applied Mechanics, Pages 247 to 256, under the heading "The Theory of Elasticity for Bodies Displaying a Strong Pore Structure". Lubinski illustrates the similarity between problems involving thermal stress and problems involving pore pressure, and devises a method by which the solution to the latter type of problem can be deduced from a solution to the former in geometrically similar bodies. His paper takes into account not only the elastic properties of the porous medium treated as a homogeneous material, but also the elastic properties of the interpore matter.

Lubinski's Stress-Strain Relation.

The stresses in a porous material are considered to be of two types; microstresses which are the stresses in the interpore material, and macrostresses which are the average stresses on plane sections through pores and interpore material, i.e., the macrostress is the common conception of stress in concrete or rock when they are regarded as homogeneous materials.

The relationship between macrostress and microstress is then, according to Lubinski,

$$\text{macrostress} = \text{microstress}\ (1-f)$$

where f is the volumetric porosity or the sectional porosity of a plane section. The writer does not agree with this relation for the same reasons that objection was made in Chapter 4 to Lubinski's expression for the body force caused by pore pressure. Lubinski's relation between

macrostress and microstress does not take into account the internal structure of concrete and natural rocks of similar structure in which the intergranular bonds or ligatures are responsible for the deformation of the material. In such materials the microstresses in the ligatures are quite different from the microstresses in the granules because of the much smaller cross-sectional area of the former, and since Lubinski's analysis concerns only microstresses caused by pore pressure, the relation which should be used is

$$\text{macrostress} = \text{microstress}\,(1-n)$$

where n is the area factor which has been discussed at length in Chapter 4. Lubinski's ultimate results are still valid if n is substituted for f.

The strain caused by a constant pressure p all round the body and inside the pores is, by Hooke's law,

$$\epsilon' = -\frac{1-2\nu_i}{E_i}p \qquad (2)^*$$

where E_i and ν_i are, respectively, Young's modulus and Poisson's ratio of the interpore material and p is a microstress.

If the same body is made impervious so that no pore pressure exists within the pores, then the strain caused by an all round pressure p is

$$\epsilon = -\frac{1-2\nu}{E}p$$

where E and ν are, respectively, Young's modulus and Poisson's ratio of the porous material and p is a macrostress.

To obtain a general stress-strain relationship for a porous body, stress and strain are each considered to be composed of two parts. One part of the stress, a microstress, is related to the corresponding part of the

---

* The numbers of the equations correspond to those in Lubinski's paper.

strain by the elastic contents of the interpore material. This relation is expressed in equation (2). The second part of the stress, which is a macrostress, is related to the corresponding part of the strain by the elastic constants of the porous material. Denoting the components of this macrostress by σ_x'', σ_y'' and σ_z'' and the corresponding components of strain by ϵ_x'', ϵ_y'' and ϵ_z'' the relations between them are, again by Hooke's law:

$$\begin{aligned} \epsilon_x'' &= \frac{1}{E}\left[\sigma_x'' - \nu(\sigma_y'' + \sigma_z'')\right] \\ \epsilon_y'' &= \frac{1}{E}\left[\sigma_y'' - \nu(\sigma_z'' + \sigma_x'')\right] \\ \epsilon_z'' &= \frac{1}{E}\left[\sigma_z'' - \nu(\sigma_x'' + \sigma_y'')\right] \end{aligned} \tag{6}$$

The total strain being the sum of the two parts of strain, it follows that:

$$\begin{aligned} \epsilon_x &= \epsilon_x'' + \epsilon' = \frac{1}{E}\left[\sigma_x'' - \nu(\sigma_y'' + \sigma_z'')\right] - \frac{1-2\nu_i}{E_i}p \\ \epsilon_y &= \epsilon_y'' + \epsilon' = \frac{1}{E}\left[\sigma_y'' - \nu(\sigma_z'' + \sigma_x'')\right] - \frac{1-2\nu_i}{E_i}p \\ \epsilon_z &= \epsilon_z'' + \epsilon' = \frac{1}{E}\left[\sigma_z'' - \nu(\sigma_x'' + \sigma_y'')\right] - \frac{1-2\nu_i}{E_i}p \end{aligned} \tag{7}$$

Further since macrostress is equal to microstress $(1-f)$, (where f is in fact the area factor and not the sectional porosity), the total stress components are:

$$\begin{aligned} \sigma_x &= \sigma_x'' - (1-f)p \\ \sigma_y &= \sigma_y'' - (1-f)p \\ \sigma_z &= \sigma_z'' - (1-f)p \end{aligned} \tag{8}$$

Solving for σ_x'', σ_y'' and σ_z'' in (8) and substituting into (7),

Lubinski's basic stress-strain relationships are found to be:

$$\epsilon_x = \frac{1}{E}\left[\sigma_x - \nu(\sigma_y + \sigma_z)\right] + \frac{1-2\nu}{E}(1-\beta-f)\,p$$

$$\epsilon_y = \frac{1}{E}\left[\sigma_y - \nu(\sigma_z + \sigma_x)\right] + \frac{1-2\nu}{E}(1-\beta-f)\,p \qquad (9)$$

$$\epsilon_z = \frac{1}{E}\left[\sigma_z - \nu(\sigma_x + \sigma_y)\right] + \frac{1-2\nu}{E}(1-\beta-f)\,p$$

where

$$\beta = \frac{E/(1-2\nu)}{E_i/(1-2\nu_i)}$$

i.e., β is the ratio of the compressibility of the interpore material to the compressibility of the porous material. This can be determined by measuring the contraction of jacketed and unjacketed specimens of the material subjected to an all round hydrostatic pressure.

Analogy with Thermal Stresses.

Lubinski compares his expressions (9) to Timoshenko's stress-strain relations for thermal expansion:

$$\epsilon_x = \frac{1}{E}\left[\sigma_x - \nu(\sigma_y + \sigma_z)\right] + \alpha T$$

$$\epsilon_y = \frac{1}{E}\left[\sigma_y - \nu(\sigma_z + \sigma_x)\right] + \alpha T \qquad (11)$$

$$\epsilon_z = \frac{1}{E}\left[\sigma_z - \nu(\sigma_x + \sigma_y)\right] + \alpha T$$

where α is the coefficient of thermal expansion and T is the temperature.

By making $\alpha = \frac{1-2\nu}{E}(1-\beta-f)$ and $T = p$, expressions (11) are identical to expressions (9). This is the basis of Lubinski's thermal analogy method of solving problems of porous bodies. He points out that the analogy between pore pressure and thermal problems is not complete simply because of the similarity of the stress-strain relations, and he goes on to establish what adjustments must be made to the terms of a thermal

analysis to account for the boundary and body forces in pore pressure problems. These adjustments are finally set out in a table from which it is possible to convert solutions for one type of problem to those for the other type.

		Porous body problem	Thermal problem
Body forces (for displacements and stresses)		$-(1-\beta)\frac{\partial p}{\partial x}$	$-\frac{\alpha E}{(1-2\nu)}\cdot\frac{\partial T}{\partial x}$
Surface forces at: (for displacements and stresses)	Permeable boundaries	$+(1-\beta)p \quad -p$	$+\frac{\alpha E}{1-2\nu}\cdot T$
	Impermeable boundaries	$+(1-\beta)p \quad -p_c$	$+\frac{\alpha E}{1-2\nu}\cdot T$
Stress equal in all directions (for stresses only)		$-(1-\beta)p + f p$	$-\frac{\alpha E}{1-2\nu}\,T$

The chief merit of this method lies in overcoming some of the difficulties of integration which can be met in the solution of pore pressure problems by more conventional methods: many thermal problems have been solved and the results have been published, so that it is only necessary to refer to these results and make the necessary adjustments to obtain the solution to pore pressure problems for geometrically similar bodies.

Lubinski's Solution to the Problem of Radial Drainage in a Cylinder.

As an illustration of his method, Lubinski gives the solution to the problem of radial drainage in a porous cylinder, based on Timoshenko's solution for the thermal stresses in a similar body of solid material. Lubinski's expressions for radial and tangential stress are:

$$\sigma_r = (1-\beta)\frac{1-2\nu}{1-\nu}\,\frac{p_a-p_b}{2}\left[\frac{\log r/a}{\log b/a} - \frac{b^2(r^2-a^2)}{r^2(b^2-a^2)}\right] - \frac{a^2b^2(p_a-p_b)}{r^2(b^2-a^2)}$$

$$+\frac{a^2p_a-b^2p_b}{(b^2-a^2)} + f\left[p_a-(p_a-p_b)\frac{\log r/a}{\log b/a}\right] \qquad (33)$$

$$\sigma_\theta = \frac{(1-\beta)(1-2\nu)}{1-\nu}\left(\frac{p_a - p_b}{2}\right)\left[\frac{1+\log r/a}{\log b/a} - \frac{b^2(r^2+a^2)}{r^2(b^2-a^2)}\right] + \frac{a^2b^2(p_a-p_b)}{r^2(b^2-a^2)}$$

$$+ \frac{a^2p_a - b^2p_b}{(b^2-a^2)} + f\left[p_a - (p_a-p_b)\frac{\log r/a}{\log b/a}\right] \qquad (33)$$

The corresponding expressions derived by the writer are:

$$\sigma_r = \eta\frac{(1-2\nu)}{(1-\nu)}\left(\frac{p_a-p_b}{2}\right)\left[\frac{\log r/a}{\log b/a} - \frac{b^2(r^2-a^2)}{r^2(b^2-a^2)}\right] - \frac{a^2b^2(p_a-p_b)}{r^2(b^2-a^2)}$$

$$+ \frac{a^2p_a - b^2p_b}{(b^2-a^2)} + \eta\left[p_a - (p_a-p_b)\frac{\log r/a}{\log b/a}\right]$$

$$\sigma_\theta = \eta\frac{(1-2\nu)}{(1-\nu)}\left(\frac{p_a-p_b}{2}\right)\left[\frac{1+\log r/a}{\log b/a} - \frac{b^2(r^2+a^2)}{r^2(b^2-a^2)}\right] + \frac{a^2b^2(p_a-p_b)}{b^2-a^2}$$

$$+ \frac{a^2p_a - b^2p_b}{b^2-a^2} + \eta\left[p_a - (p_a-p_b)\frac{\log r/a}{\log b/a}\right]$$

It will be noted that the only difference between these expressions, assuming that Lubinski's f denotes the area factor and not the porosity, is that in the former case the first term of each expression is multiplied by $(1-\beta)$ whereas in the latter case it is multiplied by η.

Terzaghi has shown that β for concrete, under ideal laboratory conditions, is less than 1/200, so that β might be safely ignored in Lubinski's expressions if it assumed that a concrete cylinder is being considered. There is apparently still a serious discrepancy between the two sets of results if η or f is appreciably less than unity.

There is in fact no discrepancy at all once it is realized that $(1-\beta)$ is equal to η by the following reasoning.

Lubinski has pointed out that β can be measured by noting the contraction of jacketed and unjacketed specimens of the material subjected to a hydrostatic pressure p. Writing this in symbols:

$$\beta = \frac{E}{1-2\nu} \Big/ \frac{E_i}{1-2\nu_i} = \frac{p/\epsilon}{p/\epsilon_i} = \frac{\epsilon_i}{\epsilon}$$

where ϵ is the measured strain in the jacketed specimen with no pore pressure and ϵ_i is the measured strain in the unjacketed specimen which is also the strain in the interpore material. Furthermore, the contraction in each case is proportional to the applied macrostress which is constant throughout the specimen, so that:

$$\frac{p(1-n)}{p} = \frac{\epsilon_i}{\epsilon} = (1-n)$$

Thus it is seen that n is equal to $(1-\beta)$

The above argument holds good whether f is considered equal to n or to the porosity, for if the latter, then the macrostress in the unjacketed specimen must be taken as $p(1-f)$

From the relation which has been established, it is seen that the last term of Lubinski's expressions (9) is equal to zero, a fact which he has obviously not realized, especially since in a numerical example he has taken $\beta = 0.25$ and $f = 0.15$. Replacing $(1-\beta)$ by f in his expressions (33), it is seen that they no longer contain any elastic constants of the interpore material, and they are identical with those derived from more simple principles by the writer. The only fault in Lubinski's analysis is in his conception of the factor f.

β has only been measured under ideal static conditions and the value of f or n, as discussed in Chapter 4, is still in dispute; but whatever values are chosen for these constants they are always complimentary fractions of unity.

Lubinski's table could be amended for more convenient use by replacing β by $(1-f)$, but it is convenient to retain the term $(1-\beta-f)$ in expressions (9) to provide a basis for the analogy with thermal stresses.

APPENDIX C

The solution of equation (54),

$$F'' - F = \frac{nae^t}{(1-\vartheta)} p' + nae^t p'' \qquad (54)$$

for the case where

$p = p_a \frac{\log c/r}{\log c/a}$ in the region $a < r < c$ (or $0 < t < \log c/a$)

$p = 0$ in the region $c < r < b$ (or $\log c/a < t < \log b/a$)

If $f(t)$ is a function of t, the Laplace transofrmation of $f(t)$, which is denoted by $\bar{f}(t)$, is defined in the following manner:

$$\bar{f}(t) = \int_0^\infty e^{-mt} f(t)\,dt$$ where m is a positive integer.

The transformation will be applied to each term of equation (54) in turn.

i) $\int_0^\infty e^{-mt} F\,dt = \bar{F}$

ii) $\int_0^\infty e^{-mt} F''\,dt = m^2\bar{F} - mF_0 - F_0''$ (integrating by parts)

where F_0 and F_0' are the values of F and F' when $t = 0$

iii) p' is a step function (see Chapter 7, Figure 50) with the values

$p' = -\frac{p_a}{\log c/a}$ in the region $a < r < c$ or $0 < t < \log c/a$

$p' = 0$ in the region $r > c$ or $t > \log c/a$

Thus:

$$\int_0^\infty e^{(1-m)t} p' \, dt = \int_0^{\log c/a} \frac{-p_a}{\log c/a} e^{(1-m)t} \, dt$$

$$= \frac{-p_a}{\log c/a} \left[\frac{e^{(1-m)\log c/a}}{1-m} - 1 \right]$$

iv) $\int_0^\infty e^{(1-m)t} p'' \, dt$, integrating by parts, is

$$\left| p' e^{(1-m)t} \right|_0^\infty - (1-m) \int_0^\infty p' e^{(1-m)t} \, dt$$

$$= \frac{p_a}{\log c/a} + \frac{p_a}{\log c/a} \left[e^{(1-m)\log c/a} - 1 \right]$$

$$= \frac{p_a}{\log c/a} e^{(1-m)\log c/a}$$

Substituting the transformed expressions into the original equation (54)

$$\bar{F} = \frac{m F_0 + F_0'}{m^2 - 1} - \frac{n a p_a (1+k')}{\log c/a \, (m^2-1)(m-1)} + \frac{n a p_a (k'+m)}{\log c/a \, (m^2-1)(m-1)} e^{(1-m)\log c/a}$$

where

$$k' = \frac{v}{1-v}$$

Expressing the above equation in partial fractions to facilitate the use of transformtables:

$$\bar{F} = \frac{A}{m-1} + \frac{B}{m+1} - \frac{Q}{4}\left[\frac{1}{m+1} + \frac{2}{(m-1)^2} - \frac{1}{(m-1)}\right]$$

$$+ Q\frac{(1-v)}{4} e^{(1-m)\log c/a}\left[\frac{(1-k')}{(1-m)} + 2\frac{(1+k')}{(1-m)^2} - \frac{(1-k')}{(1+m)}\right]$$

where $Q = \frac{mkp_a}{(1-v)\log c/a}$, $A = F_0 + \frac{F_0'}{2}$ and $B = F_0 - \frac{F_0'}{2}$

Applying standard transform tables, the value of $\bar{F}$ is found to be:

$$F = Ae^{t} + Be^{-t} - \frac{Q}{4}(e^{-t} + 2te^{t} - e^{t})$$

$$+ Q\frac{(1-v)}{4}\frac{c}{a}\left[(1-k')e^{t-\log c/a} + 2(1+k')(t-\log c/a)e^{t-\log c/a} - (1-k')e^{t-\log c/a}\right]H(t-\log c/a)$$

where $H = 0$ for $0 < t < \log c/a$

$H = 1$ for $\log c/a < t < \log b/a$

This is the required solution in terms of the variable t.

APPENDIX D

The solution of equation (54):

$$F'' - F = \frac{na\,e^t}{1-\nu}\,p' + na e^t\,p''$$

for the case where

$p = p_a$ in the region $a < r < c$ $\quad (a\ 0 < t < \log c/a)$

$p = 0$ in the region $c < r < b$ $\quad (a\ \log c/a < t < \log r/a)$

The Laplace transformation will be applied to each term of equation (54)

(i) $$\int_0^\infty e^{-mt} F\,dt = \bar{F}$$

(ii) $$\int_0^\infty e^{-mt} F''\,dt = m^2\bar{F} - m F_0 - F_0'$$

(iii) + (iv) $$\int_0^\infty e^{(1-m)t}\left(\frac{p'}{1-\nu} + p''\right)dt$$

$$= \int_0^\infty \frac{p'}{1-\nu}\,e^{(1-m)t}\,dt + \Big|\underset{(=0)}{p' e^{(1-m)t}}\Big|_0^\infty - \int_0^\infty p'(1-m)\,e^{(1-m)t}\,dt$$

$$= \int_0^\infty p'\,e^{(1-m)t}\left(\frac{1}{(1-\nu)} - 1 + m\right)dt \qquad \left[\begin{matrix} e^{(1-m)t} = 0 \text{ at } t = \infty \\ p' = 0 \text{ at } t = 0 \end{matrix}\right]$$

$$= (k'+m)\left[\Big|e^{(1-m)t}\,p\Big|_0^\infty - (1-m)\int_0^\infty p\,e^{(1-m)t}\,dt\right] \qquad \left[\text{inserting } k' = \frac{\nu}{(1-\nu)}\right]$$

$$= 1-$$

$$= (k'+m)\left[-p_a - (1-m)\,p_a(1-H)\int_0^{\infty} e^{(1-m)t}\,dt\right]$$

$$\left[\begin{array}{l} H=0 \text{ for } r<c \\ \quad \text{or } t<\log c/a \\ H=1 \text{ for } r>c \\ \quad \text{or } t>\log c/a \end{array}\right]$$

$$=(k'+m)\,p_a - (k'+m)(1-m)\int_0^{\infty} p_a\, e^{(1-m)t}\,dt + (k'+m)(1-m)\,p_a \int_{\log c/a}^{\infty} e^{(1-m)t}\,dt$$

$$=-(k'+m)\,p_a\, e^{(1-m)\log c/a}$$

Substituting the transformed terms into the oringinal equation (54):

$$\bar{F} = \frac{F_0' + m F_0 - n(k'+m)a\,p_a\, e^{(1-m)\log c/a}}{m^2-1}$$

or, expressing $\bar{F}$ in partial fractions:

$$\bar{F} = \frac{A}{m-1} + \frac{B}{m+1} - \frac{na\,p_a}{2}\, e^{(1-m)\log c/a}\left[\frac{1+k'}{m-1} + \frac{1-k'}{m+1}\right]$$

where $A = \dfrac{F_0 + F_0'}{2}$ and $B = \dfrac{F_0 - F_0'}{2}$.

Applying standard transform tables, F is found to be:

$$F = Ae^{t} + Be^{-t} - \frac{n\,p_a\,c}{2}\left[(1+k')\,e^{t-\log c/a} + (1-k')\,e^{-(t-\log c/a)}\right]H(t-\log c/a)$$

where $H(t-\log c/a) = 0$ for $0<t<\log c/a$ $(a<r<c)$

$H(t-\log c/a) = 1$ for $\log c/a<t<\log b/a$ $(c<r<b)$

This is the required solution in terms of the variable t.

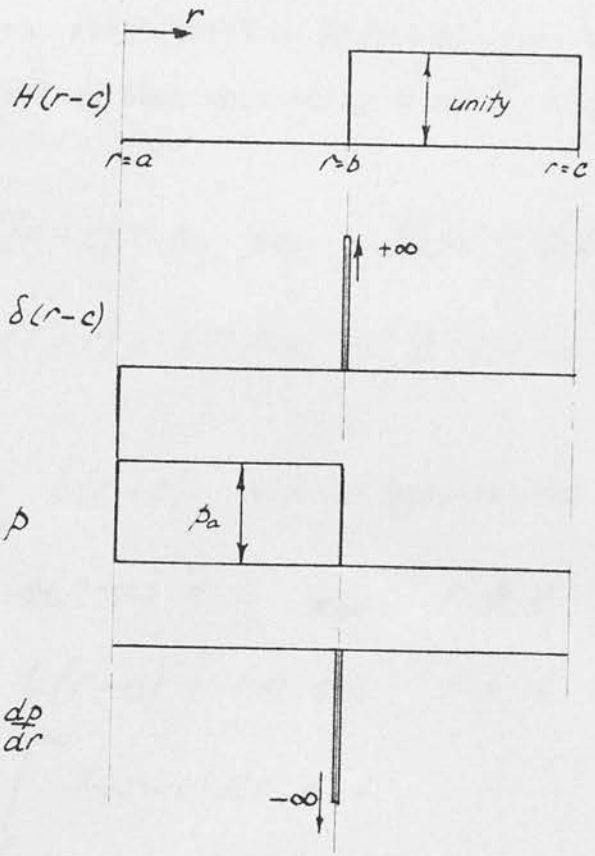

Figure 52

APPENDIX E
THE INFINITE TERMS OF EQUATION (62b)

Examining the latter two terms of equation (62b), $\frac{d}{dr} H(r-c)$ the derivative of the step function $H(r-c)$, is, by definition, an impulse function such as that defined by Dirac.[6] $H(r-c)$ has the properties:

$$H(r-c) = 0 \quad \text{for} \quad a < r < c$$

$$H(r-c) = 1 \quad \text{for} \quad c < r < b$$

$\frac{d}{dr} H(r-c) = \delta(r-c)$, has the properties:

$$\delta(r-c) = 0 \quad \text{for} \quad r \neq c$$

$$\delta(r-c) = +\infty \quad \text{for} \quad r = c$$

$$\int_{-\infty}^{+\infty} \delta(r-c)\,dr = 1$$

The functions are illustrated in Figure 52.

In the last term of equation (62a), $\frac{dp}{dr}$ is also an impulse function because p is a step function. If differs from $\delta(r-c)$ in that it has the value minus infinity at $r = c$ in accordance with the sign conventions which have been adopted. There is the further difference that $\frac{dp}{dr}$ is the derivative of a step function whose finite value is p_a rather than of the unit step function $H(r-c)$ whose finite value is unity. The difference is only in the value of a constant K_1 such that:

$$\frac{dp}{dr} = K_1\,\delta(r-c)$$

K_1 can be found by integrating both sides of this equation from $a<r<c$ to $c<r<b$, thus:

$$\int_{a<r<c}^{c<r<b} \frac{dp}{dr}\,dr = K_1 \int_{a<r<c}^{c<r<b} \delta(r-c)\,dr$$

therefore:

$$K_1 = -p_a$$

Thus it has been shown that the latter two terms of equation (62b) can be expressed as impulse functions. To determine the effect of these terms in equation (62b), the value of their integrals must be considered.

Each term will be integrated over the range minus infinity to plus infinity:

$$\text{(i)} \quad -\frac{n p_a}{2}\int_{-\infty}^{+\infty} r\left[(1+k') + (1-k')\frac{c^2}{r^2}\right]\frac{d}{dr}H(r-c)\,dr$$

$$= -\frac{n p_a}{2}\int_{-\infty}^{+\infty} r\left(1+\frac{c^2}{r^2}\right)\delta(r-c)\,dr - \frac{n p_a k'}{2}\int_{-\infty}^{+\infty} r\left(1-\frac{c^2}{r^2}\right)\delta(r-c)\,dr$$

If $f(r)$ is a continuous function of r in the neighbourhood of $r=c$ then

$$\int_{-\infty}^{+\infty} f(r)\,\delta(r-c)\,dr = f(c)$$ *

Applying this property to the above integrals, the first has the value $-n p_a c$ and the second has the value zero.

---

* See Chapter XI of reference 6.

(ii) $$\int_{-\infty}^{+\infty} nr \frac{dp}{dr}\, dr = -n p_0 \int_{-\infty}^{+\infty} r\, \delta(r-c)\, dr$$

$$= -n p_0 c \qquad \text{(by the above rule).}$$

Thus the two infinite terms have finite integrals of equal magnitude and opposite sense.

APPENDIX F
BIBLIOGRAPHY

1. BERNAL, J. D., "The Structures of Cement Hydration Compounds", London, Cement and Concrete Association, Proceedings of the Symposium on the Chemistry of Cement, September, 1952.

2. BERNAL, J. D., JEFFREY, J. W. and TAYLOR, H. F. W., "Crystallographic Research on the Hydration of Portland Cement : A First Report on Investigations in Progress", Magazine of Concrete Research, No. 11, October, 1952.

3. BLAINE, R. L. and VALIS, H. J., "Surface Available to Nitrogen in Hydrated Portland Cement Paste", Journal of Research, National Bureau of Standards, U.S.A., Vol. 42, 1949, Page 247.

4. BLEE, C. E. and RIEGEL, R. M., "Methods and Instruments for the Measurement of Performance of Concrete Dams of the Tennessee Valley Authority", Report No. 45, Third International Congress on Large Dams, Stockholm, 1948.

5. BRAHTZ, J. H. A., "The Stress Function and Photoelasticity Applied to Dams", Trans. Amer. Soc. Civ. Engrs., Vol. 101, 1936, Page 1240.

5a. BRAHTZ, J. H. A., "Pressures Due to Percolating Water and their Influence upon Stresses in Hydraulic Structures", Trans. Second International Congress on Large Dams, Vol. 5, Page 43, Washington, D.C. 1936.

6. CARSLAW, H. S. and JAEGER, J. C., "Operational Methods in Applied Mathematics", Second Edition, Oxford University Press, 1953.

7. CREAGER, W. P., JUSTIN, J. D. and HINDS, J., "Engineering for Dams", Vol. II, New York, Wiley, 1945.

8. EMMETT, P. H., Symposium on New Methods for Particle Size Determination in the Sub-Sieve Range, Amer. Soc. Testing Materials, 1941.

9. FILLUNGER, P., "Der Auftrieb in Talsperren", Oesterr. Wochenschrift f.d. Offentl. Baudienst, No. 31, 1913, Page 34.

10. FILLUNGER, P., "Auftrieb und Unterdruck in Staumauern", Vol. 9, Trans. Second World Power Conference, Berlin, 1930.

11. GHERARDELLI, L., "The Static Effects of Interstitial Pressures in Porous Elastic Solids", L'Energia Elettrica, May, 1954.

12. GLANVILLE, W. H., "The Permeability of Portland Cement Concrete", Building Research Technical Paper No. 3, 1926.

13. GRIGGS, D. T., "Deformation of Rocks Under High Confining Pressures", Journal of Geology, Vol. 44, 1936, Page 541.

14. HARRISON, E. S. and KINDSVATER, C. E., "Dam Modifications Checked by Hydraulic Models", Trans. Amer. Soc. Civ. Engrs., Vol. 119, 1954, Page 73.

15. HARZA, L. F., "The Significance of Pore Pressure in Hydraulic Structures", Trans. Amer. Soc. Civ. Engrs., Vol. 114, 1947, Page 193.

16. HENNY, D. C., "Stability of Straight Concrete Gravity Dams", Trans. Amer. Soc. Civ. Engrs., Vol. 60, 1934, Page 1041.

17. HINDS, J., "Upward Pressure Under Dams", Trans. Amer. Soc. Civ. Engrs., Vol. 92, 1928.

18. HOUK, I. E., "Uplift Pressures in Masonry Dams", Civil Engineering, (U.S.A.), September, 1932.

19. KEENER, K. B., "Uplift Pressure in Concrete Dams", Trans. Amer. Soc. Civ. Engrs., Vol. 116, 1951, Page 1218.

20. KHOSLA, Discussion of General Report on Uplift, Trans, Third International Congress on Large Dams, Stockholm, 1948.

21. LE CHATELIER, H., "Experimental Researches on the Constitution of Hydraulic Mortars", (Translation by J. L. Mack), McGraw Hill, New York, 1905.

22. LEGGETT, R. F., "Geology and Engineering", McGraw Hill, 1939, Page 305.

23. LELIAVSKY, S., "Structural Methods for Reducing Uplift and Leakage in Dams", The Engineer, 11th and 18th of March, 1949.

24. LELIAVSKY, S., "Experiments on Effective Uplift Area in Gravity Dams", Trans. Amer. Soc. Civ. Engrs., Vol. 112, 1947, Page 443.

25. LEVY, M., "Quelques Considerations sur la Construction des Grands Barrages", Comptes Rendues de l'Academie des Sciences, Vol. 12, 1895 Page 288.

26. LEVY, M., Comptes Rendues de l'Academie des Sciences, 1898.

27. LUBINSKI, A., "The Theory of Elasticity for Porous Bodies Displaying a Strong Pore Structure", Proceedings Second U.S. National Congress of Applied Mechanics.

28. McHENRY, D., "The Effect of Uplift Pressure on the Shearing Strength of Concrete", Report No. 48, Trans. Third International Congress on Large Dams, Stockholm, 1948.

29. POLANYI, M. and SCHMIDT, E., "Ist die Gleitreibung vom Druck Normal zu den Gleitflachen Abhangig",. Zeitschrift fur Physik, Vol. 16, 1923, Page 336.

30. POWERS and BROWNYARD, Journal of the American Concrete Institute, Vol. 18, 1946, Page 469.

31. REINIUS, E., Report No. 57, Trans. Third International Congress on Large Dams, Stockholm, 1948.

32. RUBINSKY, I. A. and RUBINSKY, A., "A Preliminary Investigation of the Use of Fibre-Glass for Prestressed Concrete", Magazine of Concrete Research, No. 17, September, 1954.

33. SACHS, G., "Die Technologischen Eigenschaften von Aluminiumkristallen", Zeitschrift Ver. Deutsch. Ing., Vol. 71, 1927, Page 777.

34. SERAFIM, J. L., "A Subpressao nas Barragens", Paper No. 55, Laboratorio Nacional de Engenharia Civil, (Ministerio das Obras Publicas), Lisbon.

35. SIMMONS, J. C., "Poisson's Ratio of Concrete : A Comparison of Dynamic and Static Measurements", Magazine of Concrete Research, No. 20, July, 1955.

36. SIMONDS, A. W., "Final Foundation Treatment at Hoover Dam", Trans. Amer. Soc. Civ. Engrs. Vol. 118, 1953, Page 78.

37. JEFFREY, J. W., "Apparatus and Methods Employed in the X-Ray Examination of Cement Compounds at Birkbeck College Research Laboratories", Magazine of Concrete Research, No. 2, June, 1949.

38. TERZAGHI, K., "Simple Tests Determine Hydrostatic Uplift", Engineering News-Record, 18th of June, 1936.

39. TERZAGHI, K., "Stress Conditions for the Failure of Saturated Rock and Concrete", Proceedings Amer. Soc. Testing Materials, Vol. 45, 1945, Page 777.

40. TIMOSHENKO, S. and GOODIER, J. N., "Theory of Elasticity", Second Edition, McGraw Hill, 1951.

41. WILSON, J. S. and GORE, W., "Stresses in Dams : An Experimental Investigation by Means of India-Rubber Models", Proceedings of the Institution of Civil Engineers, Vol. 172, 1907-8, Part 2, Page 107.

42. ZIENKIEWICZ, O. C., "The Stress Distribution in Gravity Dams", Journal of the Institution of Civil Engineers, Vol. 27, 1946-7, Page 244.

43. ALLEN, D. N. de G., CHITTY, L., PIPPARD, A. J. S. and SEVERN, R. T., "The Experimental and Mathematical Analysis of Arch Dams with Special Reference to Dokan", Proceedings of the Institution of Civil Engineers, Vol. 5, May, 1956, Part 1, Page 198.